



National Library
of Canada

Bibliothèque nationale
du Canada

Canadian Theses Service

Services des thèses canadiennes

Ottawa, Canada
K1A 0N4

CANADIAN THESES

THÈSES CANADIENNES

NOTICE

The quality of this microfiche is heavily dependent upon the quality of the original thesis submitted for microfilming. Every effort has been made to ensure the highest quality of reproduction possible.

If pages are missing, contact the university which granted the degree.

Some pages may have indistinct print especially if the original pages were typed with a poor typewriter ribbon or if the university sent us an inferior photocopy.

Previously copyrighted materials (journal articles, published tests, etc.) are not filmed.

Reproduction in full or in part of this film is governed by the Canadian Copyright Act, R.S.C. 1970, c. C-30.

**THIS DISSERTATION
HAS BEEN MICROFILMED
EXACTLY AS RECEIVED**

AVIS

La qualité de cette microfiche dépend grandement de la qualité de la thèse soumise au microfilmage. Nous avons tout fait pour assurer une qualité supérieure de reproduction.

S'il manque des pages, veuillez communiquer avec l'université qui a conféré le grade.

La qualité d'impression de certaines pages peut laisser à désirer, surtout si les pages originales ont été dactylographiées à l'aide d'un ruban usé ou si l'université nous a fait parvenir une photocopie de qualité inférieure.

Les documents qui font déjà l'objet d'un droit d'auteur (articles de revue, examens publiés, etc.) ne sont pas microfilmés.

La reproduction, même partielle, de ce microfilm est soumise à la Loi canadienne sur le droit d'auteur, SRC 1970, c. C-30.

**LA THÈSE A ÉTÉ
MICROFILMÉE TELLE QUE
NOUS L'AVONS REÇUE**

A PERFORMANCE STUDY OF
NLA 64-STATE QAM

Tricia Hill

Thesis presented to the School of Graduate Studies
in partial fulfillment of the requirements for the
degree of Master of Applied Science.

UNIVERSITY OF OTTAWA
OTTAWA, CANADA, 1983



Patricia (Tricia) Hill, Ottawa, Canada, 1984.

Permission has been granted to the National Library of Canada to microfilm this thesis and to lend or sell copies of the film.

The author (copyright owner) has reserved other publication rights, and neither the thesis nor extensive extracts from it may be printed or otherwise reproduced without his/her written permission.

L'autorisation a été accordée à la Bibliothèque nationale du Canada de microfilmer cette thèse et de prêter ou de vendre des exemplaires du film.

L'auteur (titulaire du droit d'auteur) se réserve les autres droits de publication; ni la thèse ni de longs extraits de celle-ci ne doivent être imprimés ou autrement reproduits sans son autorisation écrite.

ISBN 0-315-30960-1

ABSTRACT

This thesis investigates the performance characteristics of Nonlinearly Amplified 64-state Quadrature Amplitude Modulation (NLA 64-state QAM) for terrestrial microwave radio systems. These studies include computer simulation analyses, hardware design and experimental investigations.

A comparison of various 64-ary modulation techniques is made which shows the advantages offered by NLA 64-state QAM. In addition, a brief review of its theoretical probability of error (P_e) versus the ratio of energy per bit to noise power in a 1 Hz bandwidth (E_b/N_0) performance and spectral performance are presented.

A prototype NLA 64-state QAM modem was designed which operated at a scaled bit rate of 384 kb/s. A detailed description of the prototype modem design is presented. The principles of operation and practical constraints of the modem are analyzed. The modem design and evaluation indicate that the use of NLA 64-state QAM in a commercial product is viable.

Computer simulation models of 64-state QAM systems are introduced, important features of which are outlined. In addition, the analysis of the P_e performance used in the computer simulation is derived.

A study of the effects of commonly encountered microwave radio transmission and operating conditions on the P_e performance of NLA 64-state QAM is presented. The conditions analyzed include co-channel and adjacent channel interference,

anomalous signal levels and phase shifts in the state space, channel amplitude distortions, channel group delay distortions, and multipath fading. For systems incorporating 64-state QAM, it is evident that careful measures must be taken to combat practically encountered distortions.

An analysis of the spectral efficiency of the prototype modem translated to practical North American terrestrial radio bit rates and frequencies is presented. It is shown that in the Federal Communications Commission (FCC) authorized bandwidth of 20 MHz, 30 MHz, and 40 MHz spectral efficiencies in the order of 4.7 b/s/Hz, 5.0 b/s/Hz, and 5.1 b/s/Hz are achievable.

An estimation of the P_e performance degradation from ideal resulting from the prototype modem's hardware configuration is presented. It is shown that the prototype's filtering introduces a degradation to performance in the order of 1.9 dB. In addition, the lack of Gray coding in the modulator increased the bit error rate by a factor of 1.57.

ACKNOWLEDGEMENT

The author would like to gratefully acknowledge the help provided by many individuals during the course of this research.

Sincere thanks go to her supervisor, Dr. Kamilo Feher, for his encouragement and support. A special thanks goes to Doug Prendergast for his invaluable guidance, technical advice, and assistance.

Thanks is also extended to Patrick Vandamme, Tho Le Gnoc, Hiep Phan Van, Shuzo Kato and Dr. V. Arunchalam for their help and time spent in useful discussion.

Appreciation is expressed to all graduate students for their assistance and support.

Finally, the author expressed whole-hearted thanks to both Farinon Canada and Farinon Electric for enabling the completion of this research.

TABLE OF CONTENTS

	Page
LIST OF FIGURES	iii
LIST OF TABLES	vii
LIST OF ABBREVIATIONS	viii
CHAPTER 1. INTRODUCTION	
1.1 Trends in Digital Microwave Radio	1
1.2 Outline of Thesis	4
1.3 Comparing 64-ary Signal Set Designs	7
1.4 Performance Analysis of Rectangular 64-state APK	9
1.5 A Comparison of 8-L QAM and NLA 64-state QAM	18
CHAPTER 2. MODEM DESIGN	
2.1 Introduction	27
2.2 The Modulator	28
2.3 The Demodulator	40
CHAPTER 3. COMPUTER SIMULATION	
3.1 Introduction	46
3.2 Simulation Model	47
3.3 Probability of Error Calculations	52
CHAPTER 4. PERFORMANCE OF 64-STATE QAM WITH TRANSMISSION IMPAIRMENTS	
4.1 Introduction	56
4.2 Interference	58
4.3 Anomalous Amplitude and Phase in the State Space	60
4.4 Channel Amplitude Distortions	72
4.5 Channel Group Delay Distortions	79
4.6 Selective Fading	86

	Page
CHAPTER 5. PERFORMANCE OF MODEM	
5.1 Introduction	91
5.2 Spectral Efficiency of the Modem	92
5.3 P_e Performance of the Modem	98
CHAPTER 6. THESIS SUMMARY AND SUGGESTED RESEARCH TOPICS	
6.1 Thesis Summary	102
6.2 Suggested Research Topics	108
APPENDICES	
APPENDIX A. TECHNICAL INFORMATION - 64-STATE QAM MODEM	109
APPENDIX B. SIMULATION PROGRAMS	138
REFERENCES	205

LIST OF FIGURES

	Page
CHAPTER 1.	
Figure 1.4.1 A single Rectangular Decision Region	10
Figure 1.4.2 Rectangular 64-APK Constellation	11
Figure 1.4.3 P_e versus E_b/N_0 for Ideal Rectangular 64-APK	14
Figure 1.4.4 Power Spectral Density of 64-APK	17
Figure 1.5.1 8-Level QAM Modem Block Diagram	20
Figure 1.5.2 NLA 64-State QAM Modem Block Diagram	22
CHAPTER 2.	
Figure 2.2.1 NLA 64-State QAM Modulation Block Diagram	30
Figure 2.2.2 Block Diagram of a Predistortion Equalizer	32
Figure 2.2.3 Photograph of Measured Unequalized Pulse Response and Equalized Pulse Response	34
Figure 2.2.4 Measured Amplitude Response of Modified Fifth-Order Butterworth Low-Pass Filter	36
Figure 2.2.5 A Block Diagram of a QPSK Modulator .	37
Figure 2.2.6 QPSK Modulated Carrier Wave Forms ...	38
Figure 2.3.1 A Block Diagram of the NLA 64-State QAM Demodulator	41
Figure 2.3.2 A Block Diagram of Quadrature Demodulator	42
Figure 2.3.3 Eye Diagrams at the Post Detection Low-Pass Filter Output	44
Figure 2.3.4 Signal State Space Diagram at the Post Detection Low-Pass Filter Output	44

	Page
CHAPTER 3.	
Figure 3.2.1 Computer Simulation Model	49
Figure 3.3.1 64-State QAM Composite State Space ..	55
CHAPTER 4.	
Figure 4.2.1 P_e versus E_b/N_0 Performance for Co-Channel Interference	60
Figure 4.2.2 P_e versus E_b/N_0 Performance for Adjacent Channel Interference	61
Figure 4.3.1 P_e versus E_b/N_0 for First Modulator Power Level Variations	64
Figure 4.3.2 P_e versus E_b/N_0 for Second Modulator Power Level Variations	65
Figure 4.3.3 P_e versus E_b/N_0 Third Modulator Power Level Variations	66
Figure 4.3.4 A Measured Eye-Diagram with the Two Decision Thresholds Indicated	67
Figure 4.3.5 Degradation of E_b/N_0 versus the Variation on the Power Levels from Ideal	69
Figure 4.3.6 Degradation of E_b/N_0 versus the Variation of the Phase from Ideal ...	71
Figure 4.4.1 P_e versus E_b/N_0 for Linear Amplitude Distortions	74
Figure 4.4.2 P_e versus E_b/N_0 for Parabolic Amplitude Distortions	75
Figure 4.4.3 P_e versus E_b/N_0 for Sinusoidal Amplitude Distortions	77
Figure 4.4.4 Degradation of E_b/N_0 for Linear, Parabolic, and Sinusoidal Amplitude Distortions	78

	Page
Figure 4.5.1 P_e versus E_b/N_0 for Linear Group Delay Distortions,	80
Figure 4.5.2 P_e versus E_b/N_0 for Parabolic Group Delay Distortions	82
Figure 4.5.3 P_e versus E_b/N_0 for Sinusoidal Group Delay Distortions	83
Figure 4.5.4 Degradation of E_b/N_0 for Linear, Parabolic, and Sinusoidal Group Delay Distortions	85
Figure 4.6.1 P_e versus E_b/N_0 for Minimum Phase Fades	88
Figure 4.6.2 P_e versus E_b/N_0 for Nonminimum Phase Fades	89
 CHAPTER 5.	
Figure 5.2.1 Measured Power Spectral Density of 64-State QAM Signal of Transmitter Output	93
Figure 5.2.2 FCC Mask Applied to 64-State QAM ...	97
Figure 5.3.1 Measured Eye Diagram at the 8-to-2 Level Converter Input in the Demodulator	99
Figure 5.3.2 64-State QAM State Space to Bit Error Relationship	101
 APPENDIX A	
Figure A.1.1 Serial-to-Parallel Circuit Diagram .	111
Figure A.1.2 Serial-to-Parallel Circuit Board ...	112
Figure A.2.1 Predistortion Equalizer and Low-Pass Filter Circuit Diagram	115
Figure A.2.2 Predistortion Equalizer and Low-Pass Filter Circuit Board	116
Figure A.3.1 Quadrature Modulator Circuit Diagram	119

	Page
Figure A.3.2 Quadrature Modulator Circuit Board	120
Figure A.4.1 Hard Limiter Circuit Diagram	122
Figure A.5.1 Combiner Circuit Diagram	125
Figure A.5.2 Combiner Circuit Board	126
Figure A.6.1 Quadrature Demodulator Circuit Diagram	129
Figure A.6.2 Quadrature Demodulator Circuit Board	130
Figure A.7.1 Post Detection Low-Pass Filter Circuit Diagram	133
Figure A.8.1 8-to-2 Level/Parallel-to-Serial Converter Circuit Diagram	136
Figure A.8.2 8-to-2 Level/Parallel-to-Serial Converter Circuit Board	137

APPENDIX B

Figure B.1.1 64-State QAM Simulation Model	140
Figure B.1.2 NLA 64-State QAM Simulation Model ..	179
Figure B.1.3 64-State QAM Co-Channel and Adjacent Channel Simulation Model	191

LIST OF TABLES

	Page
CHAPTER 1.	
Table 1.3.1 Comparing P_e Performance of 64-ary Signal Set Designs	7
CHAPTER 2.	
Table 2.1.1 Performance of Eight-to-two Level Converter	45
CHAPTER 5.	
Table 5.1.1 Normalized Transmit Spectrum	96
APPENDIX A	
Table A.1.1 Serial-to-Parallel Converter Technical Summary	110
Table A.2.1 Predistortion Equalizer/Low-Pass Filter Technical Summary	114
Table A.3.1 Quadrature Modulator Technical Summary	118
Table A.4.1 Hard Limiter Technical Summary	
Table A.5.1 Combiner Technical Summary	124
Table A.6.1 Quadrature Demodulator Technical Summary	128
Table A.7.1 Post Detection Low-Pass Filter Technical Summary	132
Table A.8.1 8-to-2 Level/Parallel-to-Serial Converter Technical Summary	135

LIST OF ABBREVIATIONS

A(f)	Amplitude Function
AM	Amplitude Modulation
APK	Amplitude Phase Keying
AWGN	Additive White Gaussian Noise
BPF	Bandpass Filter
BPSK	Binary Phase Shift Keying
BWN	Double-sided Nyquist Bandwidth
b/s/Hz	Bits per second per Hertz
CIR	Carrier-to-Interference ratio
E_b	Energy per bit
erfc	Complementary Error Function
E_s	Energy per symbol
f_N	Nyquist frequency
f_C	Carrier frequency
f_f	3 dB single-sided filter bandwidth
G(f)	Power spectral density
Hz	Hertz
I	Inphase
ISI	Intersymbol Interference
kb/s	kilobits per second
LPF	Low-pass Filter
Mb/s	Megabits per second
MSK	Minimum Shift Keying
N_0	Noise Power density

NLA	Nonlinear Amplified
NRZ	Non Return to Zero
P_s	Signal Power
P_e	Probability of error
PM	Phase Modulation
Q	Quadrature-phase
QPSK	Quaternary Phase Shift Keying
$R_x(f)$	Receiver filter transfer function
SNR	Signal-to-noise ratio
T_{8-L}	Unit eight-level symbol duration
T_b	Unit bit duration
TWT	Travelling Wave Tube
$T(f)$	Group delay function
α	Raised cosine filtering roll-off factor
8-L QAM	Eight-Level Quadrature Amplitude Modulation
8PSK	Eight Phase Shift Keying
16-QAM	Sixteen State Quadrature Amplitude Modulation

CHAPTER 1

CHAPTER 1

1.1 Trends in Digital Microwave Radio

Digital microwave radio systems have become an important part of the total voice and data transmission picture in a very short period of time. [U] In the early 1970's the number of microwave radio systems using digital modulation techniques was very small relative to the number of systems using analog modulation techniques. However, with the advances in digital technology, significant cost reductions and improved performance were realized in the telephone systems using digital techniques. Today, digital transmission systems are widely used in many telephone systems throughout the world.

With increased popularity of digital radio systems came the need to improve such systems. The crowded conditions prevailing in many regions of the radio spectrum, the necessity to meet communication regulations, and the pressure to increase transmission capacity helped create this need. The satisfaction of this need, however, is not easily achieved.

When designing these systems many factors must be dealt with. There are regulatory constraints on occupied bandwidth, spectrum shape, and bandwidth utilization. In addition to these constraints, there is a need to meet standard digital interfaces on factors such as transmission rates, number of voice circuits per channel, and numerous others.

For instance, the Federal Communications Commission (FCC) in Docket 19311, has decreed a minimum channel capacity of 1152 voice channels for the 4, 6, and 11 GHz bands. Since existing digital banks digitize voice signals on the basis of 24 channels per 1.544 Mb/s (DS-1 signal) the 1152 voice channel requirement implies a minimum of 48 DS-1 signals. However, most digital radios at 6 and 11 GHz utilize a higher capacity of 1344 voice channels or 90Mb/s (two DS-3 signals). This rate facilitates the handling of larger digital cross sections, thereby reducing the multiplexing requirements and hence the costs.

Providing 90 Mb/s in existing authorized radio bandwidths is not an easy task. Using 4 GHz as an example, the authorized FCC bandwidth is only 20 MHz thus requiring a 4.5 b/s/Hz capacity. This transmission capacity implies the use of higher order modulation techniques.

Modulation techniques for digital radio are still undergoing an evolutionary period. Early systems used Quaternary Phase Shift Keying (QPSK), to achieve transmission efficiencies of approximately 1 b/s/Hz [1]. Today, Eight Phase Shift Keying (8 PSK) and Sixteen-state Quadrature Amplitude Modulation (16-state QAM) systems are achieving efficiencies of approximately 3 b/s/Hz [2]. In the future, systems featuring efficiencies of over 4 b/s/Hz will be available. Companies such as Nippon Telephone and Telegraph of Japan, Rockwell Collins of U.S.A., and Northern Telecom of Canada have all announced the future introduction of products with transmission capacity of over 4 b/s/Hz.

Digital radio technology has moved at a rapid pace in the past few years and there is every reason to believe this trend will continue. The struggle for higher capacity and efficiency is in its infancy. The coming years look exciting indeed.

In this thesis an in depth study is made of the implementation and viability of NonLinearly Amplified (NLA) 64-state QAM, a modulation technique with a potential transmission capacity of over 4 b/s/Hz. In the succeeding sections of this chapter we:

- 1) Provide an outline of the thesis that shows how the various studies relate to the thesis topic;
- 2) Discuss the various 64-ary modulation techniques and show the advantages offered by rectangular 64-ary Amplitude and Phase Keying (APK);
- 3) Review the theoretical performance of rectangular 64-state APK; and
- 4) Compare the implementation of Eight-Level QAM (8-L QAM) to that of NLA 64-state QAM and show the advantages to NLA 64-state QAM.

1.2 Outline of Thesis

The first study presented is introductory in nature and contained in Sections 1.3 and 1.4. It reviews various 64-ary modulation techniques and compares their probability of error performance. Specifically, the following techniques are reviewed:

64 PSK

(6,12,19,27) Concentric Circular APK

(6,13,19,26) Concentric Circular APK

Triangular 64-state APK

Rectangular 64-state APK

The basis for the selection of a rectangular 64-state APK modulation technique is justified in this review.

The final part of this introductory study reviews the theoretical performance of rectangular 64-state APK. The probability of error performance relative to the energy per bit versus noise power density ratio is presented together with the power spectral density of rectangular 64-state APK. The purpose of this review is to form a base of understanding of the ideal performance of the technique that will be helpful when studying the more detailed material presented in the remaining chapters.

The next study, contained in Section 1.5, is not a review but is introductory in nature. In it a comparison is made of implementations of rectangular 64-state APK. Specifically, we compare 8-L QAM and NLA 64-state QAM. A brief description of the implementation of each technique is presented followed by

a comparison of the two. It is as a result of this study and the previous study that the selection of NLA 64-state QAM for further research was made.

Next, in Chapter 2 a description is presented of the prototype modem that has been implemented for this research. The subsystems of the modulator and demodulator are briefly described and explained. An understanding of the operation of the modem and the function of the various subsystems is inherent in this study. A more detailed technical description of each of the subsystems is contained in Appendix A.

In Chapter 3, the computer simulation programs that have been used to aid in the performance analyses of NLA 64-state QAM systems are presented. Important features of the simulation models are outlined and the method of computing probability of error described. Appendix B contains complete listings of the simulation programs.

In Chapter 4 a study of the probability of error performance of 64-state QAM during various operating and transmission conditions is presented. Specifically, the following conditions are considered:

- cochannel and adjacent channel interference,
- anomalous amplitude and phase in the state space,
- channel amplitude distortions,
- channel group delay distortions, and
- selective fading.

In Chapter 5, the final study of the thesis is presented. The performance of a digital radio system with the same basic hardware design as our prototype modem is determined. The laboratory measurements of the eye diagram indicate a high quality eye diagram representing a minimal degradation to performance from ideal. The bandwidth efficiency of systems in the 20 MHz, 30 MHz, and 40 MHz FCC bandwidths with the same basic filtering as our prototype modem is determined.

Chapter 6 concludes the thesis and presents suggestions for future research based on this thesis.

1.3 Comparing 64-ary Signal Set Designs

The approach employed in this investigation is based on one employed by Thomas, Weidner, and Durrani [3] which uses the error performance as a guideline in the selection of a signal set design. Designability and realizability are also used as guidelines in the selection. Reasonable designs are selected as candidates for error probability evaluation. While the selected design might not offer the optimum performance, the performance should not be greatly inferior to that of the best candidate considered.

It has been shown [2] that for an alphabet size of over 4, a hybrid modulation scheme combining both amplitude and phase keying requires less power than PSK for the same error performance. For this reason, APK designs are selected for further investigation.

The signal set designs selected for error probability evaluation will now be described. They fall into three basic categories: those with signals arranged on concentric circle (6,12,19,27) and (6,13,19,26) with radii (1,1.93,3.04,4.29) and (1,2.08,3.08,4.15), and those with triangular or rectangular patterns. For notational convenience the circular sets are designated as (a,b,c,d) meaning there are four circles with "a" signals on the inner circle, "b" signals on the next larger circle, etc. The same notation applies for the circular radii, for example, (x,y,z,w) indicates the inner circle radius is

normalized to "x" units, the next larger radius is "y" units, etc.

Thomas et al [3] have shown that for the above mentioned designs, under an average signal-to-noise ratio (SNR) constraint the 64-ary triangular design yields the optimum performance. The rectangular and circular designs require about 0.5 dB greater SNR for a P_e of 10^{-5} . As expected, the 64-ary APK performance is superior to the PSK performance, in fact by approximately 10 dB.

Signal Set	SNR for a P_e of 10^{-5}
64 PSK	37.4
(6,12,19,27) Concentric Circular APK	26.6
(6,13,19,26) Concentric Circular APK	26.4
Triangular 64-state APK	25.9
Rectangular 64-state APK	26.4

Table 1.3.1 Comparing P_e performance of 64-ary signal set designs

As summarized in Table 1.3.1 it is evident that for 64-ary designs the triangular design yields the best performance on an average SNR basis. This is to be expected because of its sphere-packing properties. However, the most easily realizable rectangular design is within 0.5 dB of the best set.

Based on the above results, the rectangular APK design was selected for further study over the other candidates because of its comparable performance and its ease of design. The next section will look more closely at the theoretical performance of rectangular 64-state APK.

1.4 Performance Analysis of Rectangular 64-state APK

The P_e performance of any digital communication system is a function of the filtering applied to the system, the added noise, and unwanted interference. However, before discussing this topic, which is considered in Chapters 3, 4 and 5, the theoretical P_e performance of rectangular 64-state APK in an AWGN environment and an infinite bandwidth channel is derived.

The decision regions $[R^{(i)}]$, $i = 1, \dots, 64$ for this signal configuration are rectangular and $S^{(K)} + n$ falls within $R^{(K)}$ whenever simultaneously,

$(a_1 < n_1 < B_1)$ and $(a_2 < n_2 < B_2)$. [14] (1.4.1) where a_1 , B_1 , a_2 , and B_2 form the decision region boundaries. (An example of this is given in Fig. 1.4.1). Thus, the conditional probability of a correct decision given that $A^{(i)}$ was sent is given by

$$p[C|A^{(i)}] = p[a_1 < n_1 < B_1] p[a_2 < n_2 < B_2] \quad (1.4.2)$$

The determination of this conditional probability for each of the possible sixty-four signals might seem to be laborious, however, this is in fact not the case. The ease of determining the conditional probabilities is directly attributable to the symmetry in the signal constellation. This is illustrated in Fig. 1.4.2. The conditional probabilities of all four corner signals * are equivalent as are the conditional probabilities of all twenty-four outer edge signals o and all

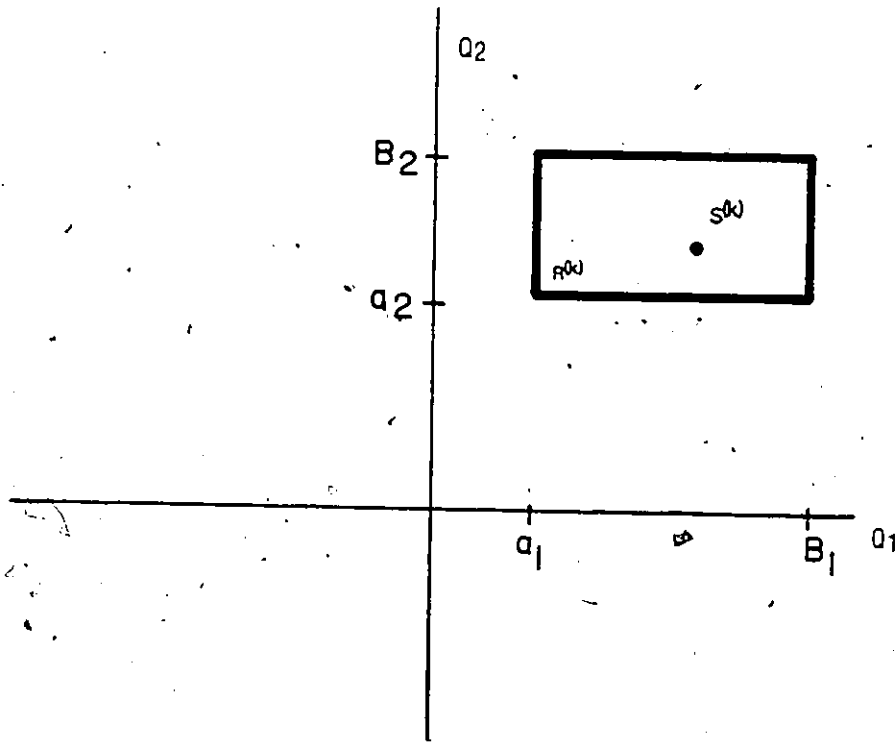


FIGURE 1.4.1 A SINGLE RECTANGULAR DECISION REGION

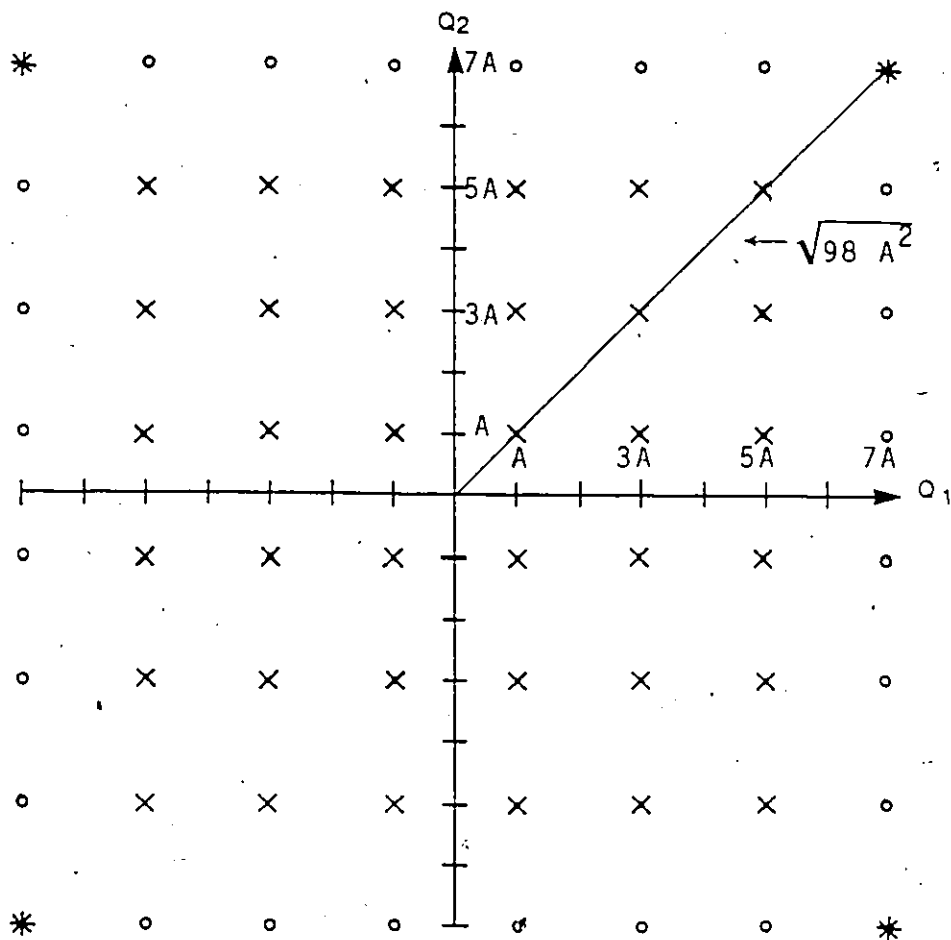


FIGURE 1.4.2 RECTANGULAR 64-APK SIGNAL CONSTELLATION

thirty-six inner grid signals x . The three different conditional probabilities $p[C|*]$, $p[C|o]$ and $p[C|x]$ are

$$p[C|*] = (1-p)(1-p) \quad (1.4.3a)$$

$$p[C|o] = (1-2p)(1-p) \quad (1.4.3b)$$

$$\text{and } p[C|x] = (1-2p)(1-2p) \quad (1.4.3c)$$

where $p = \int_A^{\infty} \frac{1}{\sqrt{2\pi}} \frac{e^{-v^2/2}}{\sqrt{N_0}} dv$ is the probability of error

of two signals separated by a distance $2A$ and $N_0/2$ is the noise power density.

$$\begin{aligned} \text{Thus } P_c &= 4/64 (1-p)^2 + 24/64 (1-p)(1-2p) \\ &+ 36/64 (1-2p)^2 \\ &= 1 - 14/4p + 49/16p^2 \end{aligned} \quad (1.4.4)$$

and

$$P_e = 14/4p + 49/16p^2. \quad (1.4.5)$$

For the practical case of high S/N ratios Eq. (1.4.4) simplifies to

$$P_e \approx 14/4p \quad (1.4.6)$$

To determine the $P_e (E_b/N_0)$ of rectangular 64-APK the average energy of the symbol E_s in terms of A must initially be derived.

$$E_s = \frac{1}{64} \sum_{i=1}^8 \sum_{j=1}^8 (a^{(i)^2} + b^{(j)^2}) \quad (1.4.7)$$

Referring to Fig. 1.4.2, that is,

$$\begin{aligned} E_s &= \frac{1}{64} \times A^2 ((1^2 + 1^2) \times 4 + (3^2 + 3^2) \times 4 + \\ &(5^2 + 5^2) \times 4 + (7^2 + 7^2) \times 4 + (1^2 + 3^2) \times 8 + (1^2 + 5^2) \times 8 \\ &+ (1^2 + 7^2) \times 8 + (3^2 + 5^2) \times 8 + (3^2 + 7^2) \times 8 + (5^2 + 7^2) \times 8) \\ &= 42 A^2 \end{aligned} \quad (1.4.8)$$

The average energy of a bit E_b is E_s divided by the number of bits per symbol. Thus,

$$E_b = \frac{E_s}{6} \quad (1.4.9)$$

and

$$\frac{E_b}{N_0} = \frac{7\Lambda^2}{N_0} \quad (1.4.10)$$

Substituting Eq. (1.4.10) into Eq. (1.4.6)

$$P_e = \frac{14}{4} \int_{\sqrt{\frac{E_b \cdot 2}{N_0 \cdot 7}}}^{\infty} \frac{1}{\sqrt{2\pi}} e^{-v^2/2} dv \quad (1.4.11)$$

or

$$P_e = 1.75 \operatorname{erfc} \left(\sqrt{\frac{E_b}{7\Lambda^2 N_0}} \right) \quad (1.4.12)$$

where the complementary error function $\operatorname{erfc}(x)$ is given by

$$\operatorname{erfc}(x) = \frac{2}{\sqrt{\pi}} \int_x^{\infty} e^{-y^2} dy.$$

The relationship given in Eq. (1.4.12) is shown graphically in Fig. 1.4.3.

Since overall system filtering should be decided so as to minimize intersymbol, interchannel and intersystem interference, it is quite natural to try to approach matched Nyquist filtering in order to minimize these interferences. The P_e performance, for rectangular 64-APK, derived above is in fact the P_e performance that could be expected of such a system with matched Nyquist filtering in an AWGN environment.

The rectangular 64-state APK power spectral density can be derived from the NRZ power spectral density $G_{NRZ}(f)$ as follows.

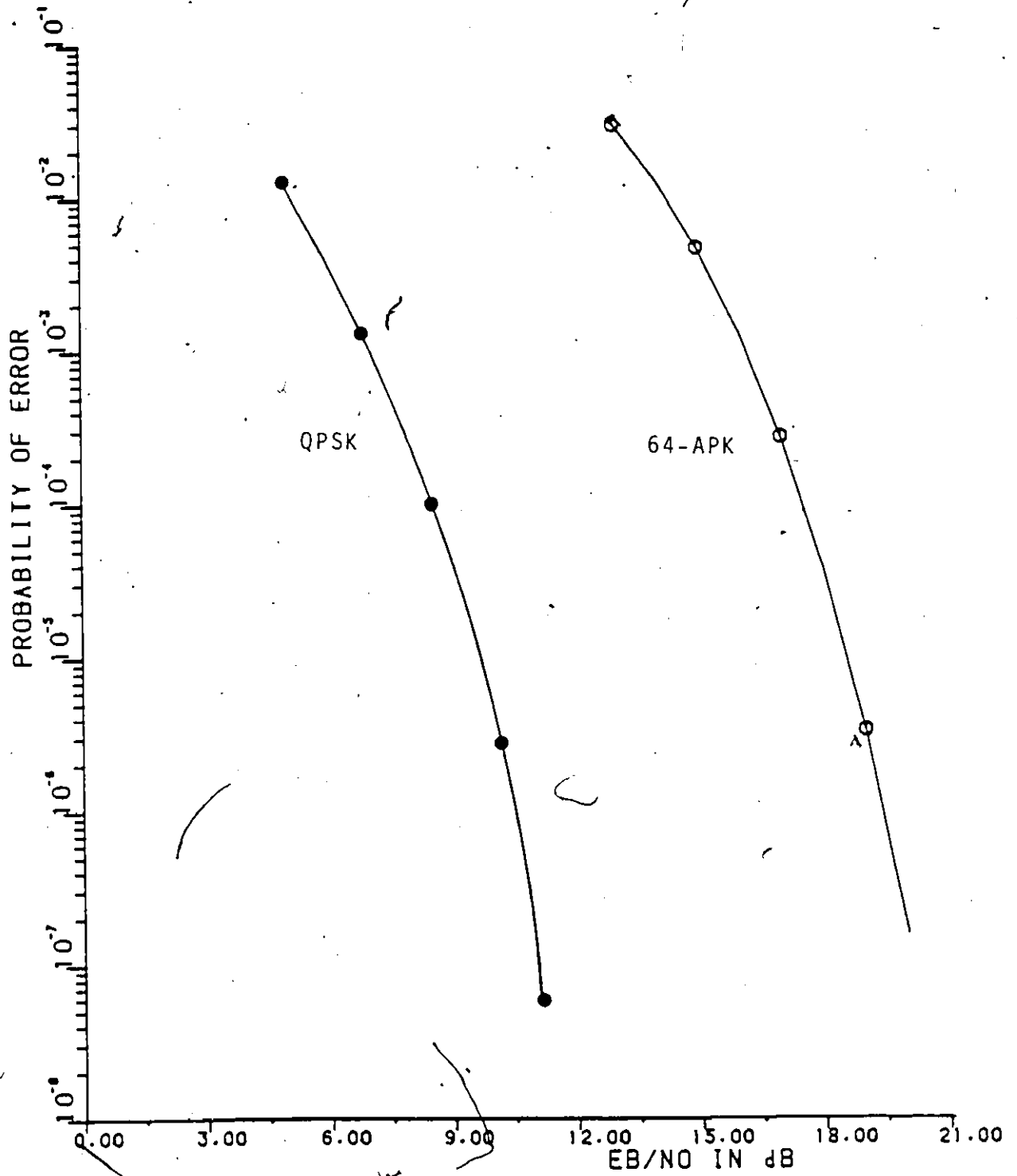


FIGURE 1.4.3

P_e VERSUS E_b/N_0 FOR IDEAL
64-APK

The power spectral density of random, equiprobable NRZ data with amplitude levels $+A$ or $-A$ is given by [2]

$$G_{\text{NRZ}}(f) = A^2 T_b \left(\frac{\sin \pi T_b f}{\pi T_b f} \right)^2 \quad (1.4.13)$$

where T_b is the bit duration.

Rectangular 64-APK can be thought of as two baseband eight-level signals in quadrature, each of whose power spectral densities are given by

$$G_{8-L}(f) = 21A^2 T_{8-L} \left(\frac{\sin \pi f T_{8-L}}{\pi f T_{8-L}} \right)^2 \quad (1.4.14)$$

where T_{8-L} is the symbol duration of the 8-level signal, $\pm A$, $\pm 3A$, $\pm 5A$, $\pm 7A$ are the possible amplitude levels, and $21A^2$ is the average power of the 8-level signal. Defining T_b as the bit duration of the NRZ input data to the 64-state APK system then,

$$T_{8-L} = 6 T_b \quad (1.4.15)$$

Thus, $G_{8-L}(f)$ as given in Eq. (1.4.14) can be rewritten as

$$G_{8-L}(f) = 126 A^2 T_b \left(\frac{\sin 6\pi f T_b}{6\pi f T_b} \right)^2 \quad (1.4.16)$$

Multiplying the baseband signals with a carrier of frequency f_0 translates the eight-level signal's power spectral density up to f_0 . That is, the modulated signal's single sided power spectral density $G_{M8-L}(f)$ is given mathematically by

$$G_{M8-L}(f) = K \left[\frac{\sin 6\pi (f-f_0) T_b}{6\pi (f-f_0) T_b} \right] \quad (1.4.17)$$

The rectangular 64-APK signal is then the result of a linear addition of the two modulated signals of identical power spectral density but with the carrier frequency shifted relative to each other by 90° . It follows therefore that the spectral shape of the rectangular 64-APK signal will be identical

to that of its component signals. Thus, the power spectral density of the rectangular 64-APK signal as shown in Fig. 1.4.4 is given by

$$G_{64\text{-APK}}(f) = 252 A^2 T_b \left(\frac{\sin 6\pi(f-f_0) T_b}{6\pi(f-f_0) T_b} \right) \quad (1.4.18)$$

Defining P_s as the power of the 64-APK signal, then Eq. (1.4.18)

can be rewritten as

$$G_{64\text{-APK}}(f) = 6 P_s T_b \left(\frac{\sin 6\pi(f-f_0) T_b}{6\pi(f-f_0) T_b} \right) \quad (1.4.19)$$

Based on the Nyquist theorem, it is theoretically possible to transmit without intersymbol interference (ISI) and using a bandpass signal at RF, 1 symbol b/s/Hz. As each of the 64 symbols contains 6 bits of information this means that 64-state APK has a theoretically maximum spectral efficiency of 6 b/s/Hz.

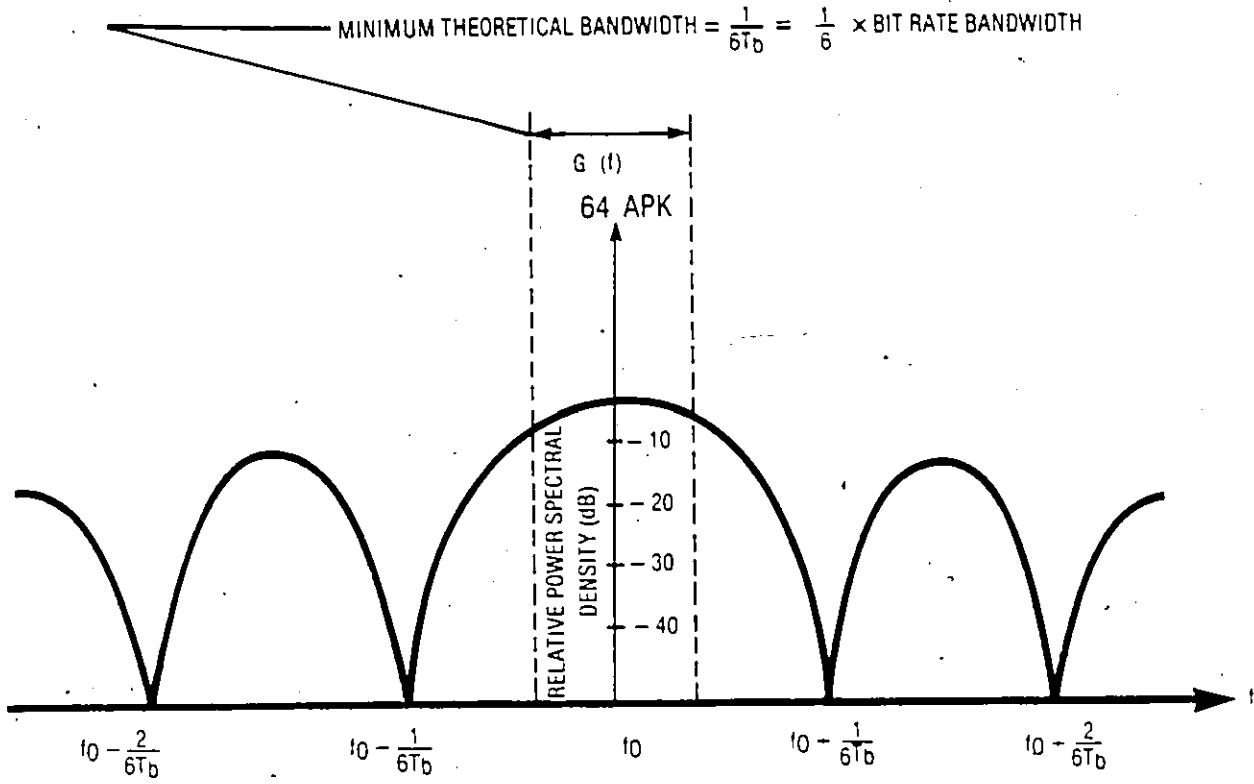
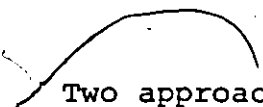


FIGURE 1.4.4 POWER SPECTRAL DENSITY OF 64 - STATE APK

1.5 A Comparison of 8-L QAM and NLA 64-state QAM



Two approaches to the implementation of rectangular 64-state APK, namely, Eight-Level QAM (8-L QAM) and Nonlinearly Amplified 64-state QAM (NLA 64-state QAM) are compared in this section. In order to avoid confusion in the differentiation of the two techniques 8-L QAM, which is in fact also 64-state QAM, will be referred to as 8-L QAM in this section. In this comparison, a brief description of the implementation of each of these schemes will be given followed by a discussion of the advantages and disadvantages associated with each scheme.

An 8-L QAM modem block diagram is given in Fig. 1.5.1. In the modulator, the incoming NRZ binary data is split into two NRZ streams labelled $I(t)$ and $Q(t)$ in a serial-to-parallel converter. Each new stream has a bit rate one-half that of the input signal's rate. The two-to-eight level converters code their incoming signals in groups of three bits to form an eight-level signal whose duration is thrice that of the incoming signal. In each of the balanced mixers, which function as analog multipliers, the signal modulates one of two carriers in quadrature. The modulated carriers are combined and band limited using a Band-Pass Filter (BPF) or premodulation Low-Pass Filter (LPF). Figure 1.5.1 depicts the QAM LPF implementation. At the output to the modulator the modulated signal is amplified and transmitted over the channel. At the demodulator input, the modulated signal is split into two parallel paths. Each mixer is

fed one of these two signals together with one of two coherent carriers in quadrature. The mixer's output signal is passed through a LPF to remove noise and interference as well as second-order and higher spectral products. The filtered signals are eight-to-two level converted and then recombined in a parallel-to-serial converter to form the recovered data.

NLA 64-state QAM employs a technique first suggested by Miyauchi et al. [4] for 16-state APK. This parallel modulation technique is extended to NLA 64-state Qam [5]. Although the techniques used in the generation of the 64-state signal differ significantly from those used in 8-L QAM, the same demodulation techniques apply to both schemes.

A block diagram of a NLA 64-state QAM modem is shown in Fig. 1.5.2. In the modulator, the NRZ data is serial-to-parallel converted into six NRZ streams labelled $I_1(t)$, $I_2(t)$, $I_3(t)$, $Q_1(t)$, $Q_2(t)$, and $Q_3(t)$. The rate of any one of the six streams is one-sixth that of the incoming bit rate. $I_1(t)$ and $Q_1(t)$ feed "QPSK modulator 1", $I_2(t)$ and $Q_2(t)$ feed "QPSK modulator 2", and $I_3(t)$ and $Q_3(t)$ feed "QPSK modulator 3". The other inputs to the modulators are two quadrature carrier signals. The outputs of the modulators are amplified using nonlinear amplifiers and combined. In order to form the rectangular 64-state APK signal, the transmit output power from the first QPSK modulator must be 6 dB above that of the second QPSK modulator and 12 dB above that of the third. One way to do this is to have the three amplifiers operate with equal output power and have two directional couplers with coupling coefficients of 0.2 (6.99 dB) and 0.238 (6.23 dB) respectively forming the combiner. Where the outputs of NLA2

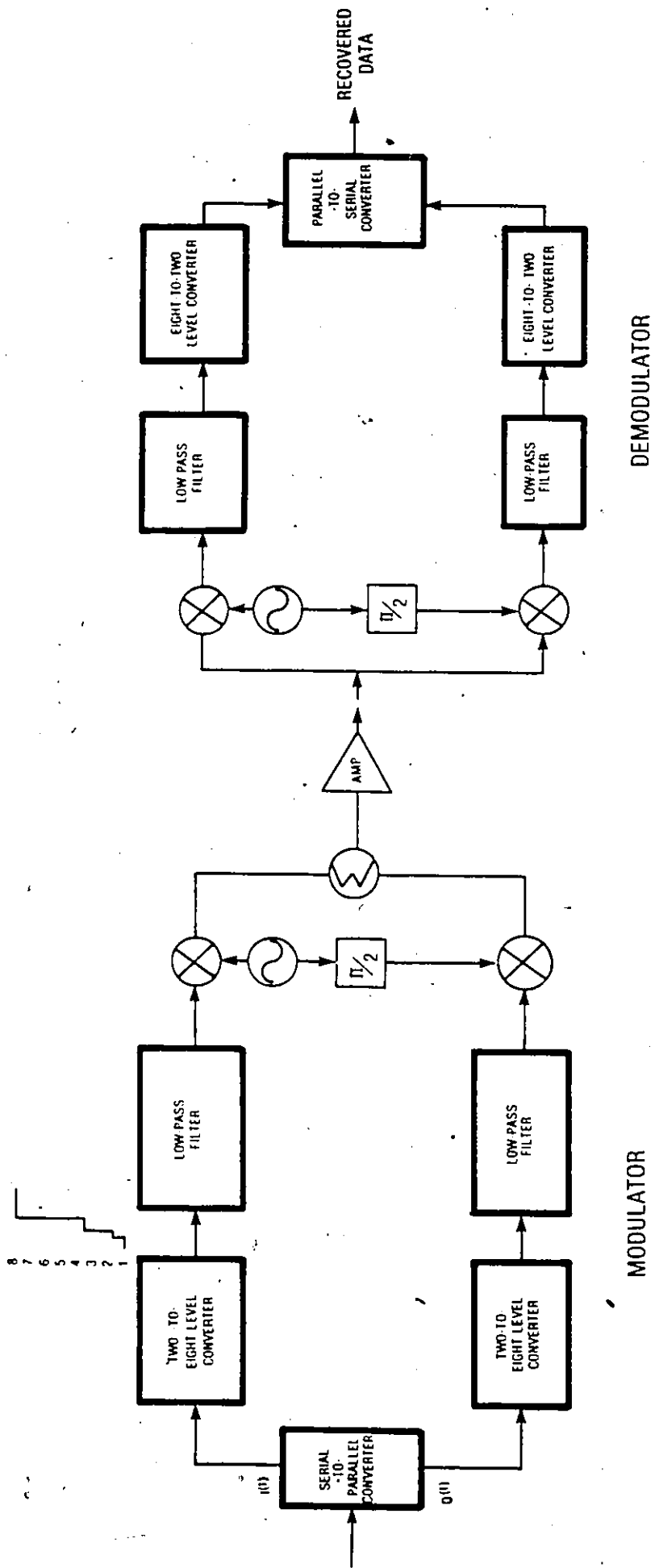


FIGURE 1.5.1 8-LEVEL QAM MODEM BLOCK DIAGRAM

and NLA3 are summed in the first hybrid which is summed with NLA1 in the second hybrid. The resulting 64-state rectangular APK signal is then filtered using an output bandpass filter to limit the transmitted signal's spectrum.

As previously stated, the NLA 64-state QAM demodulation process is identical to that used in 8-L QAM and for this reason it will not be repeated here. Many different demodulation techniques [4] , [6] could have been used in either of these multilevel schemes, however, the more conventional coherent QAM type demodulation scheme was selected for the modem implementations.

In comparing these two schemes, a few major differences become apparent. Using 8-L QAM one is constrained to employing linear transmitter power amplification. The input/output power characteristics of the power amplifier and the phase shift as a function of the input level (i.e. AM/AM conversion and AM/PM conversion) force this constraint. In order to avoid the degradation due to AM/AM and AM/PM conversion, it is necessary to operate the transmit amplifier with the average output power "backed-off" from saturation. This back-off is necessary in order for the signal to be amplified in a linear fashion. To minimize this back-off, predistortion is used to effectively linearize the power amplifier characteristics. Ideally, with perfect predistortion the amplifier would only need to be backed off enough to accommodate the peak-to-average power ratio which is 3.68 dB (see note at end of section). However, in practice, additional back-off is almost always required. Especially for multi-level schemes with their inherently high linearity

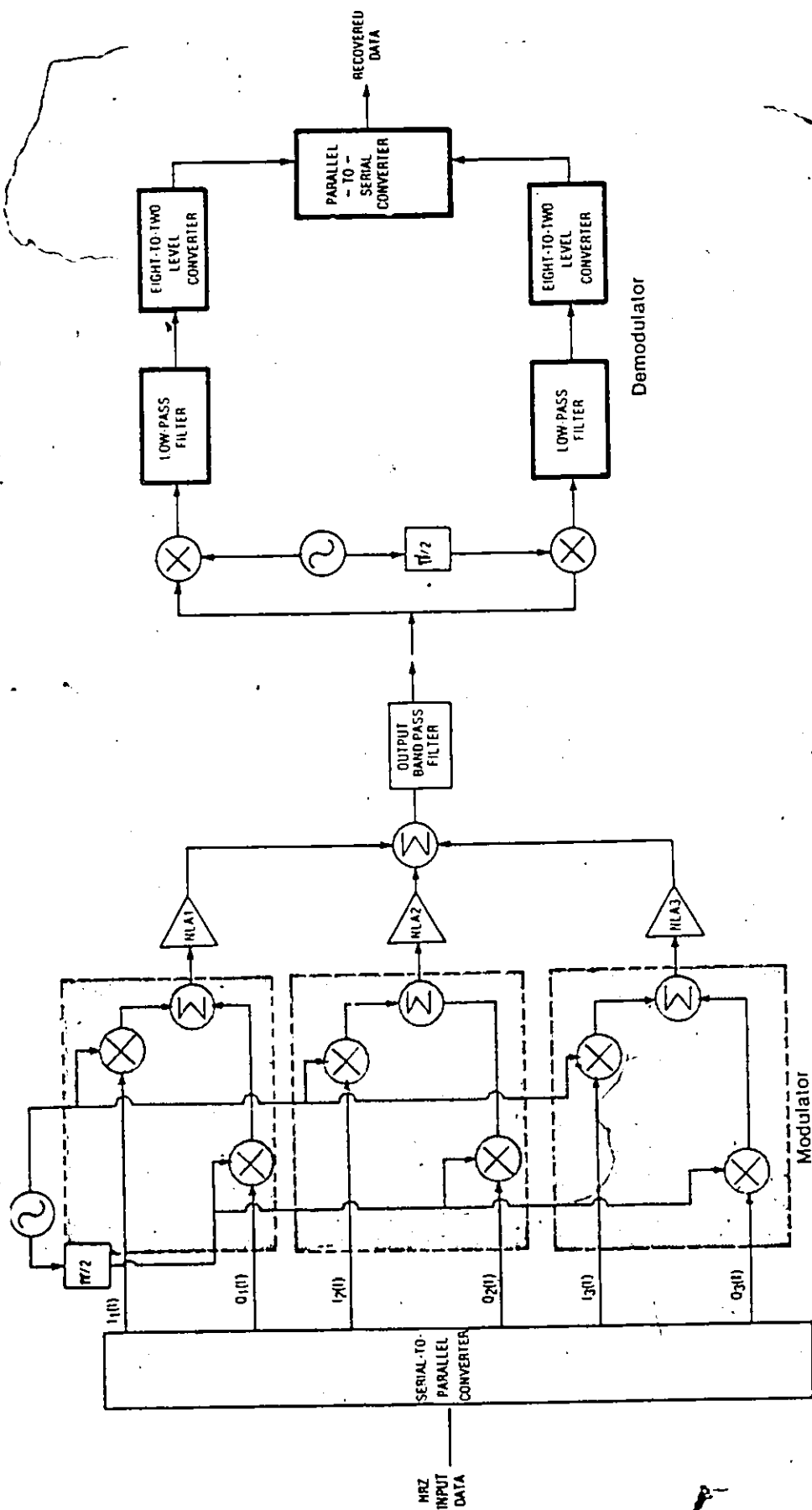


Figure 1.5.2 NLA 64-State QAM MODEM Block Diagram

requirements. NLÀ 64-state QAM, as its name implies, permits nonlinear transmit power amplification. The QPSK modulated signals are unfiltered prior to the nonlinear amplifiers, so they each contain only one power level, and as such, are unaffected by the AM/AM and AM/PM conversion characteristics of the nonlinear amplifiers. In fact this scheme removes the need for predistortion and can afford significantly more power at the modulator output as compared to that of 8-L QAM

To discuss this advantage a bit further, for the NLÀ 64-state modulator previously described, the peak power at the second hybrid's output is 3.68 dB greater than that available from any one of the amplifiers. Thus, the average power output of the modulator equals the peak power output of each amplifier which means that the highest average output power available from the modulator is the saturated output power of the amplifiers. As previously mentioned, the 8-L QAM scheme requires a theoretical minimum back-off of 3.68 dB even with perfect predistortion. A practical value of the back-off required for 8-L QAM has yet to be reported and for this reason is not given. It is however, safe to assume that this back-off would be larger than that required for 16-state QAM. The back-off required for a 16-state QAM system with no predistortion using a TWT amplifier and baseband filtering has been reported to be in the order of 8 dB [6]. For a system using predistortion techniques, a Ga As FET amplifier and baseband filtering a back-off of 5 dB was reported to be required [5].

Recalling that for NLA 64-state QAM, the maximum average output power of the modulator is the saturated output power of the amplifiers the power advantage of NLA 64-state QAM over 8-L QAM lies within one to two dB's of the practical value of the back-off required for 8-L QAM. The one to two dB's represents the loss due to RF filtering as opposed to baseband filtering [5]. We note that this gain in transmit power efficiency is at the expense of additional output power amplifiers. However, the output power rating and hence the cost of these amplifiers could be significantly lower than that of the amplifier used in the 8-L QAM scheme.

The design complexity of 8-L QAM is synonymous to that of NLA 64-state QAM. Although the block diagram of the latter might appear more complex than that of the former scheme, the novelty of 8-level modulation as compared to the commonly used quadrature modulation must be taken into account. Especially in terms of the design time of the new modulator and the training timing of the service personnel. In addition to this, the duplication of the paths in the parallel modulation scheme simplifies its design.

Another advantage to NLA 64-state QAM is that it also extends itself to other implementations. Using linear addition and a single linear transmit amplifier, the parallel modulation technique permits nonlinear modulation in the quadrature modulators. To explain a bit further, this permits the "hitting hard" of the mixers in a quadrature modulator which could significantly reduce the circuitry typically required. The scheme

also lends itself to implementations in which the modulation technique must be switchable. QAM and 16-state QAM are two of the possible modulation techniques which could be switched to.

The filtering in 8-L QAM can be either post-modulation bandpass filtering or premodulation low-pass filtering. Post-modulation bandpass filters are known to be difficult to design for systems which have a very low bit rate-to-carrier frequency ratio. As well, bandpass filters can not be used in modulators where the carrier frequency is varied. In such systems, the compatibility of their modulation technique with low-pass filtering is a necessity. NLA 64-state QAM is apparently constrained to using a post-modulation BPF, however, this is not necessarily the case. A baseband signal processing or filtering technique [7][8][9], which severely limits the nonlinearly amplified signal's transmit spectrum, can replace the bandpass filtering in the modulator. An example of such a scheme: Intersymbol Interference and Jitter Free Filtering (IJF) is presently under research in the Digital Communication Group at the University of Ottawa."

As a result of the above comparison, it was felt that the advantages of nonlinear amplification warranted further investigation of NLA 64-state QAM as a viable modulation technique. In the succeeding chapters a detailed examination of NLA 64-state QAM and its properties is undertaken.

Note: The peak-to-average power ratio figure falls from the derivations in section 1.4. Referring to Fig. 1.4.2, the peak power is $98 A^2$ when $2A$ is the voltage difference between two adjacent signal states. From Eq. 1.4.8, $42 A^2$ is the average power. Thus the peak-to-average power ratio is approximately 2.3 or 3.68 dB

CHAPTER 2

CHAPTER 2

2.1 Introduction

The baseband prototype modem developed for this research is only an illustrative, scaled down example of a microwave modem. Such an approach obviates the need for expensive RF devices and equipment. However, conclusions may be drawn which, once extrapolated, apply to practical 64-state QAM microwave systems.

The experimental modem has the following design parameters:

- o modulation technique = 64-state QAM/NLA 64-state QAM
- o bit rate = 384 kb/s
- o carrier frequency = 1 MHz
- o symbol rate = 64 kbaud.

The modem is divided in two separate units namely the modulator and the demodulator. The design of each unit is described briefly below. Appendix A provides a more detailed technical examination of each unit's design.

2.2 The Modulator

A block diagram of the modulator which was implemented for this research is shown in Fig. 2.2.1. It should be noted that this figure differs from the block diagram of NLA 64-state QAM modulator depicted in Fig. 1.5.2 with the inclusion of predistortion equalizers, premodulation low-pass filters, linear amplifiers, and the exclusion of a post-modulation bandpass filter.

This modulator has two switchable modes of operation. One being 64-state QAM with equalizers, low-pass filters and linear amplifiers. The second being NLA 64-state QAM where hardlimiters prior to linear amplifiers represent the nonlinear amplifiers. In this realization, the only filtering is done by post-detection low-pass filters.

The post-modulation bandpass filter was excluded from this modem because of the nonlinear amplification followed by bandpass filtering is essentially equivalent to that of premodulation low-pass filtering.

Predistortion equalizers were incorporated to improve the amplitude and phase response of the channel. This improvement is discussed further in Section 2.2.2.

Hardlimiters are used to practically simulate the nonlinearities resulting from nonlinear amplification. These hardlimiters produce a constant output envelope without changing the phase of the unfiltered modulated signal. These characteristics

closely approximate those of the Gunn and Impatt injection locked amplifiers.

To compare the P_e performance of the modem to the theoretical 64-state QAM P_e performance; predistortion equalizers, low-pass filters and linear amplifiers are included in the modem. The results from this comparison are discussed further in Chapter 5.

A description of each of the blocks, shown in Fig. 2.2.1 follows.

2.2.1 Serial-to-Parallel Converter

The serial-to-parallel converter accepts a 384 kb/s serial data stream and converts it into six parallel 64 kb/s binary data streams. Because this laboratory prototype modem is operating without symbol timing recovery subsystems, a 64 kHz clock is generated from the hardwired 384 kHz master clock. This provides the clock for both the modulator and the demodulator.

2.2.2 Predistortion Equalizer

Predistortion equalizers are devices used to improve the amplitude and phase response of a channel. In this discussion the channel includes the premodulation and post-detection low-pass filters. To explain the equalization process a little bit further, a bandlimited channel whose amplitude and phase

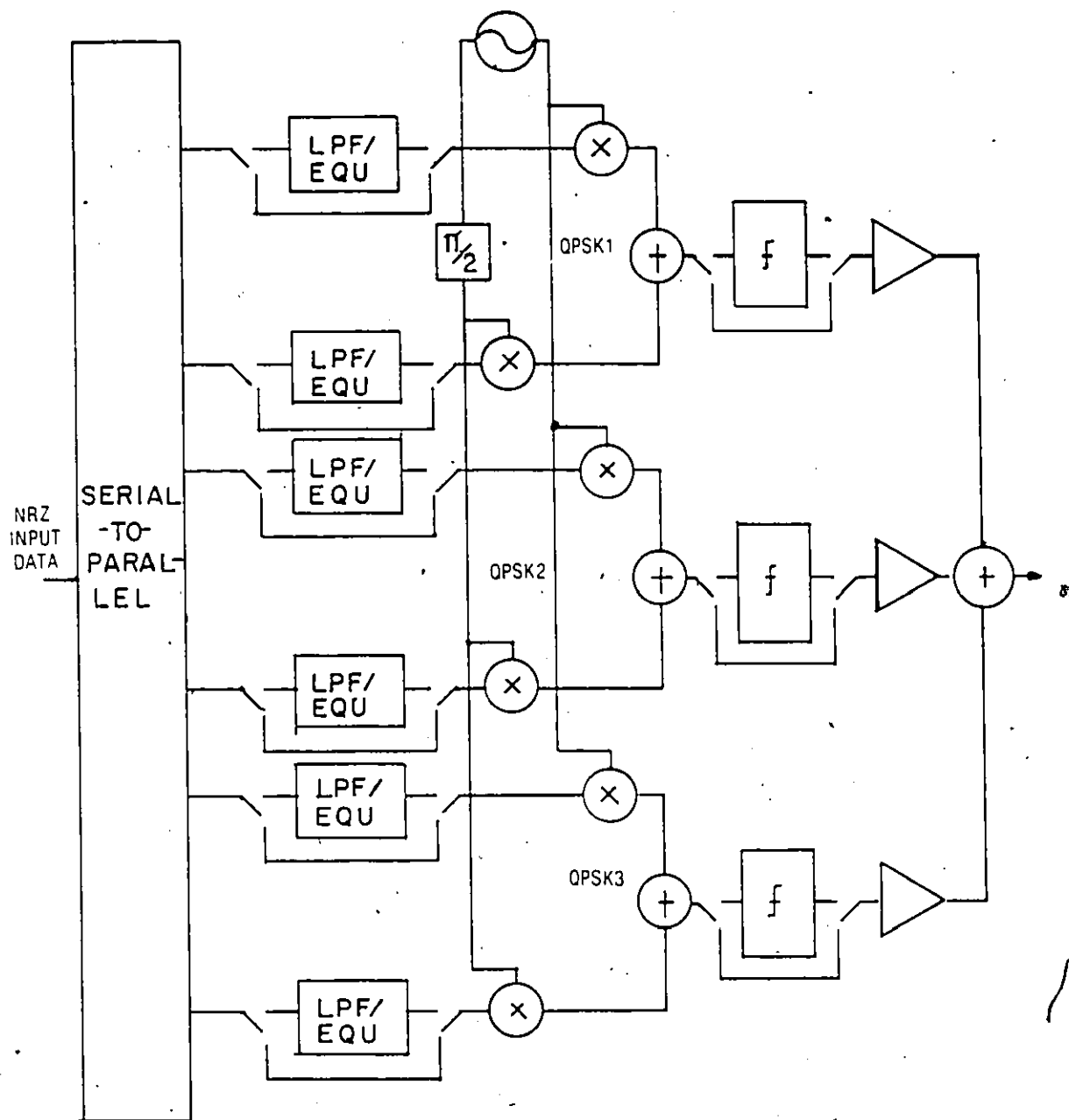


Figure 2.2.1 NLA 64-State QAM Modulator Block Diagram

characteristics are not ideal, distorts the received pulse and causes intersymbol interference (ISI). Although a complete definition of ideal channel characteristics is not given herein, one example of an ideal bandlimited channel is described. A brick-wall channel, with a cut-off frequency equal to the Nyquist frequency, ideally has linear phase and flat amplitude characteristics for an impulse input or an $x/\sin x$ amplitude correction for NRZ type pulses. When data is transmitted over a nonideal channel, it is often necessary to apply corrective means or equalization to keep the pulse distortion within reasonable limits.

The equalizers are realized using a method suggested by Bennet and Davey [10]. This method predistorts the data in such a way that the pulses have the desired shape at the output to the post-detection low-pass filter. The desired pulse shape corresponds to a maximization of the eye opening at the sampling instant and hence a minimization of ISI.

Figure 2.2.2 shows a block diagram of a predistortion equalizer. The advantage to this method is in its use of a shift register. Analog tapped delay lines are typically much more difficult to implement than are shift registers. Each shift register stage consists of a flip-flop with a potentiometer connected across the outputs to provide adjustment to the amplitude and polarity of its contribution. The summation of the contributions from each stage constitutes the predistorted

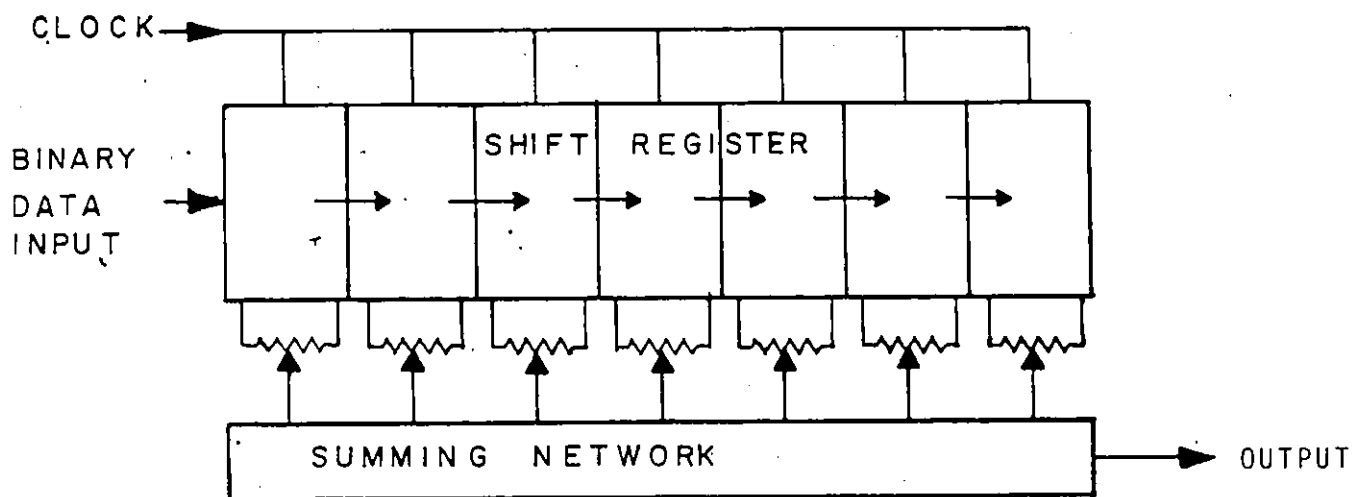


FIGURE 2.2.2 BLOCK DIAGRAM OF A PREDISTORTION EQUALIZER

data conditioned for transmission through the channel.

Figures 2.2.3 (a) and (b) show the unequalized and equalized pulse responses of the channel after the post-detection low-pass filter. The duration of the pulse at the input to the channel is $T_s = 15.6$ us and the sampling instant occurs at multiples of T_s (i.e. the rising edge of the sampling clock). We note that in Fig. 2.2.3 (a) the unequalized pulse response is not $x/\sin x$ in shape and that there is ISI present at the sampling instants. The tap coefficients of the equalizer are set to minimize ISI and force zero crossing of the pulse response at the sampling instants. The ISI is significantly reduced as seen in Fig. 2.2.3 (b) [11]

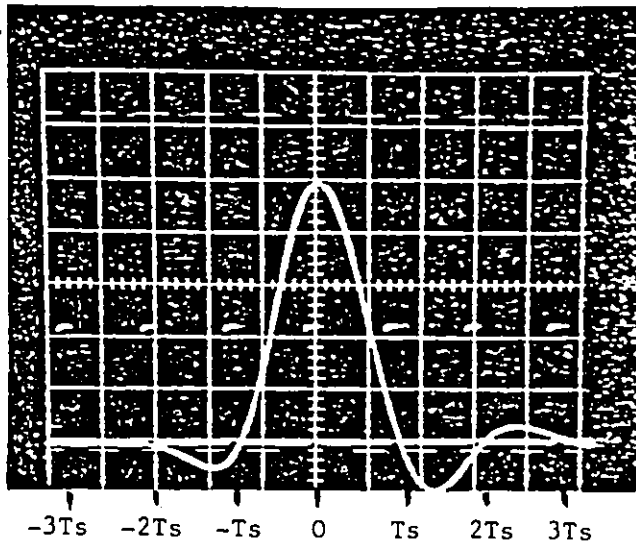
2.2.3 Low-Pass Filter

The low pass filters provide the spectral shaping of the transmitted signal. The filters are active, four pole Butterworth filters whose 3 dB frequency is 34 kHz. Butterworth type filters were chosen because of their flat response in the pass band.

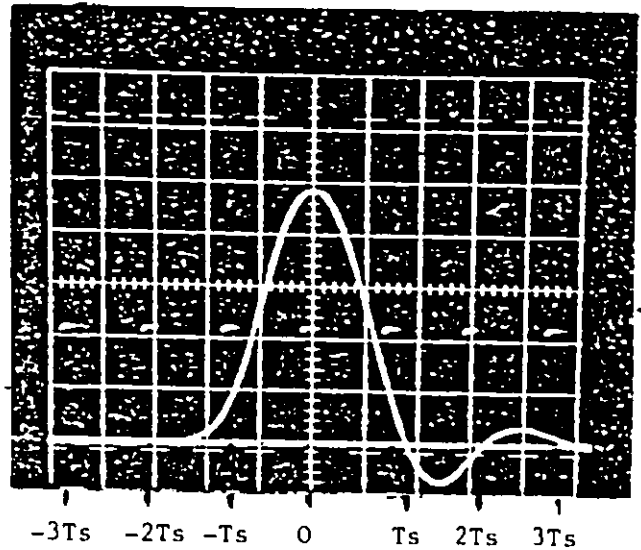
The fourth-order filter's transfer function, $A_v(s)$, can be written as [12]:

$$A_v(s) = k/(s^{**2} + 0.7654 + 1)(s^{**2} + 1.8478s + 1) \quad (2.2.1)$$

To further improve the filter's attenuation properties, an additional RC pole was added to the filter resulting in a modified fifth-order Butterworth filter. The amplitude response



(a)



(b)

FIGURE 2.2.3 PHOTOGRAPH OF MEASURED
(a) UNEQUALIZED RECEIVE PULSE RESPONSE
(b) EQUALIZED RECEIVE PULSE RESPONSE

(Photograph courtesy of D. Prendergast)

of the low-pass filter, as obtained from laboratory measurements is shown in Fig. 2.2.4. The Response shows a roll-off of 30 dB per octave and an attenuation of 3 dB at 34 kHz.

2.2.4 Quadrature Modulator

The quadrature modulator accepts two bits of data and transmits a carrier phase at 1 MHz which is a function of the two bits. A simplified block diagram is shown in Fig. 2.2.5. The 1 MHz carrier signal follows path "a" to the input of a double balanced mixer. Depending upon the polarity of the modulating data signal, the output from the mixer will either be in-phase or 180 degrees out of phase with the input signal. The carrier signal simultaneously follows path "b" through a 90 degree phase shifter to the input of the second double balance mixer. This path functions identically to path "a" except that the 90 degree phase shift causes the output signal of path "b" to be orthogonal to that of path "a". Thus, a summing of the signals from the two paths produces a QPSK modulated signal. The effect of a phase transition on the envelope of a QPSK modulated signal is shown in Fig. 2.2.6.

2.2.5 Hardlimiter

To provide the simulation of a nonlinearity, hardlimiters are included in the signal paths. By passing each of the quadrature modulated signals through a hardlimiter prior to their combining, nonlinearly amplified signals are

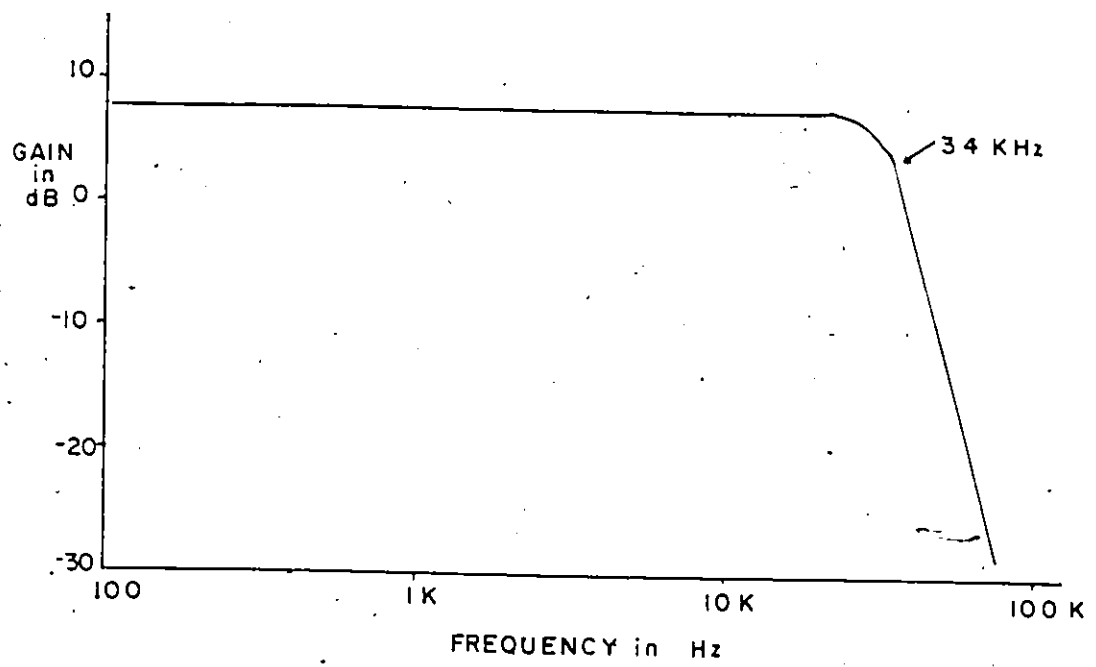


FIGURE 2.2.4 AMPLITUDE RESPONSE OF MODIFIED FIFTH-ORDER BUTTERWORTH LOWPASS FILTER

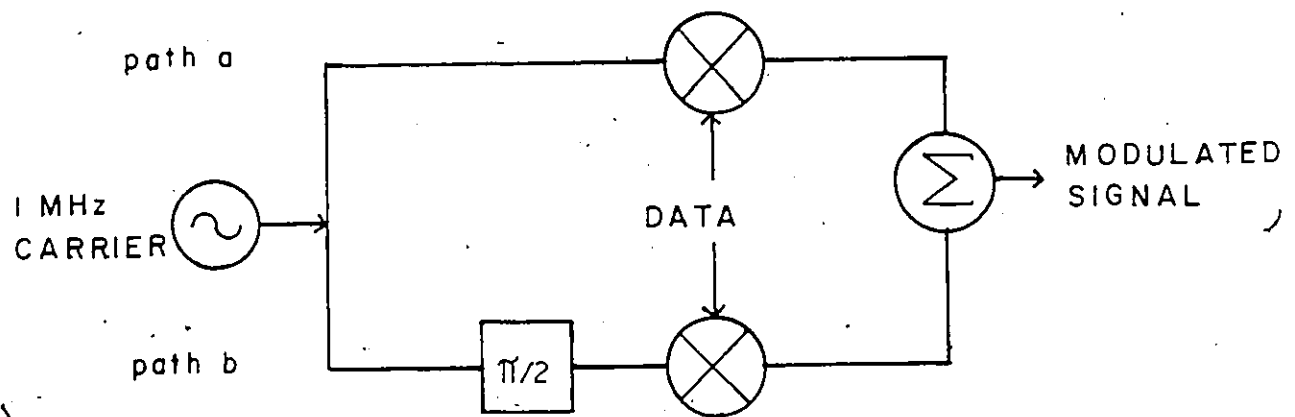
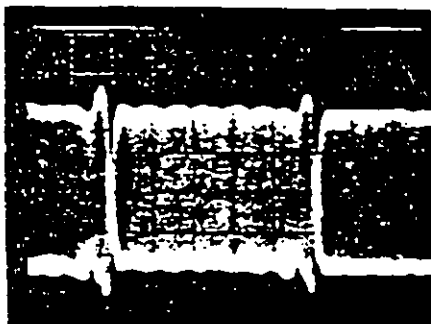
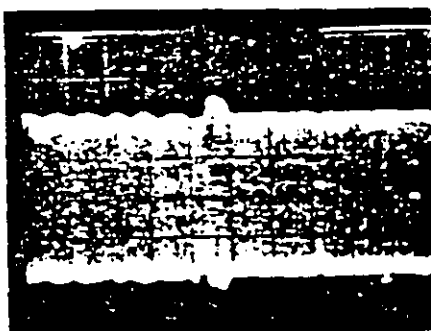


FIGURE 2.2.5 A BLOCK DIAGRAM OF A QPSK MODULATOR



180° TRANSITIONS
5 us/div



90° TRANSITIONS
5 us/div

FIGURE 2.2.6 QUADRATURE MODULATED CARRIER WAVEFORMS

emulated. The hardlimiters, modelling an ideal hardlimiter, produce a signal which has a constant envelope. For an unfiltered QPSK signal, the inclusion of a hardlimiter in the signal path does not affect its integrity.

2.2.6 Combiner

The combiner used in our laboratory prototype, amplifies and linearly sums the three QPSK modulated signals in a weighted manner to form the 64-state QAM signal. The output power from the combiner for the second and third modulator signals are 6 dB and 12 dB lower than that of the first, as previously explained. In the prototype, this combiner functionally performs as the amplifiers and combiner shown in Fig. 2.2.1. Because the laboratory prototype modem has no requirement to meet typical transmit output power requirements, no RF output power amplifiers or directional couplers were used in the combiner design.

2.3 The Demodulator

A block diagram of the demodulator which was implemented for this research is shown in Fig. 2.3.1. The demodulator can be divided into the following functional categories:

- 1) quadrature demodulator
- 2) eight-to-two level converter
- 3) parallel-to-serial converter

A description of each of these subassemblies follows.

2.3.1 Quadrature Demodulator

Since the 64-state QAM signal was generated using quadrature modulators the process must be reversed in the demodulator in order to obtain the original data. A block diagram of the prototype quadrature demodulator is shown in Figure 2.3.2.

Two balanced mixers are driven in parallel by the modulated signal. A hardwired replica of the modulator's carrier signal is used to demodulate the signal in one mixer, while the other mixer uses the same signal shifted in phase by 90 degrees. Individual phase shifters are built into the demodulating carrier legs of each mixer in order to accurately adjust the phase of demodulating signal to that of the incoming modulated signal. To complete the quadrature demodulation the output

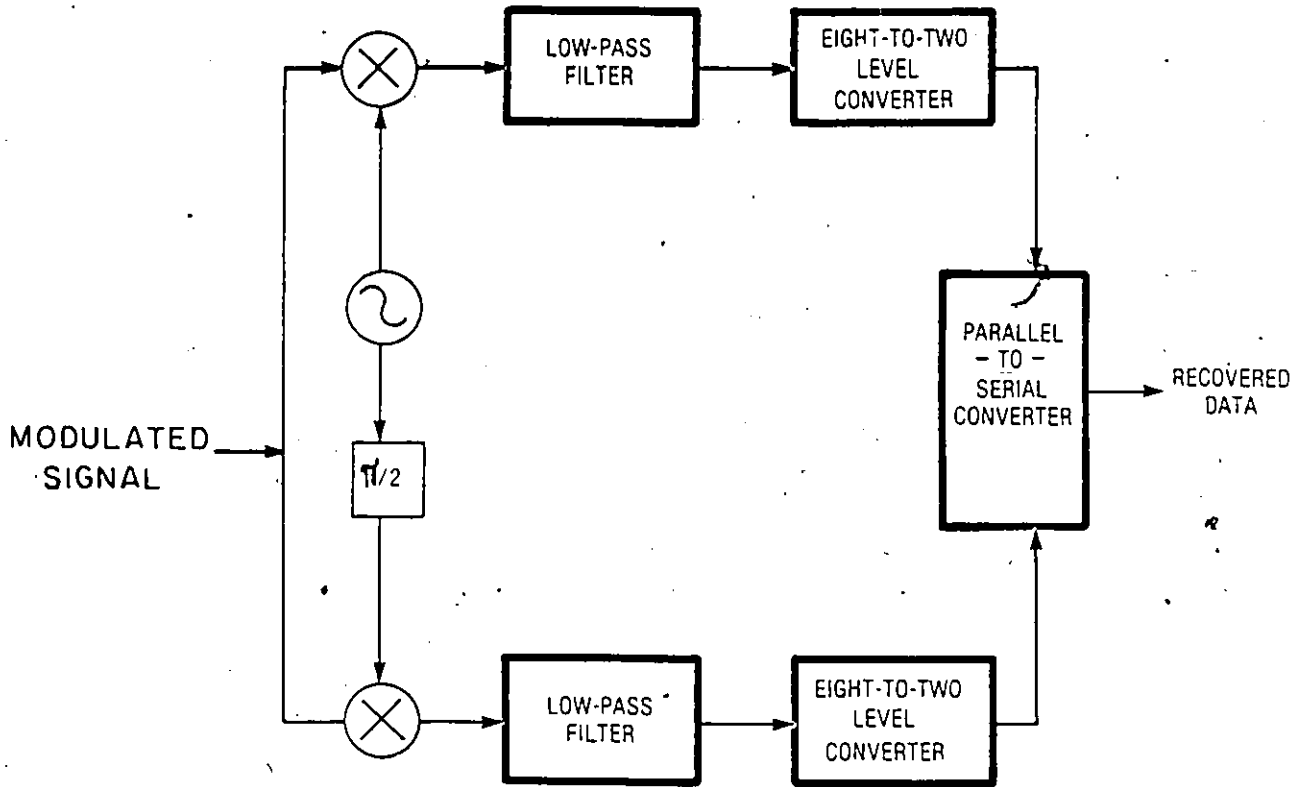


Figure 2.3.1 NLA 64-State QAM Demodulator Block Diagram

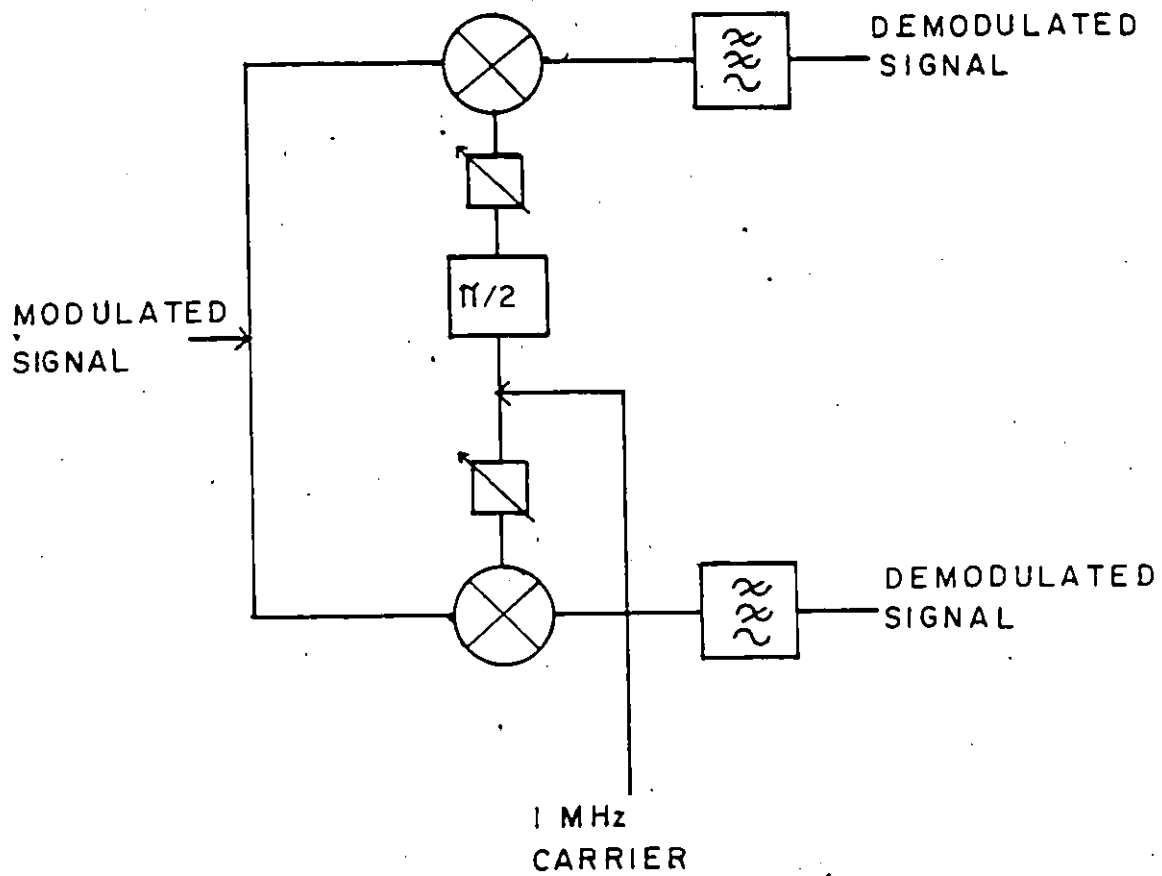


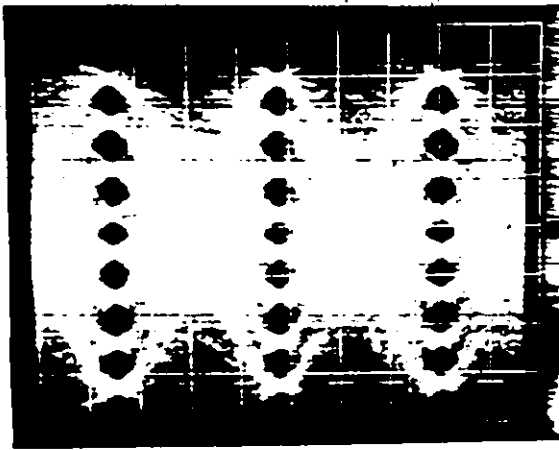
FIGURE 2.3.2 BLOCK DIAGRAM OF A QUADRATURE DEMODULATOR

from the mixers must be low-pass filtered to remove the second harmonic component. The post-detection low-pass filters used were the same as the modulator's premodulation modified fifth-order Butterworth filters. For this reason, a description of these filters will not be repeated herein but the reader can refer to Section 2.2.3 for review.

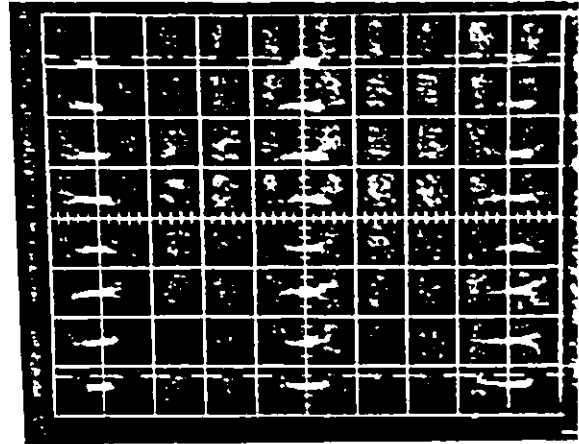
Figure 2.3.3 (a) and (b) show oscilloscope wave forms of the quadrature demodulated signal (the eye diagram). In Fig. 2.3.3 (a) the eyes are distorted, the phase of the demodulating carriers was not matched to that of the incoming modulated signal. Figure 2.3.3 (b) shows the eye diagram when the phase is adjusted correctly. In this case the eyes are open and clear. Figure 2.3.4 shows a signal space diagram at the quadrature demodulator output. This experimentally measured diagram illustrates a 64-state QAM state space as described earlier in Chapter 1. The amplitude levels are equally spaced and symmetrical, forming the rectangular pattern of 64-state QAM.

2.3.2 Eight-to-Two Level Converter

The eight-to-two level converters take the multilevel demodulated signals and convert each into three binary signals. In order to do this, each demodulated signal is sampled at the symbol rate in the center of the eyes. Each sampled signal level is then converted into three binary bits of data. A table relating the sampled signal level to the resultant binary data

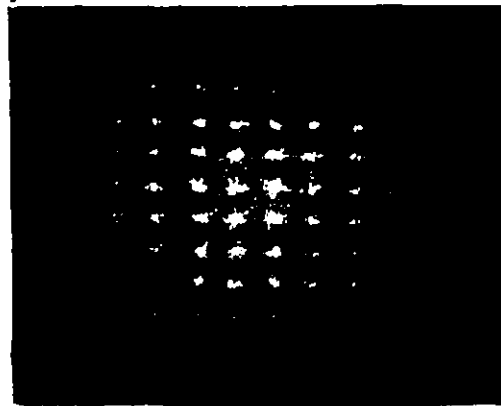


(a) 5 us/ div
8V/ div



(b) 4 us/ div
8V/ div

FIGURE 2.3.3 EYE DIAGRAMS AT THE POST DETECTION LOW-PASS FILTER OUTPUT a) WHEN PHASE OF DEMODULATING CARRIER IS NOT MATCHED TO THAT OF INCOMING MODULATED SIGNAL; b) WHEN PHASE OF DEMODULATING CARRIER IS MATCHED TO THAT OF INCOMING MODULATED SIGNAL.



2V/ div

FIGURE 2.3.4 SIGNAL SPACE DIAGRAM AT THE POST DETECTION LOW-PASS FILTER OUTPUT
(No trigger)

is shown in Table 2.1.1.

Sampled Signal (v)	I1 Logic State	I2 Logic State	I3 Logic State
-2.5	0	0	0
-1.78	0	0	1
-1.07	0	1	0
-0.35	0	1	1
0.35	1	0	0
1.07	1	0	1
1.78	1	1	0
2.5	1	1	1

Table 2.1.1 Performance of eight-to-two level converter

From this table we see, for example, that a sampled signal level of 1.07 volts corresponds to the logic states "1", "0", "1" for I1, I2, and I3 respectively.

2.3.3 Parallel-to-Serial Converter

The parallel-to-serial subassembly converts six binary signals into one binary signal representing the recovered signal. The data rate of the incoming signals is 1/6 that of the outgoing signal (i.e. 64 kb/s versus 384 kb/s). In order to recover the original transmitted data stream, the six data streams must be multiplexed so as to reverse the process of the serial-to-parallel converter of section 2.2.1. This is easily accomplished by sequencing the selection of each of the six streams in the proper order.

CHAPTER 3

CHAPTER 3

3.1 Introduction

Computer simulation provides a practical and powerful alternative to theoretical analysis or laboratory implementation when either or both of these techniques becomes extremely difficult or in some cases impossible to achieve. Systems involving a nonlinear or a frequency selective fading environment, or adjacent channel interference, often fall into this category. Computer simulation programs have been developed for this thesis to aid in the performance analysis of various 64-state QAM systems. These systems include NLA 64-state QAM, 64-state QAM with modulator impairments, 64-state QAM with transmission channel distortions, and 64-state QAM with cochannel and adjacent channel interference.

In general, the basics of the program follow those given in the Digital Communications Laboratory (DCL) Report No. 112 [13]. However, several essential modifications have been incorporated into the programs to replace the QPSK modulation, used by the DCL, with 64-state QAM. The most significant of these include: the replacement of the QPSK signal with a 64-state QAM signal in the signal generator and the replacement of the P_e calculation for QPSK with the P_e calculation for 64-state QAM in the detector.

3.2 Simulation Model

The simulation modelling used in the programs is based on the equivalent baseband concept. To explain this a bit further, in the development of a mathematical model to simulate the various systems under study, the transmitted signal $s(t)$ can be assumed to be of the form:

$$\begin{aligned} s(t) &= \operatorname{Re} [(x(t) + j y(t)) e^{jW_c t}] \\ &= x(t) \cos W_c t - y(t) \sin W_c t \end{aligned} \quad (3.2.1) \text{ where}$$

W_c is the angular carrier frequency and $x(t) + j y(t)$ is the complex baseband signal. From Eq. 3.2.1, it is seen that the digital formulation to be transmitted is contained in the complex baseband signal $x(t) + j y(t)$. Thus, the system to be studied may be modelled by specifying it in terms of its complex baseband form.

A block diagram of the 64-state QAM systems simulated is shown in Fig. 3.2.1. In the data source of the transmitter, a generator polynomial is used to produce a pseudo-random sequence of NRZ symbols of fixed length and period. In order to limit the computer memory size required by the program, five cyclically shifted versions of the original sequence are generated to give the six data streams needed to create a 64-state QAM signal.

Two methods are used to produce the two eight-level symbol streams. In the first, the two sets of three data

streams are each two-to-eight level converted to form the two eight-level symbol streams. These two symbol streams, with a set number of samples representing each symbol, form the complex data. The data's real part corresponds to the I component and the imaginary part corresponds to the Q component. This first method was adopted because it minimizes the required computer memory size. It is used in the simulation of 64-state QAM systems with transmission impairments and with adjacent channel interference.

The second method, which is depicted in Fig. 3.2.1, takes two of the six data streams to form each of the three QPSK signals. As in the previous method, the QPSK signals are represented as complex data with a set number of samples per symbol. These three signals are weighted and summed to form the two eight-level symbol streams of 64-state QAM. This latter method is used in the simulation of NLA 64-state QAM where the nonlinear devices are placed prior to the weighted summer. The effects of improper combining of the QPSK signals in the modulator are simulated using this method, by varying the weighting of any one of the signals in the weighted summer.

The transmit and receive filters are modelled in the equivalent low-pass complex formats, congruous with the format representing the modulated baseband signals in the frequency domain. The filters are raised cosine with or without $x/\sin x$ equalization. The filtering is effected by using Fast Fourier Transform (FFT) techniques. The complex baseband data is transformed into the frequency domain where it is multiplied

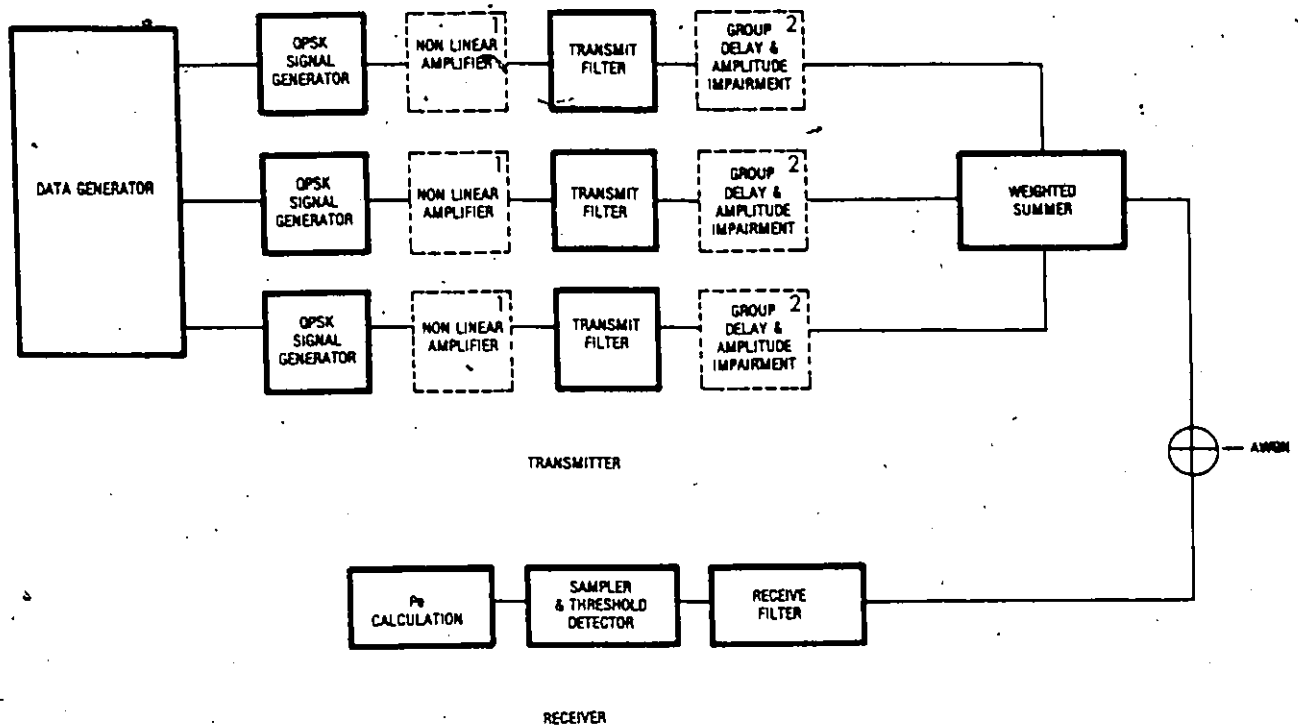


FIGURE 3.2.1 COMPUTER SIMULATION MODEL

- Note:
1. For the simulation of NLA 64-state QAM.
 2. For the simulation of hardware and/or radio propagation impairments including selective fading.

by the complex low-pass transfer function of the filter under consideration. The product of this multiplication is then transformed back to the time domain whereupon the filtering process is completed. In addition, channels with amplitude and group delay characteristics of almost any form (from flat to parabolic to sinusoidal) can be specified. Selectively fading channels are also modelled.

The nonlinear devices which are modelled include a hardlimiter and a high power amplifier (HPA). The modelling of the high power amplifier uses information on the input/output backoff relationship, with mean power normalization, which makes the scheme independent of absolute saturated power. These nonlinear routines are used when the maximum output power is desired (i.e. NLA 64-state QAM), however, when the digital system is to operate in a linear mode, none of these routines is incorporated into the program.

In the receiver, the detector takes the form of a sampler and threshold detector. At the input to the sampler, the incoming received data is synchronized to compensate for the delay and phase shift caused by the filters and nonlinearities. This "synchronized" data is then sampled at the point representing the maximum eye opening. The program calculates the symbol P_e for a number of values of E_b/N_0 and then prints and/or plots this information.

When adjacent channel simulation is desired, the generation of the main channel signal remains the same as was discussed in the preceding paragraphs. Two adjacent channel signals are added to the main channel signal at the output to the transmitter. These two signals are generated in the same manner as the main channel signal, however, they are assumed to have a carrier offset, time and phase shift, and attenuation/amplification with respect to the main channel [13].

3.3 Probability of Error Calculations

In this section the method of calculating the symbol P_e versus E_b/N_0 performance for the simulation of various 64-state QAM systems is described. The P_e performance is in fact, one of the most critical performance parameters of a digital communication system.

In the calculation of error performance, one essential feature is the inclusion of the combined effects of intersymbol interference and noise. Intersymbol interference tends to be data dependent so the modulated data sequences must contain all possible data transitions. The number of such transitions must be balanced so that all data transitions are given equal weight in the determination of P_e performance. Pseudo-random sequences of length $2^{11}-1$ (2047) were used to generate the modulated data.

As previously mentioned, in the demodulator a synchronization routine is used to compensate for the delay caused by the filters, and the phase shift caused by the non linearities. The received signal is shifted to the right until at least one of the samples for each symbol is in the correct decision region. If the impairment introduced into the system is severe enough to cause the entire symbol to be in error the P_e is not calculated and the run is terminated. Once the received data has

been "synchronized" the optimum sampling instant is chosen by calculating the P_e , for a given E_b/N_o , for each of the sampling points representing the symbols until the minimum P_e is obtained. this set of points is then used as the sampling instant for the run.

The detector "demodulates" the complex received data into its two quadrature component parts (in-phase and quadrature) as shown in Fig. 3.3.1. For each component part the detector calculates the probability that the sampled signal vector will not remain within the correct decision region for a specified value of N_o . Once the P_e 's for the selected range of N_o and hence E_b/N_o values are obtained for each symbol, the routine averages them over the entire symbol sequence, for each value of E_b/N_o , to determine the probability of symbol error performance of the system.

Specifically, for a given value of N_o , the symbol P_e for the system is given by

$$P_e = \frac{1}{NS} \sum_{i=1}^{NS} P_{e_i} \quad (3.3.1)$$

where NS is the total number of symbols including both I and Q components and P_{e_i} is the P_e for the i^{th} symbol. If the i^{th} transmitted symbol is an endpoint P_{e_i} is given by,

$$P_{e_i} = \frac{1}{2} \text{erfc} \left(\frac{\bar{S}_i - \text{THR}_{1i}}{\sqrt{2 N_o BW}} \right) \quad (3.3.2a)$$

and, if not an endpoint, by

$$P_{e_i} = \frac{1}{2} \text{erfc} \left(\frac{\bar{S}_i - \text{THR}_{1i}}{\sqrt{2 N_o BW}} \right) + \frac{1}{2} \text{erfc} \left(\frac{\text{THR}_{2i} - \bar{S}_i}{\sqrt{2 N_o BW}} \right) \quad (3.3.2b)$$

where,

\bar{S}_i is the magnitude of the i^{th} symbol sample,

$\text{erfc}(x)$ is the complementary error function ($= \frac{2}{\pi} \int_x^\infty e^{-a^2} da$),

$2A$ is the distance between the unfiltered adjacent transmit symbol voltage levels,

THR1_i is the magnitude of the i^{th} unfiltered transmit symbol voltage level minus A (lower threshold level),

THR2_i is the magnitude of the i^{th} unfiltered transmit symbol voltage level plus A (upper threshold level),

BW is the normalized system bandwidth

and

N_0 is the additive white gaussian noise power in a 1 Hz bandwidth

Note that the term "endpoint" refers to those I or Q symbols for which the transmit symbol was $\pm 7A$. These endpoints are shown in Fig. 3.3.1.

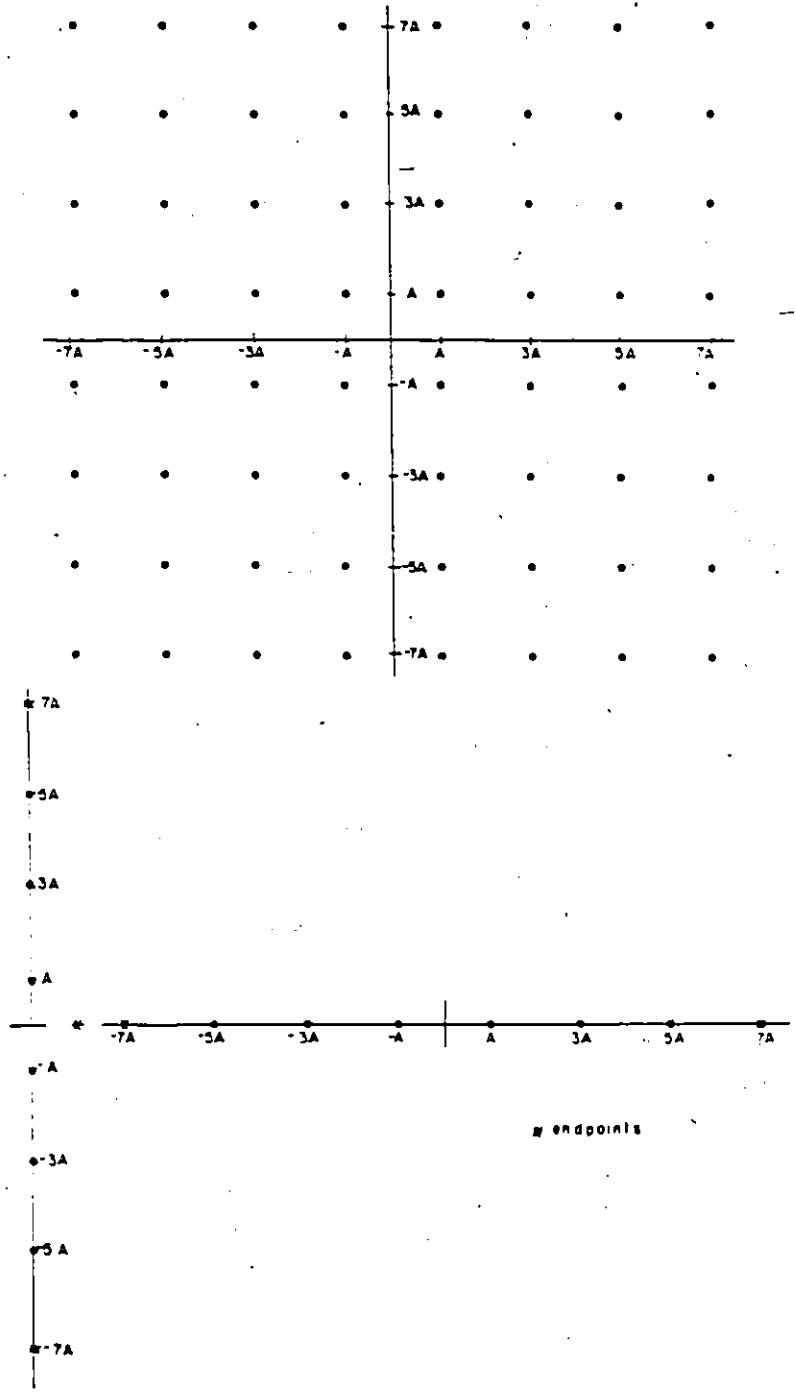


FIGURE 3.3.1 64-STATE QAM COMPOSITE STATE SPACE

CHAPTER 4

CHAPTER 4.

4.1 Introduction

The P_e performance of 64-state QAM has, up to this point, been limited to an evaluation of the performance in an environment with AWGN and ideal channel characteristics. Unfortunately, transmission systems do not operate in such an acme of perfection. For this reason, before a modulation technique can be considered viable its sensitivity to commonly encountered transmission impairments must be evaluated.

Prior to this study, the performance of 64-state QAM systems in environments with complex interference and transmission impairments had not been reported in the readily available literature. The objective of this chapter is to evaluate the P_e performance of 64-state QAM systems with some of the commonly encountered transmission and hardware impairments. The impairments or distortions included in this study are:

- 1) Interference
- 2) Anomalous signal levels in the state space
- 3) Channel amplitude distortions
- 4) Channel group delay distortions
- 5) Selective fading.

Computer simulated results are presented based on the simulation model described in Chapter 3 and Appendix B.

The system modelled in the computer analyses is a 90 Mb/s radio system with $\alpha = 0.4$ square root of raised cosine transmit and receive filters with $x/\sin x$ equalization, and a 20 MHz channel spacing [13]. The 90 Mb/s and 20 MHz are used as examples of a practical bit rate and channel spacing. However, with the appropriate considerations the succeeding results could be applied to other 64-state QAM systems.

4.2 Interference

The performance of a digital transmission system can be degraded by undue sensitivity to the effects of either cochannel or adjacent channel interference. Cochannel interference, present at the RF input of a receiver, has by definition the same (or nearly the same) nominal radio frequency as that of the desired channel. On the other hand, adjacent channel interference has a nominal frequency difference, with respect to the desired channel frequency, equal to one channel spacing. In part, the sensitivity of a system to interference can be attributed to the susceptibility of its modulation technique. Other factors such as the system's polarization isolation, filtering, and transmitted spectrum control can also contribute to the system's sensitivity to interference.

The P_e performance of a 90 Mb/s 64-state QAM system with either cochannel or adjacent channel interference is discussed in this section. In either case, the interferer is a single 64-state QAM signal which is uncorrelated with the desired signal.

Figure 4.2.1 depicts the P_e performance of 64-state QAM resulting from varying amounts of cochannel interference. In this case the interference is from a single cochannel interferer. For a carrier-to-interference ratio (CIR) of 27.8 dB, at the receiver filter's output, the E_b/N_0 requirement for a P_e of 10^{-4}

is 20.1 dB. This represents an increase in the E_b/N_0 requirement of approximately 2.6 dB.

The P_e performance resulting from varying amounts of adjacent channel interference is shown in Fig. 4.2.2. The system simulated uses raised cosine filtering with 3 dB bandwidth of 15 MHz, an alpha of 0.4, and a channel spacing of 20 MHz. As shown in Fig. 4.2.2, in the presence of a single adjacent channel interferer with a level 18.0 dB above the desired receiver level at the receive filter input, an E_b/N_0 of 18.2 dB is required for a P_e of 10^{-4} . Thus, a degradation to the performance of 64-state QAM of approximately 0.1 dB is incurred with an adjacent channel CIR of -18.0 dB.

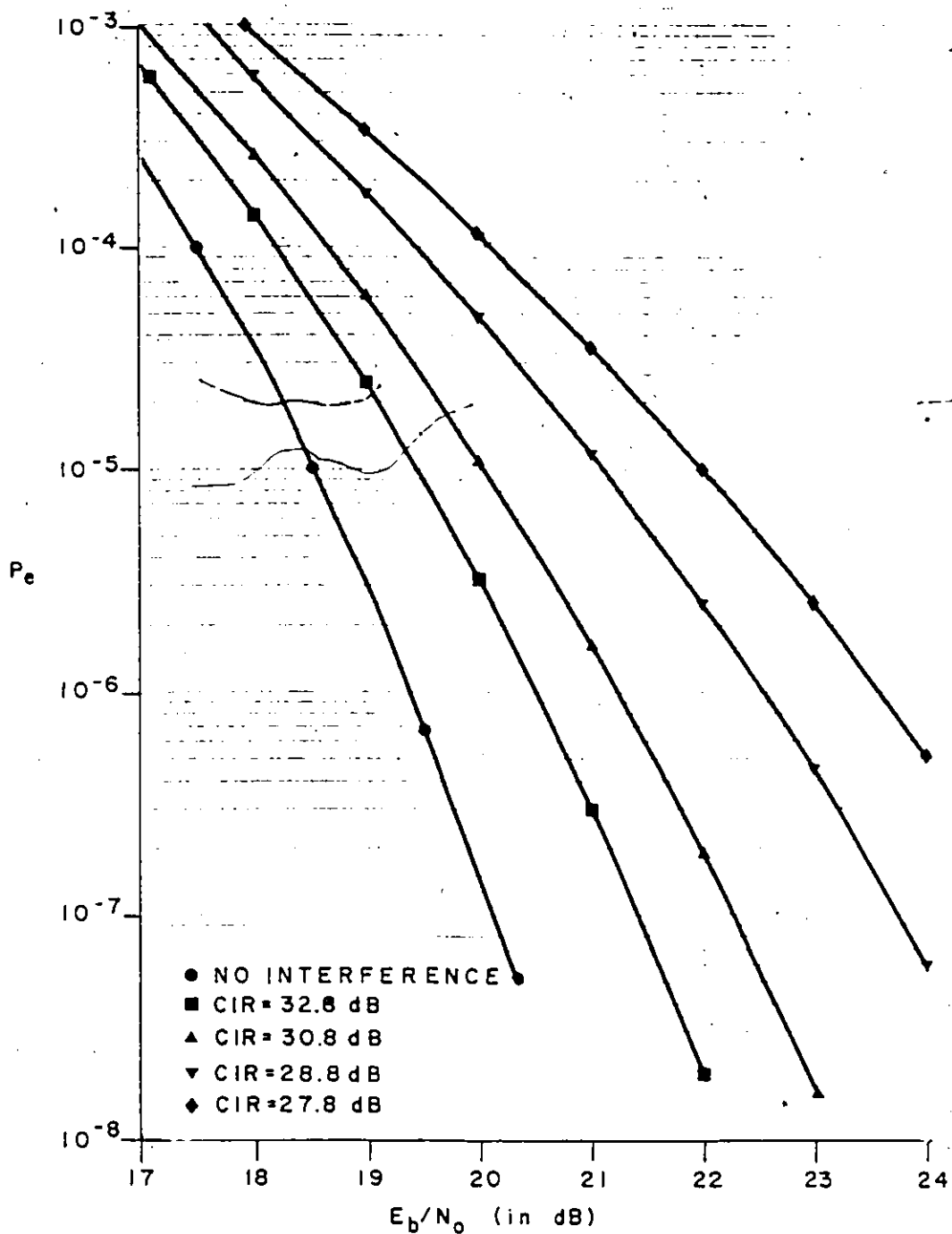


FIGURE 4.2.1 P_e VERSUS E_b/N_0 PERFORMANCE FOR CO-CHANNEL INTERFERENCE (90 Mb/s, 64-state QAM interference)

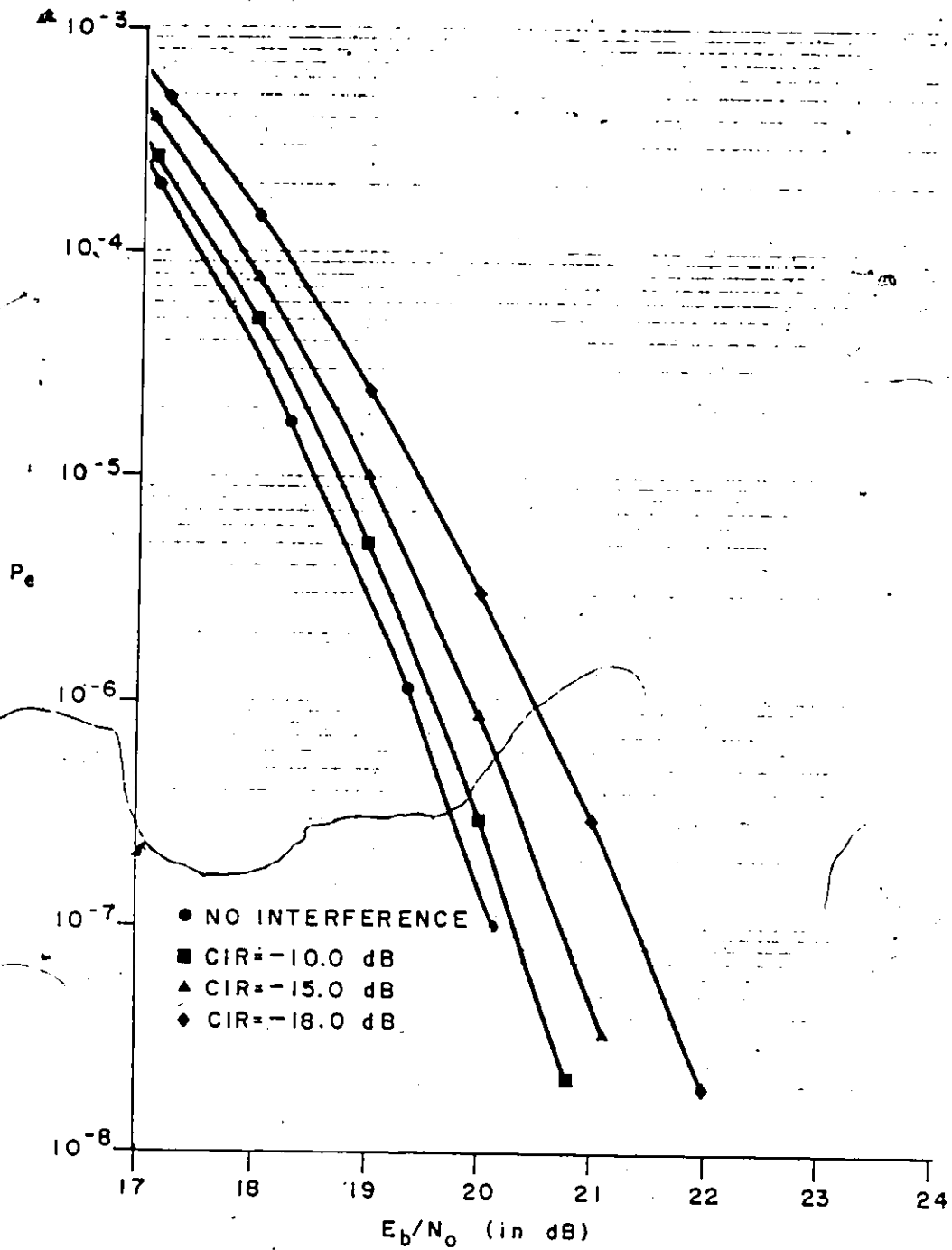


FIGURE 4.2.2 P_e VERSUS E_b/N_0 PERFORMANCE FOR ADJACENT CHANNEL INTERFERENCE (90 Mb/s, 20 MHz channel spacing, 64-state QAM interference $\alpha=0.4$ raised cosine filtering)

4.3 Anomalous Amplitude and Phase in the State Space

The sensitivity of a modulation technique to imperfections in the systems hardware must be considered when selecting the implementation of the modulation technique. Because the NLA 64-state modulation technique uses three parallel transmit amplifiers the system is susceptible to imperfect amplifier output power levels and phase. Aging and/or temperature can result in an amplifier gain or phase variation and hence a change in the output power or phase. A change in either the amplifier's output power levels or phase from the nominal levels would result in distortion of the 64-state QAM state space. Apart from amplifier output levels, multi-level modulation schemes are inherently susceptible to distortions of the signal levels. In this section, the sensitivity of 64-state QAM to amplifier output power level imperfections is determined. In addition, a limited study of the effects of amplifier phase variations is undertaken.

The P_e versus E_b/N_0 performance of 64-state QAM is evaluated for varying values of the amplifier output power levels. The results are shown in Figs. 4.3.1 (a) and (b) for varying values of P_1 , in Figs. 4.3.2 (a) and (b) for varying values of P_2 , and in Figs. 4.3.3 (a) and (b) for P_3 . Where P_1 , P_2 , and P_3 represent amplifier's 1, 2, and 3 normalize output power levels. In these figures, the solid curves represent the cases where the

decision thresholds are set at the conventional levels (i.e. 0, $\pm 2A$, $\pm 4A$, $\pm 6A$ where $2A$ represents the conventional spacing of the signal levels). The broken curves represent the cases where the decision threshold are set at the vertical center of the received eyes. An illustration of the settings of the decision thresholds is shown in Fig. 4.3.4 together with an example of a received eye diagram with anomalous signal levels. In this figure the anomalous signal levels resulted from an increase in P_1 over its nominal normalized value of 12.0 dB.

For P_1 , shown in Figs. 4.3.1 (a) and (b), the setting of the decision thresholds at the vertical center of the eyes results in a marked improvement to performance. Taking the example of $P_1 = 12.4$ dB, the degradation to performance is reduced from 1.7 dB to 0.2 dB at a P_e of 10^{-4} by readjusting the decision thresholds.

The performance curves for P_2 , Figs. 4.3.2 (a) and (b) show again that setting the decision thresholds at the vertical center of the eyes results in an improvement to performance relative to the conventional settings. Although the improvements are not quite as large as those realized in Figs. 4.3.1 (a) and (b), they are still significant. For a $P_2 = 6.4$ dB at a P_e of 10^{-4} , the degradation to performance is reduced by 0.2 dB by readjusting the decision thresholds.

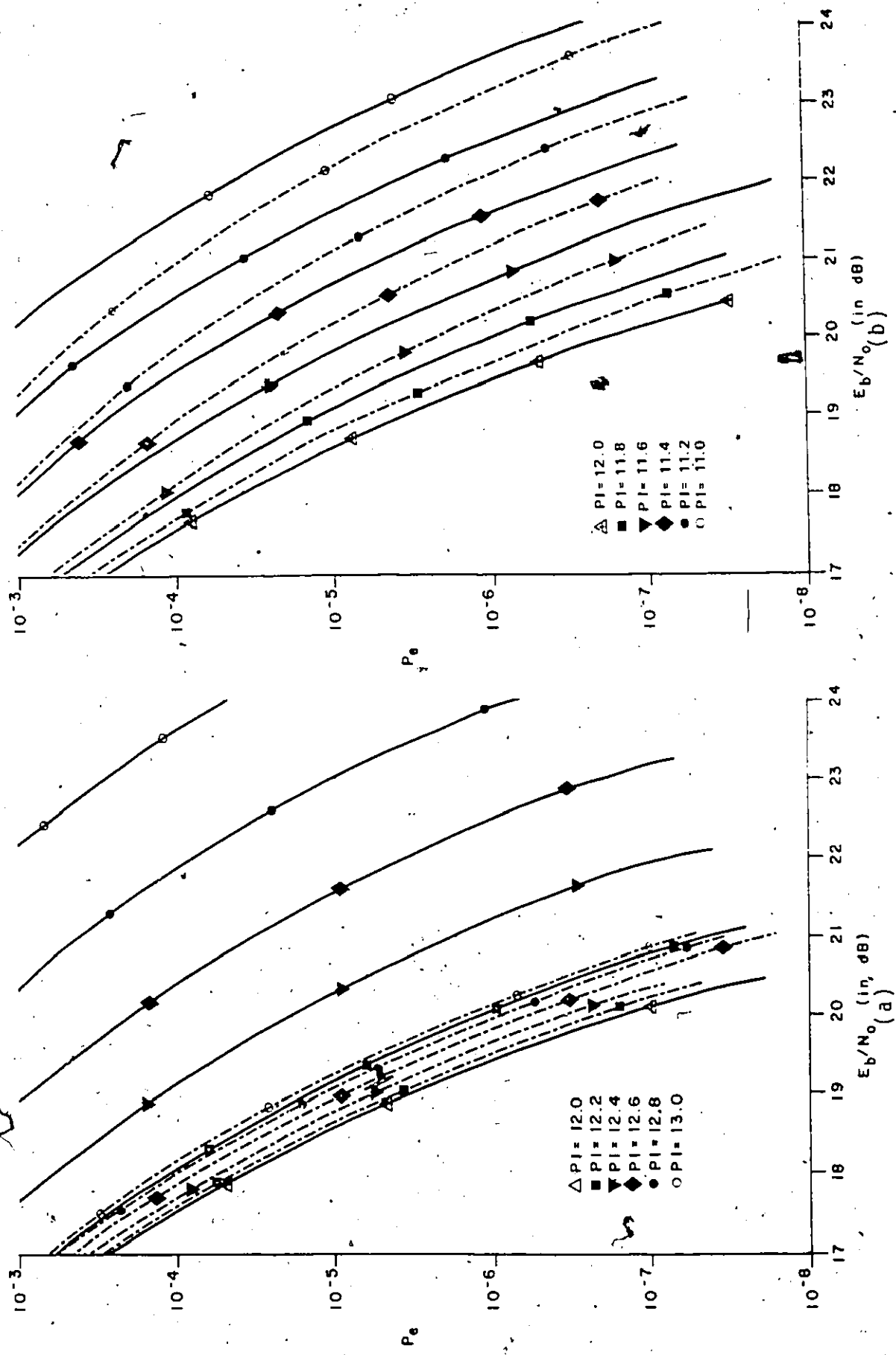


FIGURE 4.3.1 P_e VERSUS E_b/N_0 FOR FIRST MODULATOR POWER LEVEL VARIATIONS

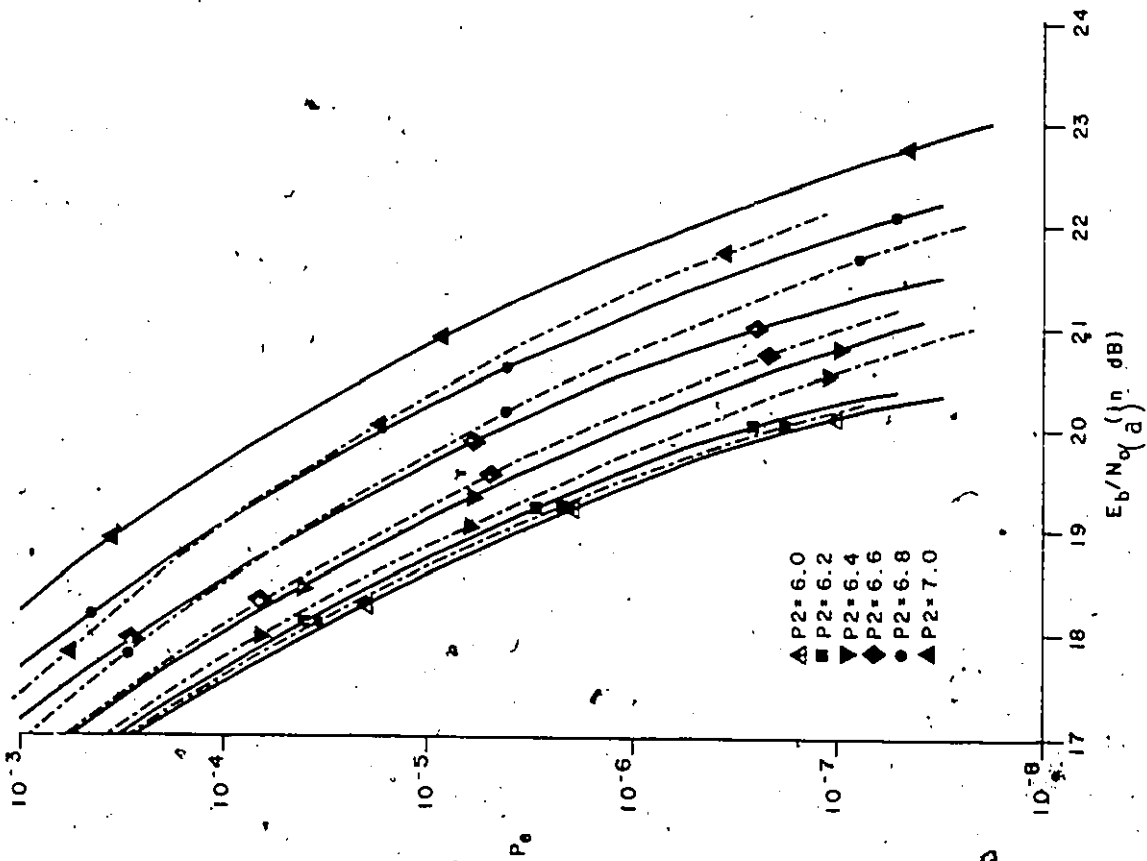
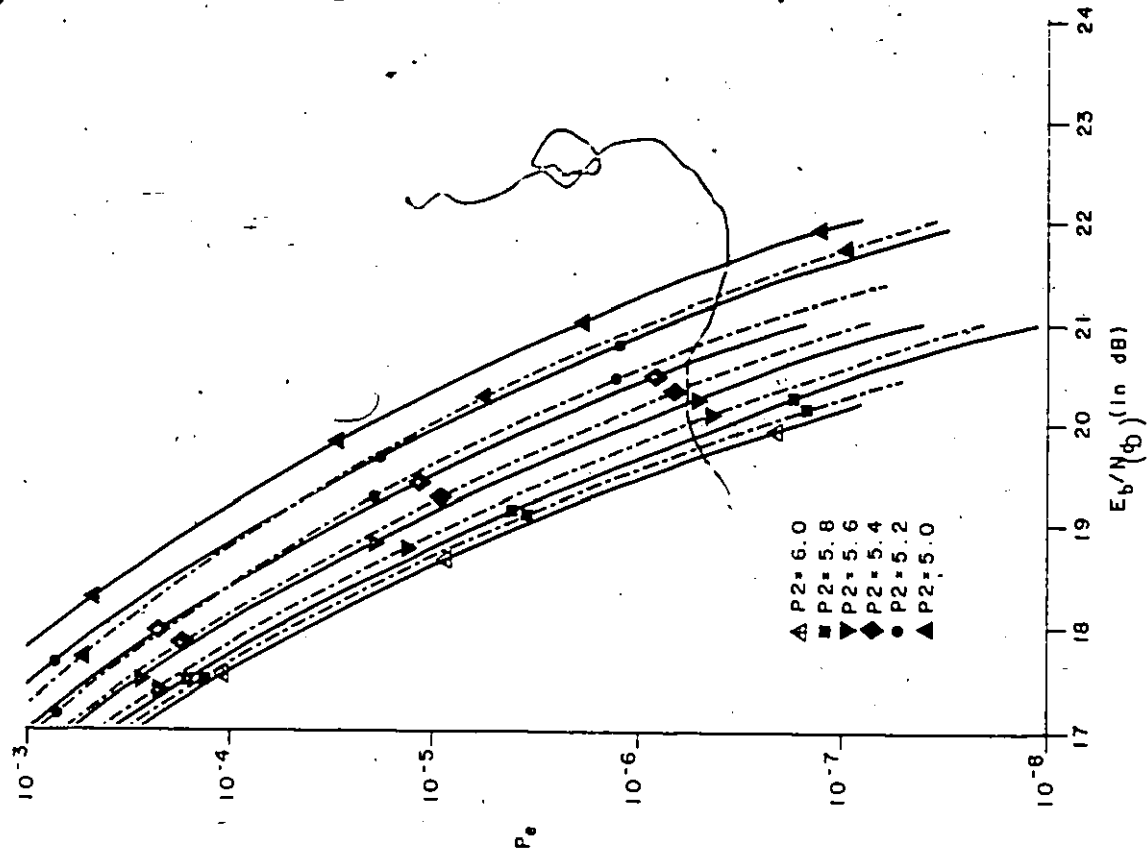


FIGURE 4.3.2 P_e VERSUS E_b/N_0 FOR SECOND MODULATOR POWER LEVELS

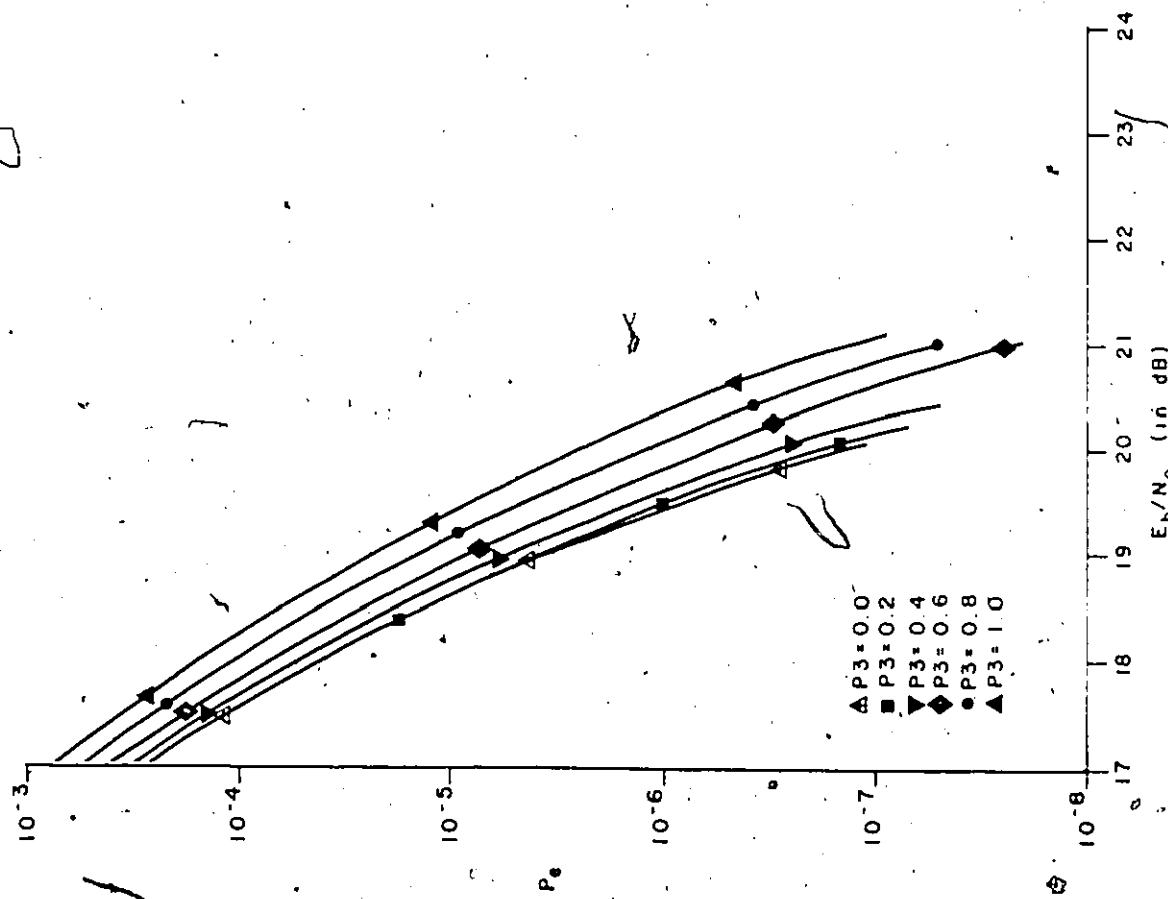
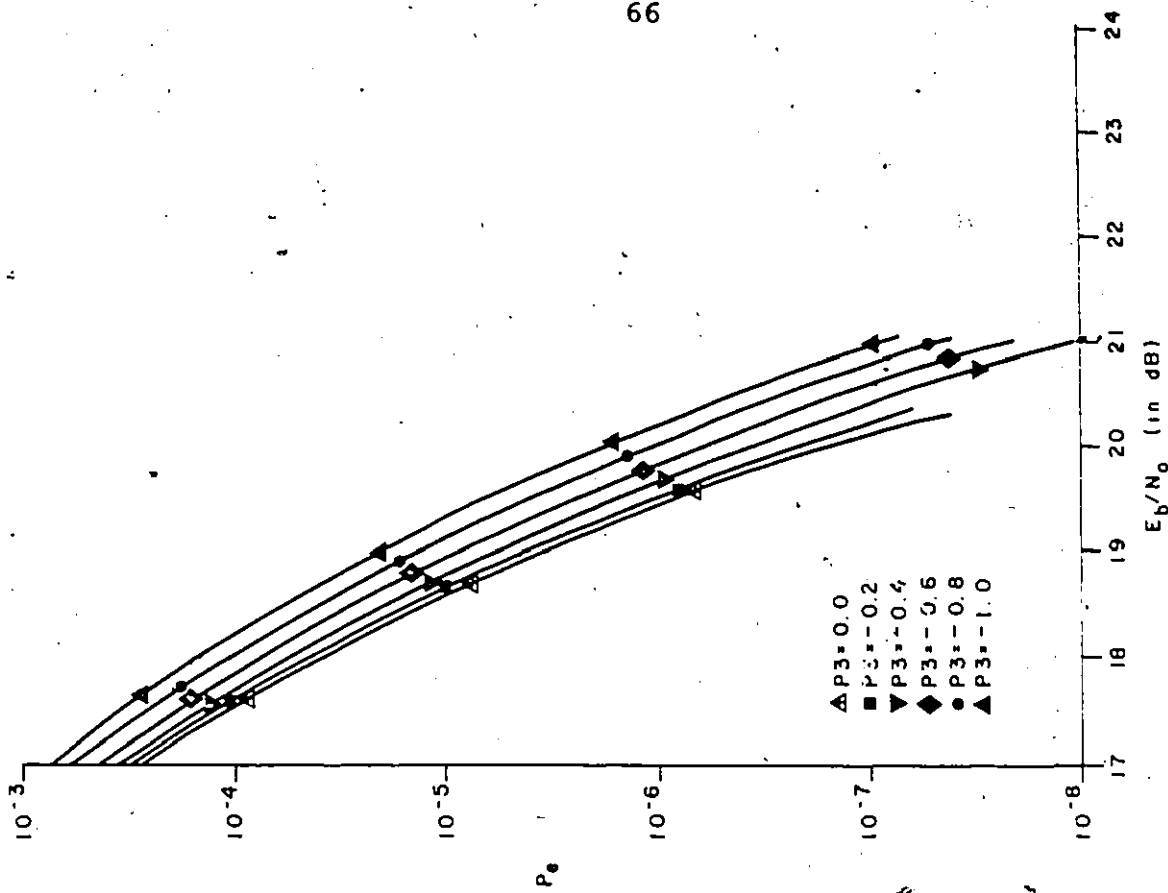


FIGURE 4.3.3 P_e VERSUS E_b/N_0 FOR THIRD MODULATOR POWER LEVEL VARIATIONS

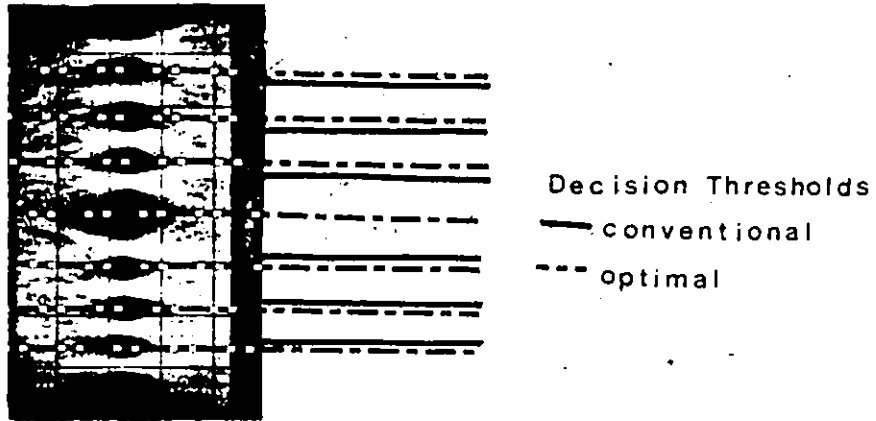


FIGURE 4.3.4 A MEASURED EYE-DIAGRAM WITH THE TWO DECISION THRESHOLDS INDICATED (See FIG. 4.3.1)

For P3 we note that only the solid curves are shown in Figs. 4.3.3 (a) and (b). This is due to the equivalence in the two settings of the decision thresholds for variations in P3.

Figure 4.3.5 shows a comparison of the degradation to E_b/N_0 resulting from the variation of each of the amplifiers' output power levels. The performance degradation as a function of the difference in dB of the specified power level from the ideal power level and relative to the nominal case for a P_e of 10^{-4} is shown for the cases where the thresholds are set at the vertical center of the eyes. What can be noticed from this figure is that the performance degradation is directly correlated to the resulting degradation of the state space. The one noticeable exception being $P_1 > 12.0$ dB. This is explainable as this increase effectively opens the distance between the levels adjacent to the in-phase and quadrature axis with the only penalty paid being an increase in the E_b/N_0 requirement.

A similar study for the effects of amplifier phase variations was undertaken and the results are shown in Fig. 4.3.6. The performance degradation as a function of the difference in degrees of the specified amplifier output phase from the ideal phase and relative to the nominal case for a P_e of 10^{-4} is shown.

The results of the first study indicated to us that a monitoring of the received eye diagram and a readjusting of the decision thresholds would be needed to maintain a reasonable performance if level variations were present. The results of the

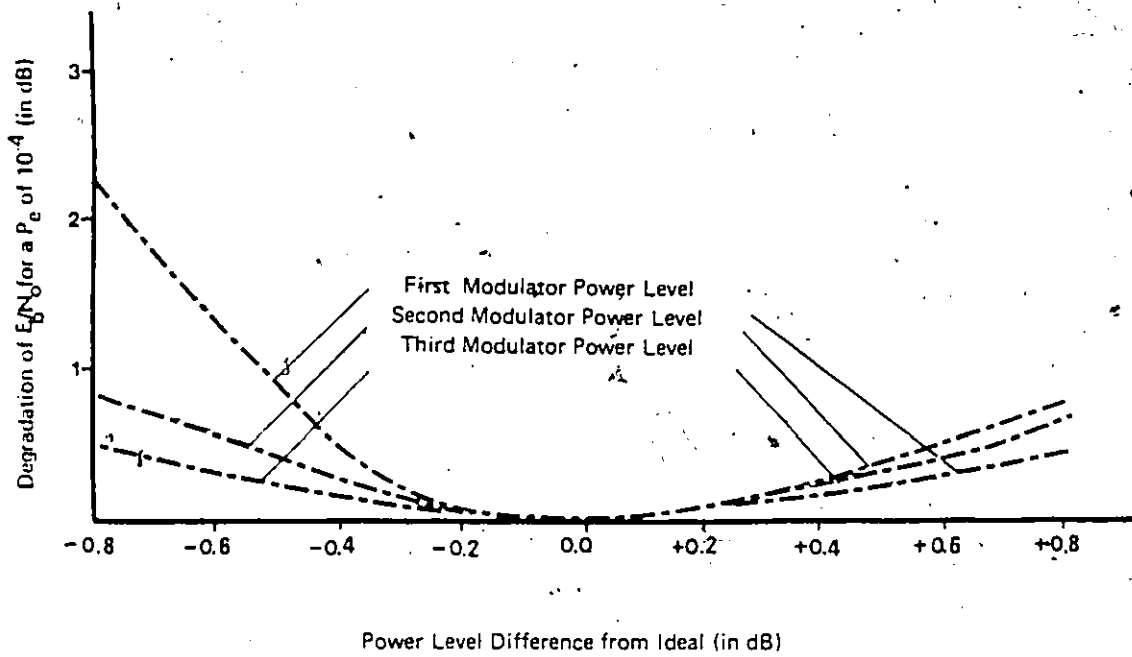


FIGURE 4.3.5 . DEGRADATION OF E_b/N_0 VERSUS THE VARIATION OF THE POWER LEVELS FROM IDEAL

second study indicated to us that a maximum amplifier phase variation in the order of 2 degrees would need to be maintained a reasonable performance. Both of the studies indicated that a careful selection of the output amplifiers used in the parallel modulation scheme would be advisable to avoid these variations.

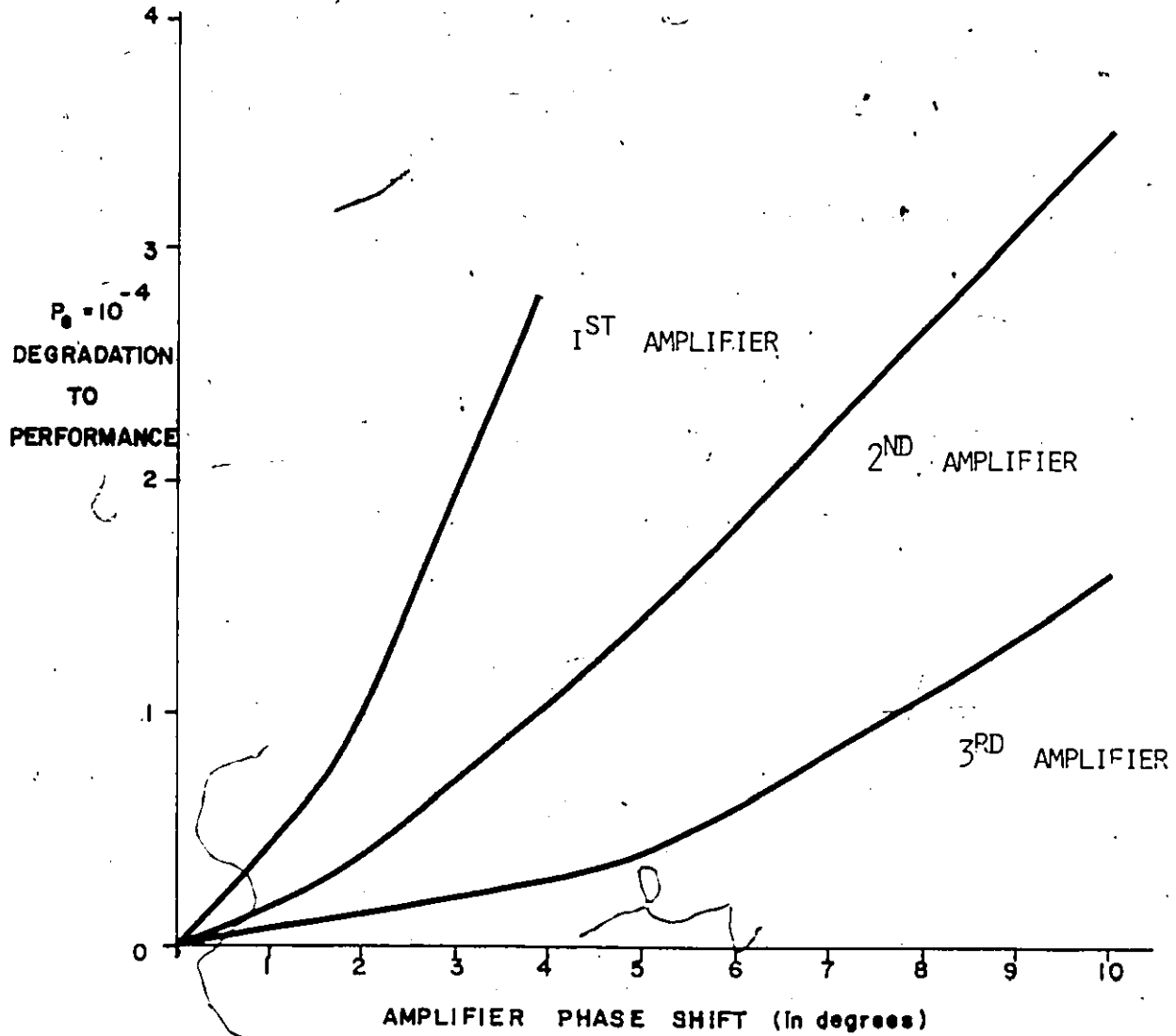


FIGURE 4.3.6 DEGRADATION TO PERFORMANCE VERSUS THE VARIATION OF PHASE FROM IDEAL

4.4 Channel Amplitude Distortions

In this section and the succeeding sections of this chapter the effects of nonideal amplitude and group delay transmission characteristics are considered. Channel amplitude and group delay distortions can result from a variety of environmental and hardware related system conditions.

Under conditions of multipath fading the transmission characteristics are often dispersive, i.e., both amplitude and group delay vary with frequency [15], [16]. These fades are due to environmental conditions and result in signal cancellations due to the reception of multiple signals propagated over paths with different amplitude and delay characteristics. Another common problem that affects the transmission characteristics is nonideal system filter characteristics. As a practical matter, the realization of ideal filter characteristics which would not degrade a system's performance in any way is very difficult.

Specifically in this section, three forms of channel amplitude distortions are considered:

- 1) Linear
- 2) Parabolic
- 3) Sinusoidal

For each of these forms of amplitude distortion the P_e performance of 64-state QAM is evaluated for varying magnitudes

of the distortion.

For linear amplitude distortion, the transfer function of the model is:

$$A(f) = Zxf \quad (4.4.1)$$

where Z is the amplitude slope in dB/MHz and $A(f)$ is the transfer function in dB. In this context, when Z is 0 the amplitude and group delay characteristics of the transmission channel are raised cosine with an alpha of 0.4, $x/\sin x$ equalization, and a flat group delay. The P_e performance of 64-state QAM with varying magnitudes of amplitude slope is shown in Fig. 4.4.1. For example, an amplitude slope of 0.152 dB/MHz the E_b/N_0 requirement increases 2.3 dB from its nominal value at a P_e of 10^{-4} .

For parabolic amplitude distortion, the transfer function of the model is:

$$A(f) = Pxf^2 \quad (4.4.2)$$

where P is in dB/MHz². Thus, when P is equal to zero the amplitude and group delay characteristics of the transmission channel are raised cosine with an alpha of 0.4, $x/\sin x$ equalization, and a flat group delay. The P_e performance of 64-state QAM with varying magnitudes of parabolic amplitude distortion is shown in Fig. 4.4.2. As shown in this figure, for parabolic amplitude distortion with a P of 7.25×10^{-3} dB/MHz² an E_b/N_0 of 18.5 dB is required for a P_e of 10^{-4} . This represents a degradation to performance of approximately 1.0 dB.

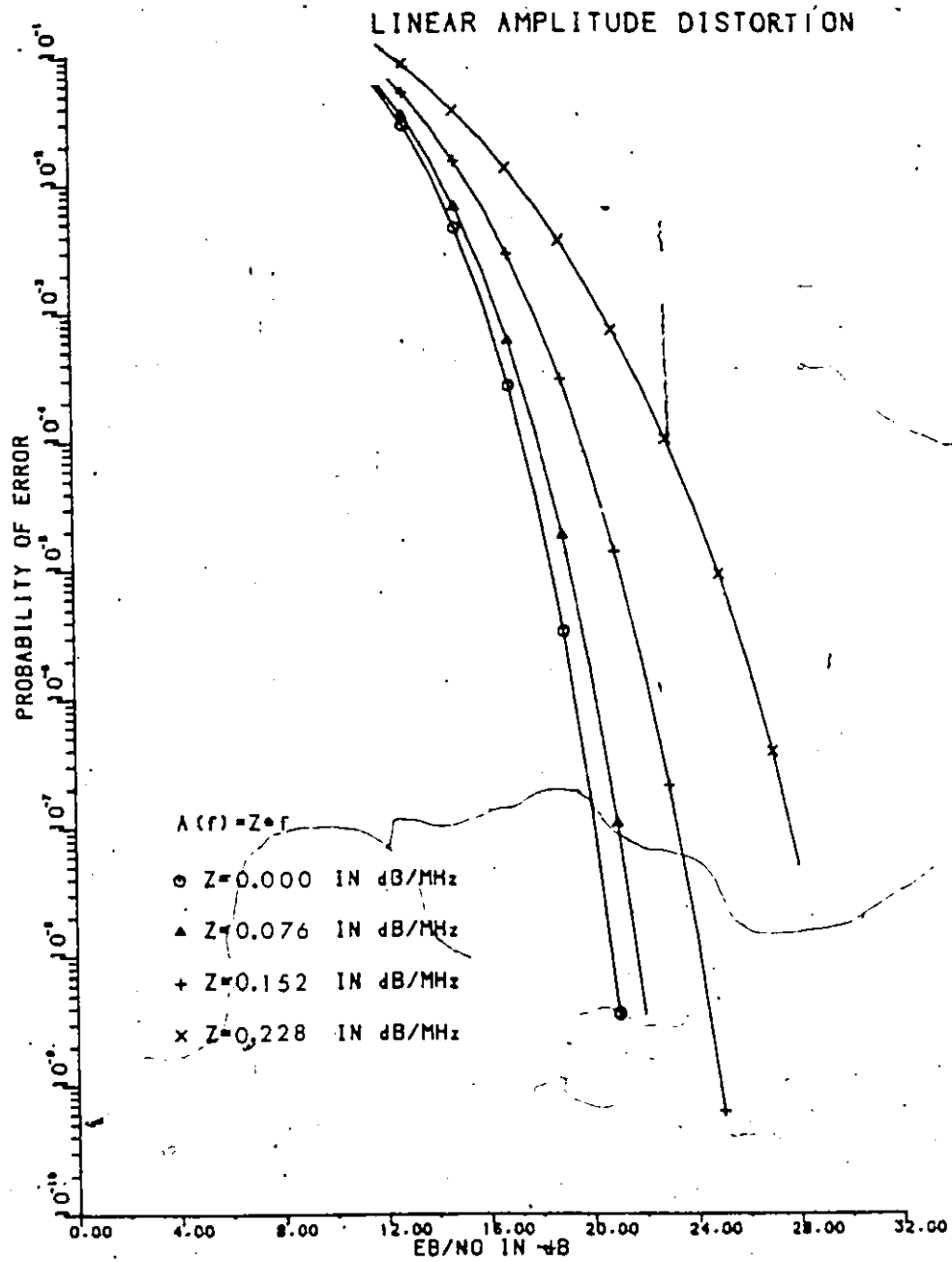


FIGURE 4.4.1 P_e VERSUS E_b/N_0 FOR LINEAR AMPLITUDE DISTORTIONS

PARABOLIC AMPLITUDE DISTORTION

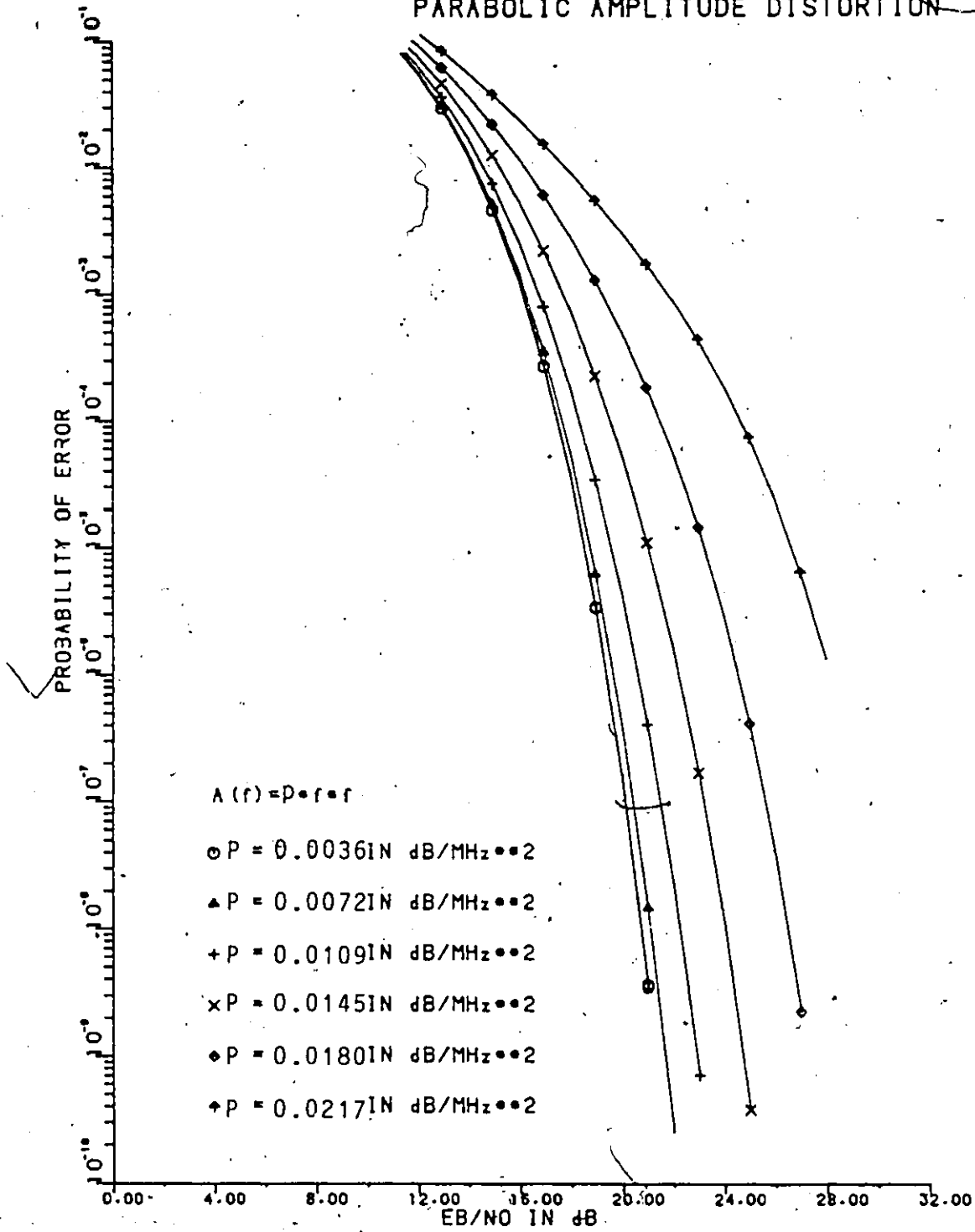


FIGURE 4.4.2 P_e VERSUS E_b/N_0 FOR PARABOLIC AMPLITUDE DISTORTIONS

For sinusoidal amplitude distortion, the transfer function of the model is:

$$A(f) = D \sin(2\pi x K x f / BWN) \quad (4.4.3)$$

where D is the magnitude of the sinusoid in dB, BWN is the double-sided Nyquist bandwidth, and K is the number of periods of the sinusoid in the Nyquist bandwidth. In this case, when D is equal to zero the amplitude and group delay characteristics of the transmission channel are raised cosine with an alpha of 0.4, with $x/\sin x$ equalization, and a flat group delay. Figure 4.4.3 shows the P_e performance of 64-state QAM for varying magnitudes of the sinusoid with $K = 4$. Taking a sinusoidal magnitude 0.8 dB as an example of the degradation than can be expected to accompany sinusoidal amplitude distortion the E_b/N_0 requirement increases 6.4 dB from its nominal value at a P_e of 10^{-4} .

Figure 4.4.4 compares the degradation to E_b/N_0 at a P_e of 10^{-4} for the maximum linear, parabolic, and sinusoidal amplitude distortion in the filter bandwidth. For a 90 Mb/s system with $\alpha = 0.4$ raised cosine filters the maximum amplitude distortion in the 21 MHz filter bandwidth which results in a 3 dB degradation to E_b/N_0 is: 3.6 dB for the linear case, 1.4 dB for the parabolic case, and 0.55 dB for the sinusoidal case. We note that for a given maximum amplitude distortion 64-state QAM is least affected by linear distortion, followed by parabolic and sinusoidal.

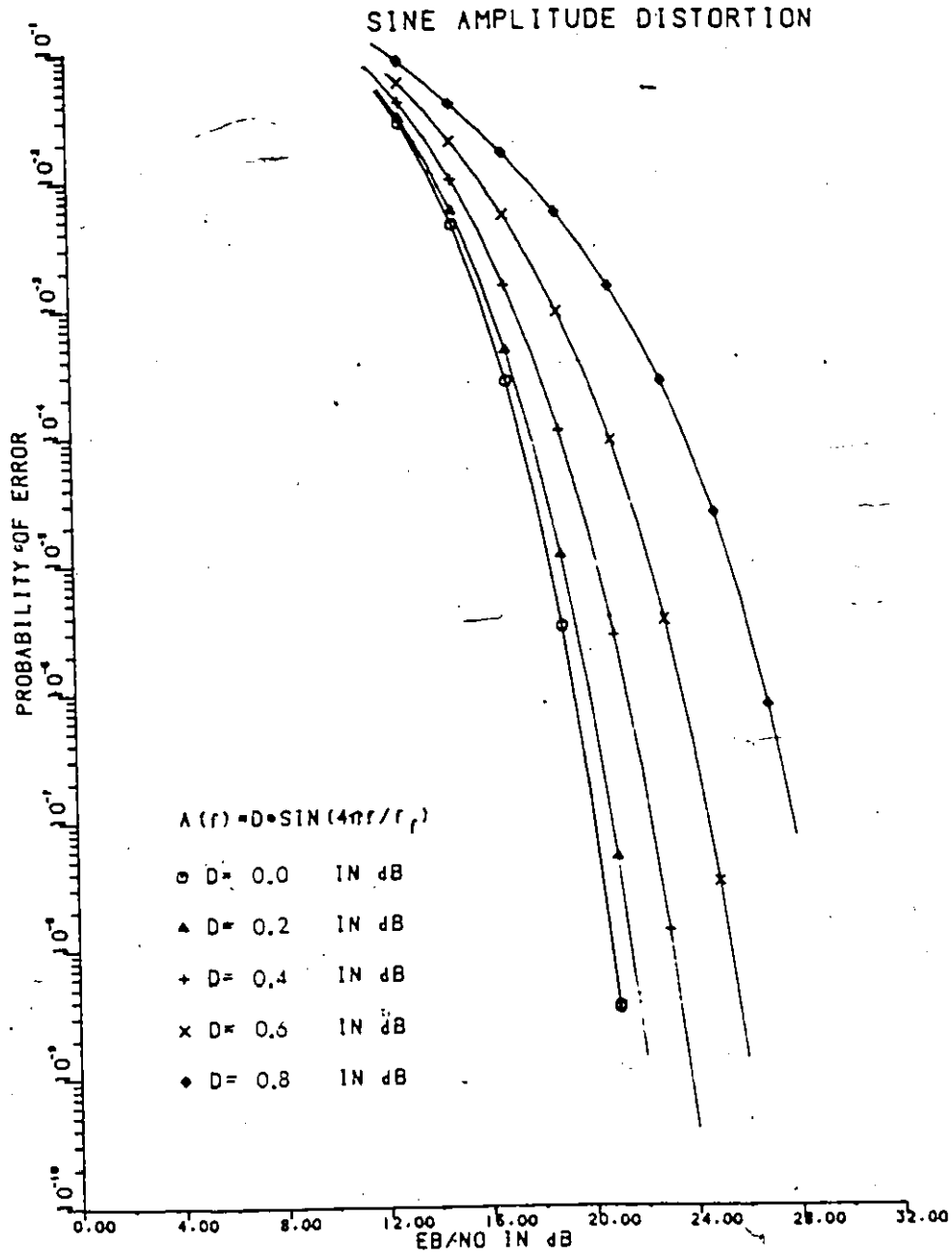


FIGURE 4.4.3 P_e VERSUS E_b/N_0 FOR SINUSOIDAL AMPLITUDE DISTORTIONS

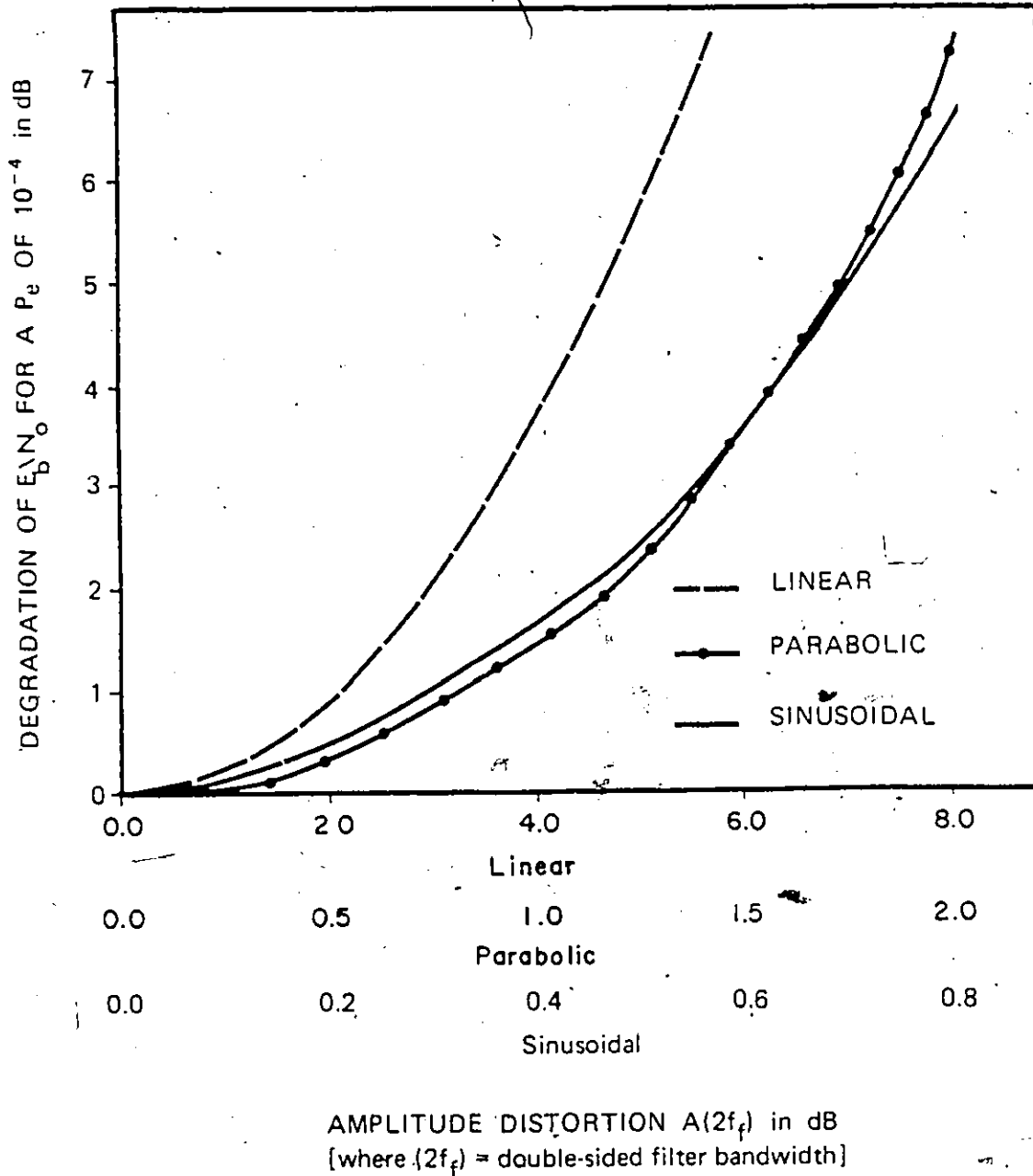


FIGURE 4.4.4 Degradation of E_b/N_0 for linear, parabolic, and sinusoidal amplitude distortions.

Note:— For a 90 Mbit/s system with $\alpha = 0.4$ raised cosine filters,

$$A(2f_p) = Z \times 21 \text{ dB (linear)}$$

$$= P \times 10.5 \times 10.5 \text{ dB (parabolic)}$$

$$= D \text{ dB (sinusoidal)}$$

4.5 Channel Group Delay Distortions

In this section, three forms of channel group delay distortions are considered namely:

- 1) Linear
- 2) Parabolic
- 3) Sinusoidal

For each of these forms of group delay the P_e performance of 64-state QAM is evaluated for varying magnitudes of the distortion.

For linear group delay, the transfer function of the model is:

$$T(f) = Bxf \quad (4.5.1)$$

where B is the delay slope in ns/MHz. In this context, when B is 0 the amplitude and group delay characteristics of the transmission channel are raised cosine with an alpha of 0.4, x/sin x equalization, and a flat group delay. The P_e performance of 64-state QAM with varying magnitudes of delay slope is shown in Fig. 4.5.1. Taking a delay slope of 0.38 ns/MHz as an example of the degradation incurred, the E_b/N_0 requirement increases 2.5 dB from its nominal value at a P_e of 10^{-4} .

For parabolic group delay, the transfer function of the model is:

$$T(f) = Sxf^{**2} \quad (4.5.2)$$

where S is in ns/MHz**2. Thus, when S is equal to zero the

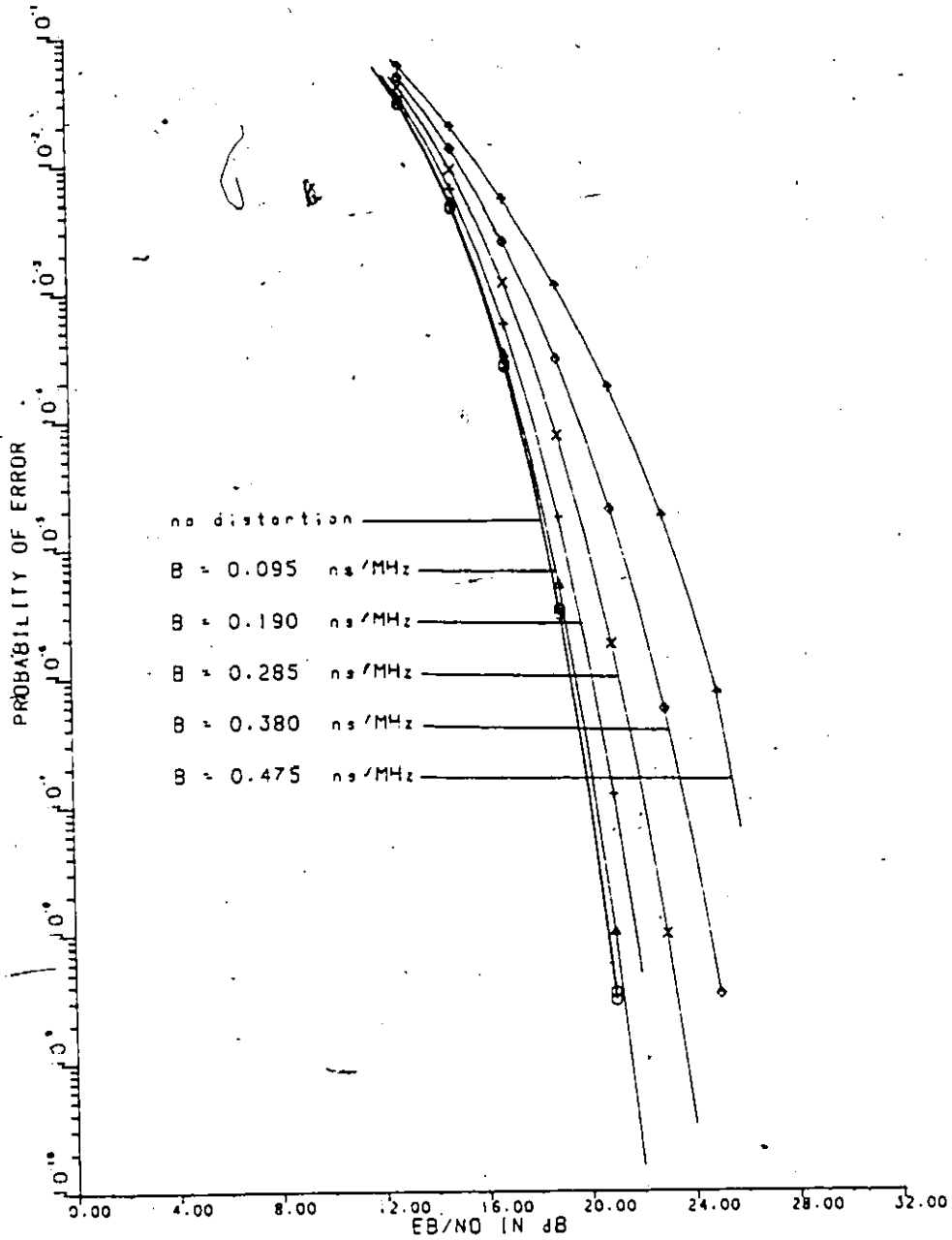


FIGURE 4.5.1 P_e VERSUS E_b/N_o FOR LINEAR GROUP DELAY DISTORTIONS

amplitude and group delay characteristics of the transmission channel are raised cosine with an alpha of 0.4, with $x/\sin x$ equalization, and a flat group delay. The P_e performance of 64-state QAM with varying magnitudes of parabolic group delay is shown in Fig. 4.5.2: As shown in this figure, for parabolic amplitude distortion with an S of 0.54 ns/MHz**2 an E_b/N_o of 19.0 dB is required for a P_e of 10^{-4} . This represents a degradation to performance of approximately 1.5 dB.

For sinusoidal group delay, the transfer function of the model is:

$$T(f) = C \sin(2\pi x K x f / BWN) \quad (4.5.3)$$

where C is the magnitude of the sinusoid in ns, BWN is the double-sided Nyquist bandwidth, and K is the number of periods of the sinusoid in the Nyquist bandwidth. In this case, when C is equal to zero the amplitude and group delay characteristics of the transmission channel are raised cosine with an alpha of 0.4, with $x/\sin x$ equalization, and a flat group delay. Figure 4.5.3 shows the P_e performance of 64-state QAM for varying magnitudes of the sinusoid with K set at four. Taking a sinusoidal magnitude 12.0 ns as an example of the degradation that can be expected to accompany sinusoidal group delay, the E_b/N_o requirement increases 1.5 dB from its nominal value at a P_e of 10^{-4} . It should be mentioned that although the results for varying the period of the sinusoid relative to the Nyquist bandwidth are not presented, in order to reduce the volume of

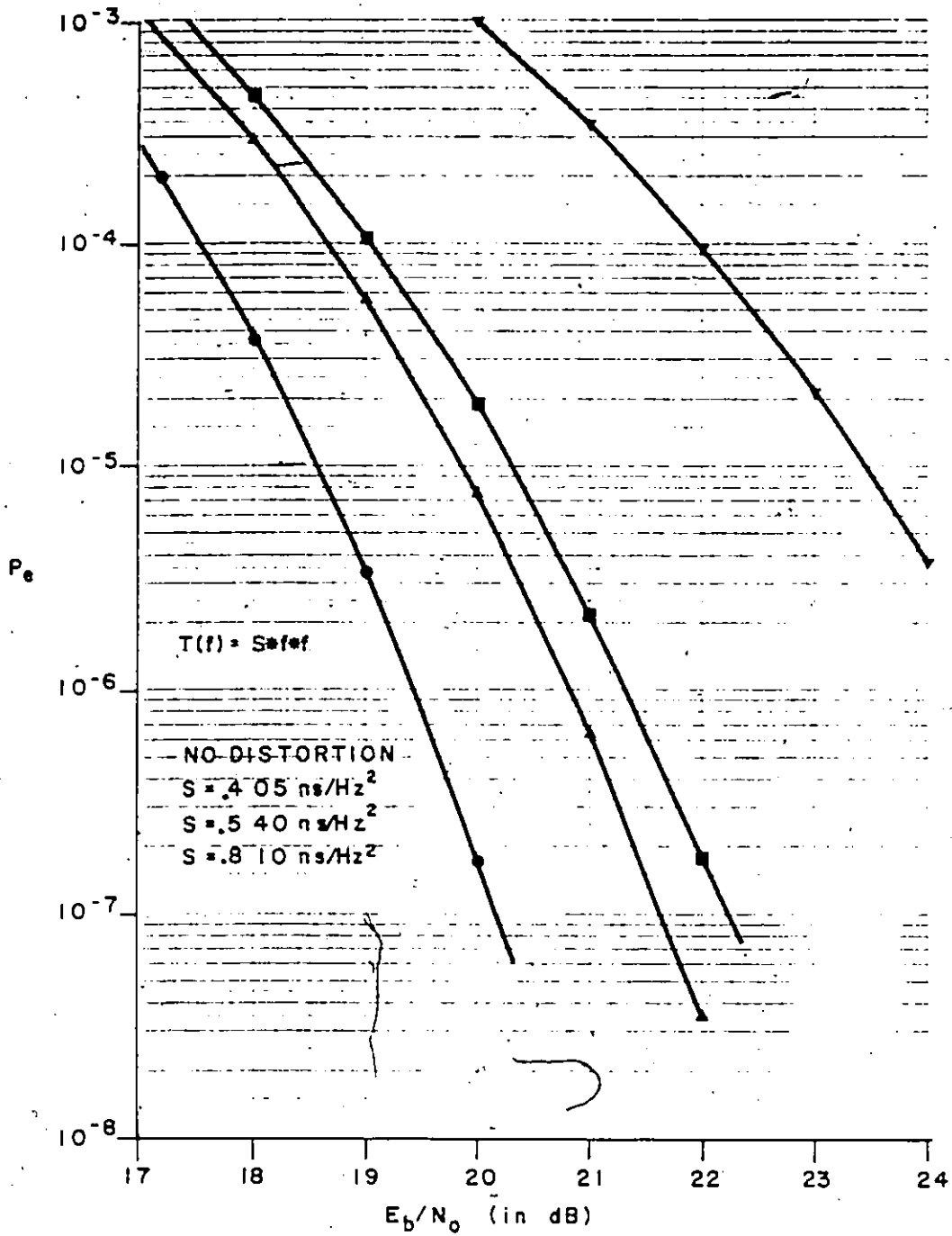


FIGURE 4.5.2 P_e VERSUS E_b/N_0 FOR PARABOLIC GROUP DELAY

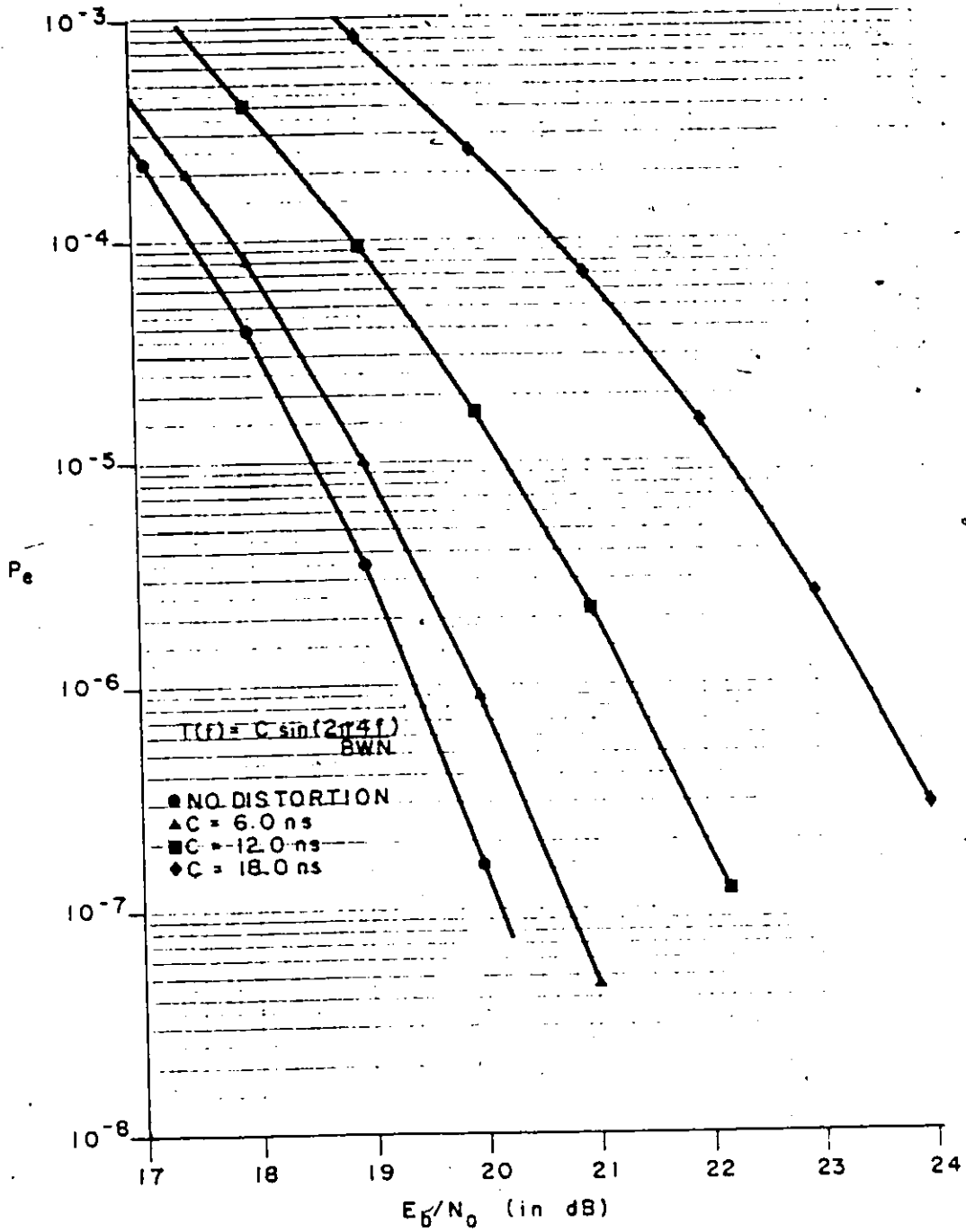


FIGURE 4.5.3 P_e VERSUS E_b/N_0 FOR SINUSOIDAL GROUP DELAY

data presented, the relative degradation to performance for a set C decreased as K increased.

Figure 4.5.4 compares the degradation to E_b/N_0 at a P_e of 10^{-4} for the maximum linear, parabolic, and sinusoidal group delay in the filter bandwidth. For a 90 Mb/s system with $\alpha = 0.4$ raised cosine filters, the maximum group delay in the 21 MHz filter bandwidth which results in a 1.0 dB degradation to E_b/N_0 is: 5.3 ns for the linear case, 52.5 ns for the parabolic case, and 103. ns for the sinusoidal case. This indicates that like QPSK, 64-state QAM is most sensitive to a group delay with linear characteristics [17].

It has been pointed out that digital radio systems with amplitude and/or group delay distortions typically exhibit error floors in their P_e performance curves. These error floors are not present in the simulated performance curves presented. However, it is felt that if larger distortion and/or longer data sequences were used in the simulation runs these floors would be present.

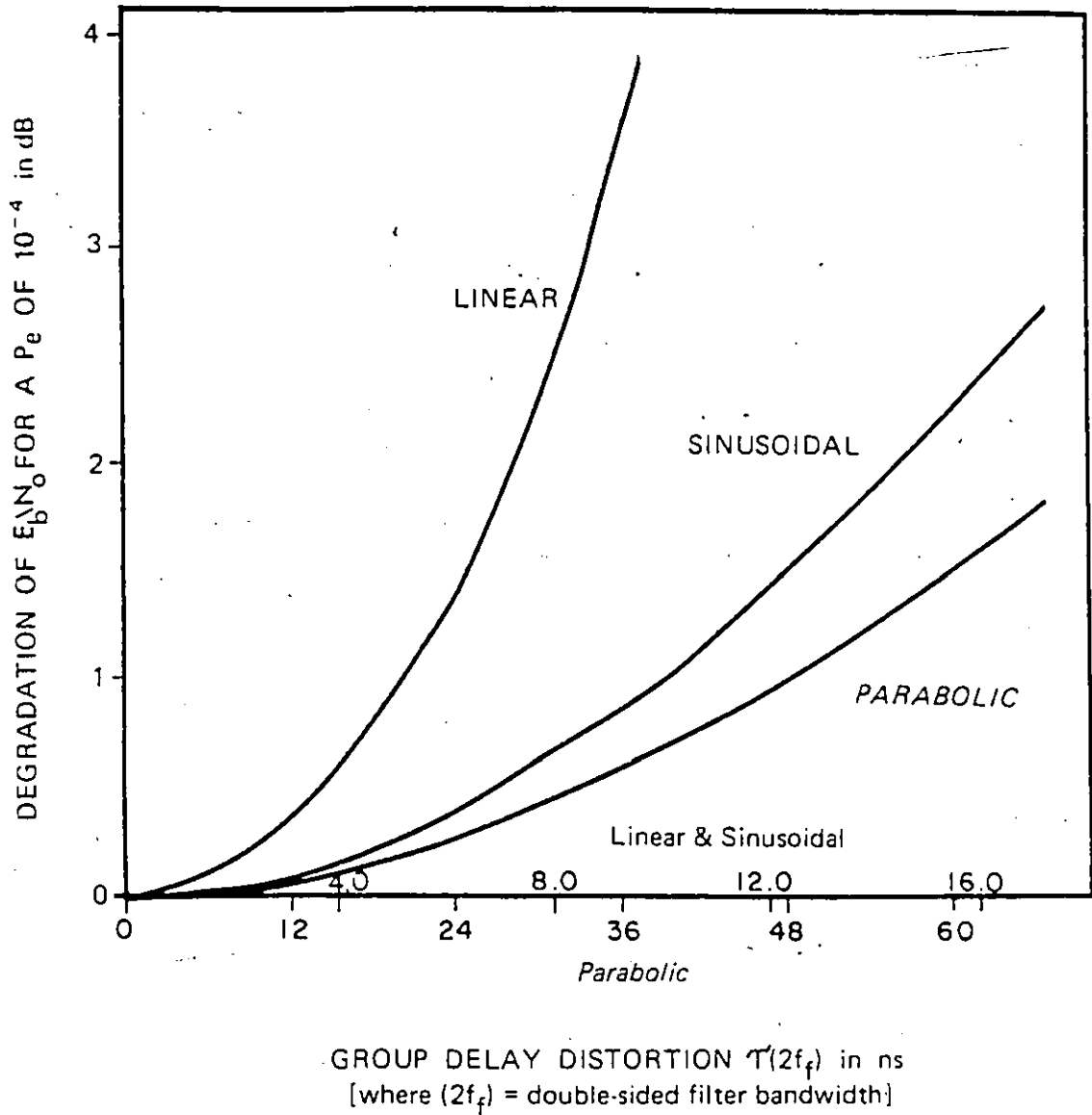


FIGURE 4.5A

Degradation of E_b/N_0 for linear, parabolic, and sinusoidal group delay distortions.

Note:— For a 90 Mbit/s system with $\alpha = 0.4$ raised cosine filters,

$$T(2f_c) = B \times 21 \text{ ns (linear)}$$

$$= S \times 10.5 \times 10.5 \text{ ns (parabolic)}$$

$$= C \text{ ns (sinusoidal)}$$

4.6 Selective Fading

One of the keys to high density digital radio communications is signal robustness over a selectively fading channel. Regardless of the modulation technique used, a selectively fading channel will affect signal robustness. How, and to what extent fading will affect the modulation technique, must be evaluated to determine the optimum technique for dealing with it. The sensitivity of 64-state QAM to a selectively fading channel is discussed in this section.

The slopes and notches of a selectively fading channel have been modelled by Rummler [18] as a three-ray multipath fade, the transfer function of which is:

$$H(\omega) = a [1 - be^{+j(\omega-\omega_0)T}] \quad (4.6.1)$$

where "a" is a real, positive parameter that represents the flat-weighting of the channel; "b" is a real, positive, time variant parameter which represents the Q or depth of the fade; " ω_0 " is the radiant frequency of the center of the fade; and "T" is the time variant delay difference in the channel. The plus and minus signs in the exponent correspond to the nonminimum and minimum phase in the channel fade respectively [23].

The model can be rewritten in terms of the channel group delay and amplitude characteristics as follows:

$$T(W) = \frac{\pm b T (\cos (W-W_0) T - 1)}{1 + b^2 - 2b \cos (W-W_0) T} \quad (4.6.2)$$

$$A(W) = (1 + b^2 \pm 2b \cos(W-W_0)T)^{1/2} \quad (4.6.3)$$

where $T(W)$ is the group delay channel characteristic and $A(W)$ is the amplitude characteristic. In this context, when the fade is minimum phase the amplitude and group delay have the same slope. When the fade is nonminimum phase, the two have opposite slopes.

Figures 4.6.1 and 4.6.2 show the performance curves of 64-state QAM in minimum and nonminimum phase fades of various depths. In either case, the fade notch is centered in the transmission channel and "T" is 6.31 nsec. As seen from these figures, equivalent minimum and nonminimum phase fades result in equivalent degradation to performance. Taking the example of a minimum or nonminimum phase fade of depth 0.45 dB, the E_b/N_0 requirement is increased 2.4 dB from its nominal value for a P_e of 10^{-4} . In practice however, systems with parabolic (minimum) group delay characteristics, which could be introduced by the system's filtering would be less sensitive to nonminimum phase fades. The filter's group delay characteristics would partially compensate for the group delay characteristics of the fade. The same could be said for minimum phase fades and a system with an inverted parabolic group delay characteristic.

The results of this study indicated to us that in order to maintain a reasonable fading performance in 64-state

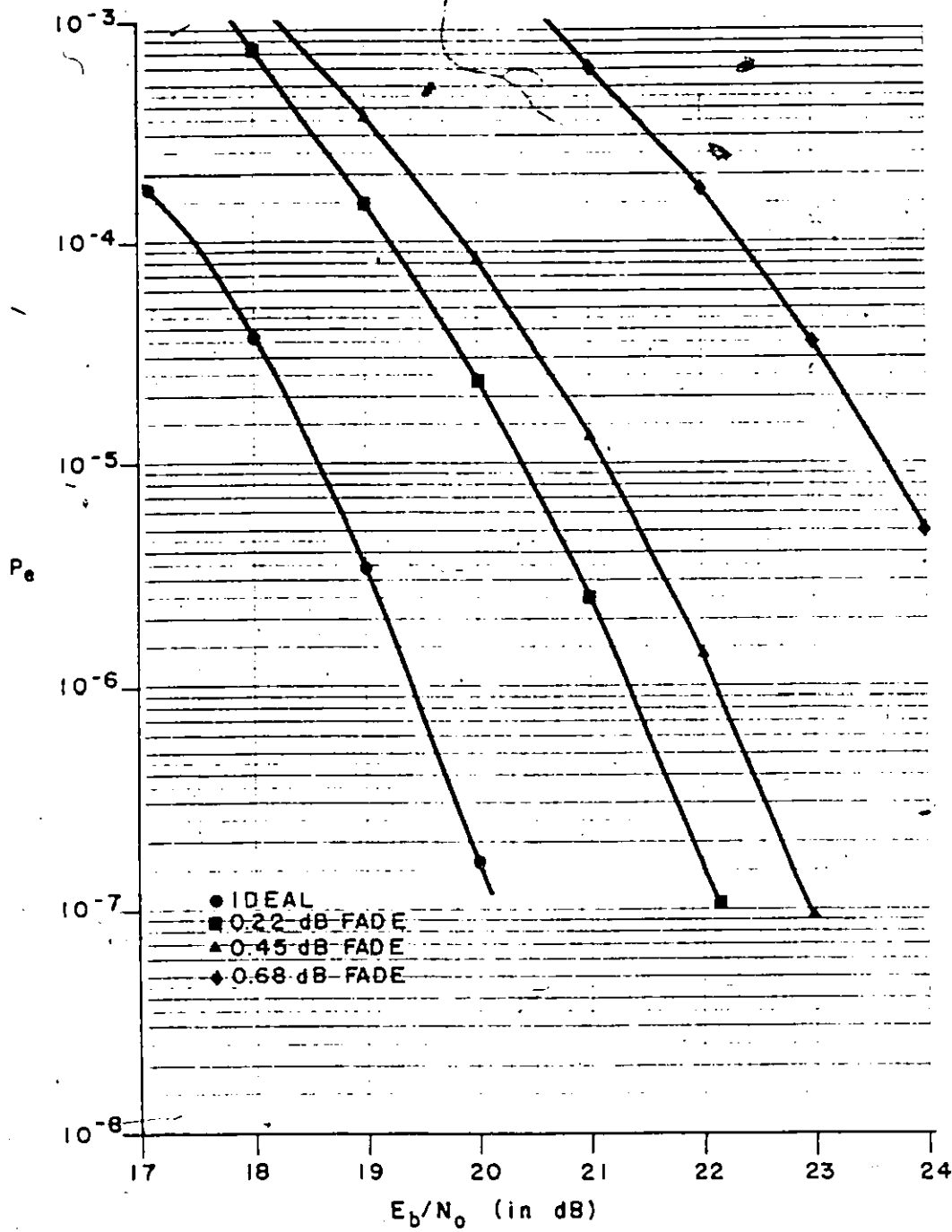


FIGURE 4.6.1 P_e VERSUS E_b/N_0 PERFORMANCE FOR MINIMUM PHASE SELECTIVE FADES (FADE CENTERED IN CHANNEL, $T=6.31$ nsec)

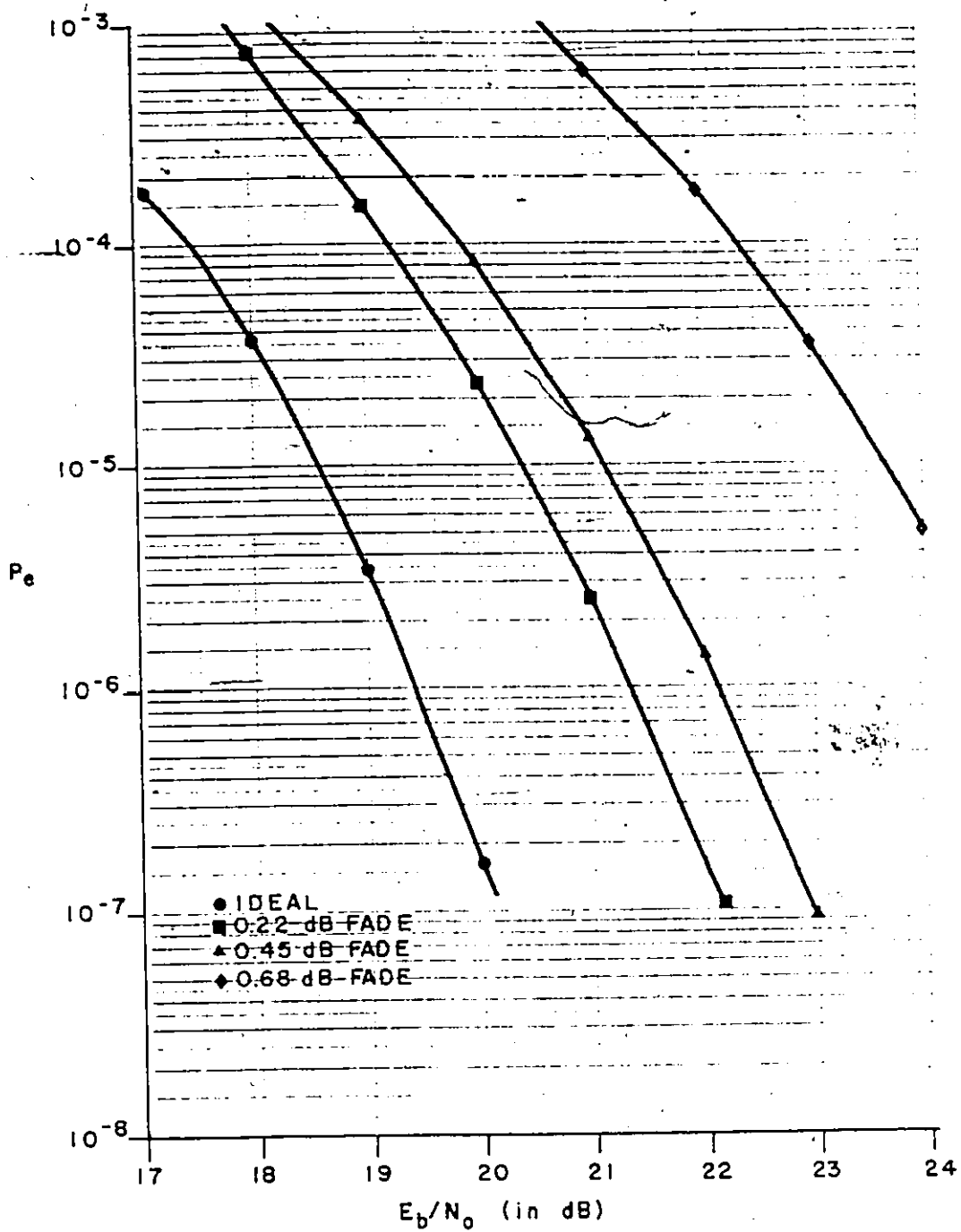


FIGURE 4.6.2 P_e VERSUS E_b/N_0 PERFORMANCE FOR NONMINIMUM PHASE SELECTIVE FADES (FADE CENTERED IN CHANNEL, $T=6.31$ nsec)

QAM systems, measures would have to be taken to combat fading. There are three major methods in use today for controlling selective fading [24]. These include larger antennas, space and frequency diversity, and the use of adaptive equalizers. Additional study is required to establish the effectiveness of these techniques in improving the fading performance of 64-state QAM systems.

5

CHAPTER 5

2

CHAPTER 5.

5.1 Introduction

In this study of NLA 64-state QAM, a prototype modem employing a "parallel type" 64-state QAM modulation technique was developed. As well as verifying the feasibility of such a technique, one of the reasons for the development of this modem was to experimentally analyse and evaluate the performance of such a system with practical design constraints. The computer simulation studies in Chapter 4 provided a good indication of the performance that could be expected under various environmental and hardware conditions. This chapter is a continuation of these studies but, deals specifically with hardware considerations. Two performance criteria are considered namely:

- 1) spectral efficiency, and
- 2) P_e performance.

Using these two criteria the performance of 64-state QAM systems with the same basic hardware design and performance as the experimental prototype modem is determined. Laboratory measurements of the prototype modem's performance as well as numerical analysis and interpretation of these measurements are presented in the succeeding sections of this chapter.

5.2 Spectral Efficiency of the Modem

In this section, the spectral efficiency of NLA 64-state QAM radio systems with the same spectral shaping as our prototype modem is determined. The digital radio systems considered are those which would operate in the FCC authorized 20 MHz, 30 MHz, and 40 MHz bandwidths.

In determining the spectral efficiency of NLA 64-state QAM systems a technique described by Amoroso [19] is employed. This technique uses the FCC mask as a standard of reference for the RF bandwidth, and the spectral performance of a modem. For these studies the spectral performance of our modem with its low bit rate and simple filters is used.

Figure 5.2.1 shows a plot of the measured power spectral density of our filtered 64-state QAM signal. The spectrum is centered at our scaled down carrier frequency of 1 MHz with null ± 64 kHz on either side, and shows spectral shaping as a result of the premodulation low-pass filtering and predistortion equalization. The spectral density is normalized to 0 dB at the center frequency ($f_c = 1\text{MHz}$).

Amoroso's method involves shifting the center frequency of the spectrum, shown in Fig. 5.2.1, up to the desired radio frequency. The bit rate of the modem and its corresponding spectrum are then conceptually increased until the new spectrum just fits within the FCC mask for the desired radio frequency. For example, for a radio frequency of 4 GHz with the authorized

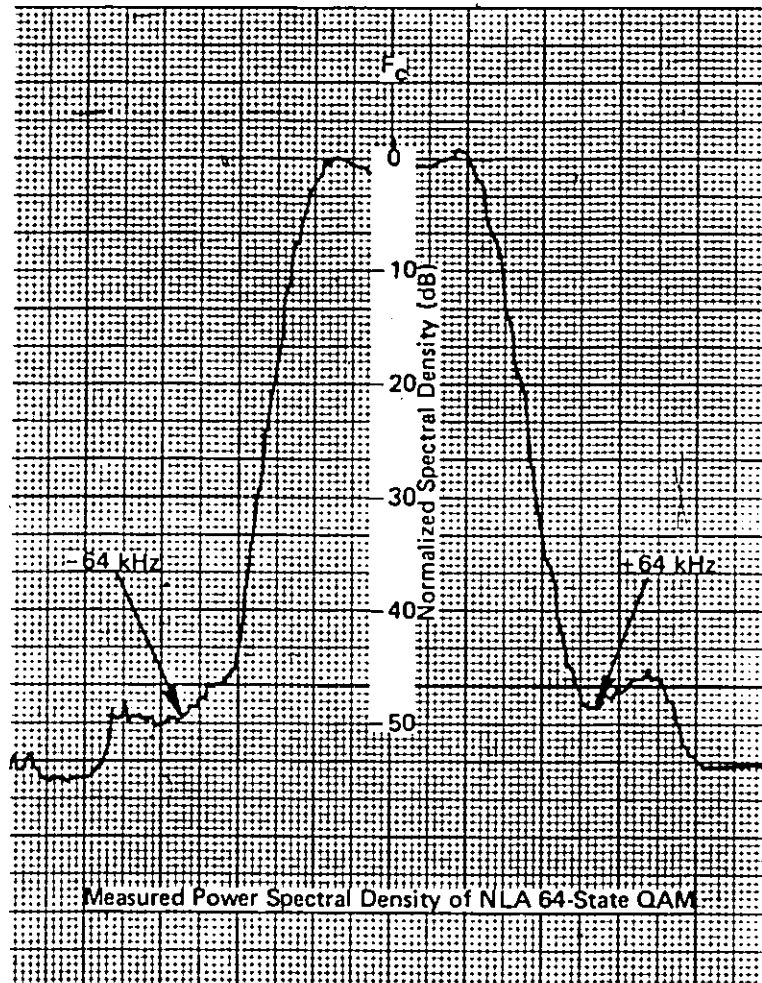


FIGURE 5.2.1 MEASURED POWER SPECTRAL DENSITY OF 64-STATE QAM SIGNAL AT TRANSMITTER OUTPUT
 $(f_b = 384 \text{ kb/s})$

bandwidth of 20 MHz, the maximum possible bit rate R is determined using the FCC 20 MHz mask and the following equation [19].

$$A(f) = 10 \log 4000 + 10 \log S_n(f) - 10 \log B_n R \quad (5.2.1)$$

where:

A(f) is the power in a 4 KHz band/total power in dB,

S_n(f) is the normalized power spectral density of the transmit spectrum,

B_n is the noise bandwidth of the transmit spectrum,

and R is the transmission bit rate in b/s.

The normalized noise bandwidth is derived using the following equation [21], [20]

$$B_n = \frac{1}{6} \int_{-5/T}^{5/T} \left(\frac{\sin \pi f}{f} \right)^2 \cdot \frac{1}{1 + (f/0.468)^2} df \quad (5.2.2)$$

where:

T is the symbol duration,

f is the frequency,

and 0.468 is the normalized 3 dB attenuation frequency for the bandlimited BPSK signal spectrum.

Solving for Eq. 5.2.5, the value of B_n is found to be 0.123.

Substituting this value of B_n into Eq. 5.2.1 and normalizing the power spectral density with respect to the bit rate as given in Table 5.1.1, the maximum possible transmission bit rate was found to be 94 Mb/s within the 20 MHz bandwidth.

Figure 5.2.2 is a plot of Eq. 5.2.1 for the 64-state QAM prototype

modem with $R = 94 \text{ Mb/s}$. This plot of $A(f)$ is shown together with the FCC mask for the 20 MHz authorized bandwidth. The translated spectrum is tangent to the FCC mask around the -50 dB level. Any further increase in the transmission bit rate would cause the mask to be violated. For this reason the maximum possible transmission bit rate in the 4 GHz band was determined to be 94 Mb/s. This rate can easily accommodate two DS3 signals, which is virtually unique in operating commercial 4 GHz digital radio systems, and represents a spectral efficiency of 4.7 b/s/Hz.

Using the same method as in the previous example, the spectral efficiencies for the 6 GHz band with an authorized bandwidth of 30 MHz and for 11 GHz with an authorized bandwidth of 40 MHz were found to be 5.0 b/s/Hz and 5.1 b/s/Hz, respectively.

The results indicate that even with simple filters, 64-state QAM systems could obtain spectral efficiencies of over 4.5 b/s/Hz.

Normalized Frequency	Normalized Power Spectral Density ($S_n(f)$ in dB)
0	0
.0521	1
.0651	3
.0781	7
.1041	15
.1302	27
.1459	35
.1563	43
.1823	46
.2083	45
.2604	51

Table 5.1.1 Normalized Transmit Spectrum

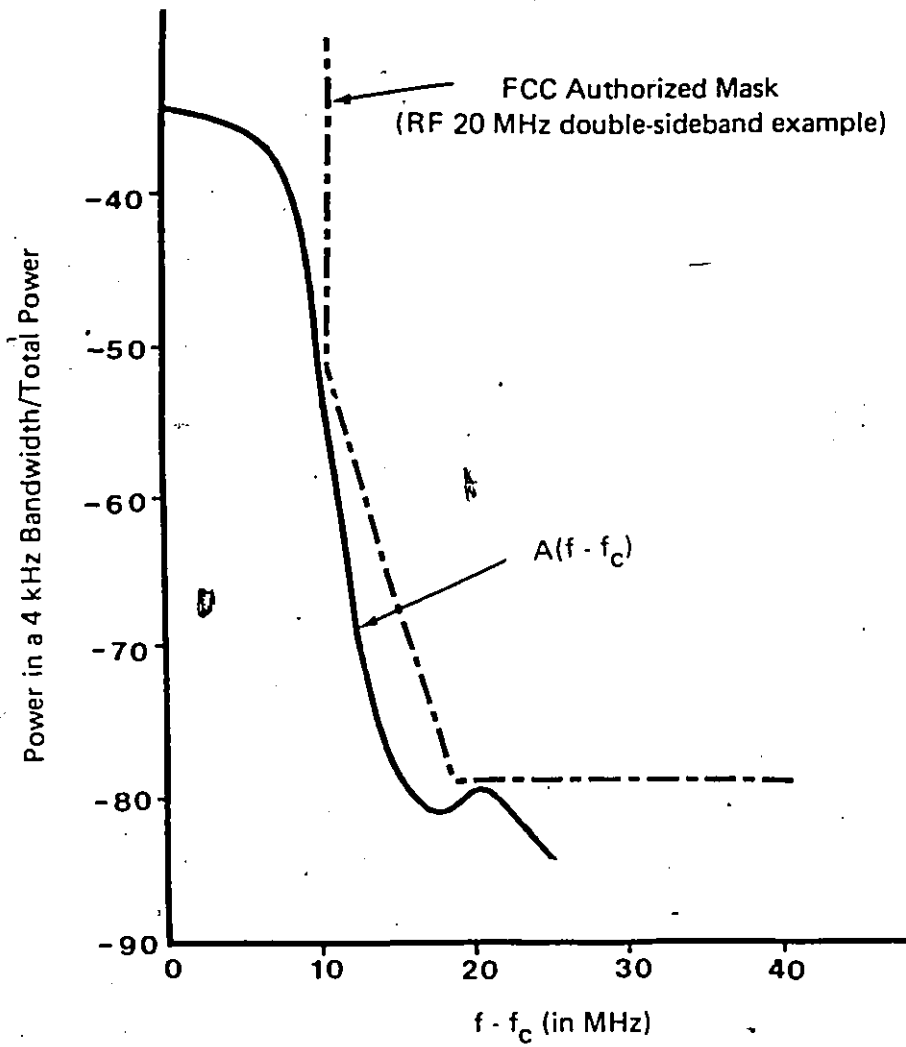


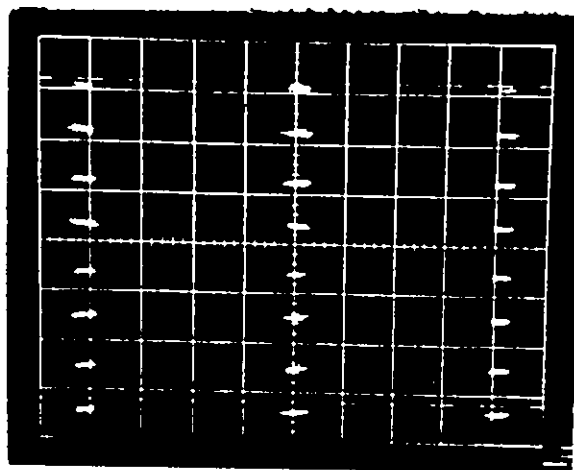
FIGURE 5.2.2 FCC MASK APPLIED TO 64-STATE QAM (single side shown)

5.3 P_e Performance of the Modem

In this section, the P_e performance degradation of digital radio systems having a hardware configuration similar to our prototype modem is determined. The feasibility of the modems hardware design is also considered.

The prototype's predistortion equalizers do not completely remove the ISI introduced by the nonideal modem (transmit and receive) filtering. The ISI contribution to the system performance degradation is estimated using the eye diagram as a quality measurement. A photograph of the prototype's 64 kBaud eye diagram at the receive filter's output is shown in Fig. 5.3.1. As can be seen from the photograph, the eye is approximately 80% open at the sampling instant. Thus, the equivalent performance degradation is $20\log_{10}(.80) = 1.94$ dB [22]. If this ISI degradation is added to the E_b/N_o requirement of an ideal 64-state QAM then the required E_b/N_o of a similar system is obtained. For example, for a P_e of 10^{-4} in 64-state QAM system with filtering and predistortion equalization similar to that of the prototype modem, an E_b/N_o of $17.5 + 1.9 = 19.4$ dB is required.

The relatively low distortion of the prototype modem's eye diagram is a qualitative proof of the feasibility of the hardware design. The lack of typical production quality design give even more credance to the design concept given the relatively high quality of the eye diagram.



0.8 V/ div
4 μ s/ div

FIGURE 5.3.1 EYE DIAGRAM AT THE 8-TO-2 LEVEL CONVERTER
INPUT IN THE DEMODULATOR

The standard binary coding scheme used in the modulator resulted in an increase in the bit error rate performance relative to that of Gray coding. Gray coding represents a symbol error to bit error ratio of 1 assuming the error is in interpreting a particular level as one of its adjacent levels. This is a common assumption used because the probability of "adjacent errors" occurring is much larger than that of "nonadjacent errors".

As can be seen in Fig. 5.3.2, a symbol error in which the sampled symbol at the receiver has been detected in the adjacent symbol's decision region can result in more than one bit error. For example, in the case where the transmitted symbol was the fifth level symbol and the detector decides erroneously that the fourth level signal was sent, a symbol error results in three bit errors. If this relationship is taken into consideration for all symbols the probability of bit error of binary coding to Gray coding ratio is found to be 1.57 as determined in Eq. 5.3.1.

$$\begin{aligned} P_e (\text{binary}) &= P_e (\text{Gray}) (3 \cdot 2 + 2 \cdot 4 + 1 \cdot 8) / 14 \\ &= 1.57 P_e (\text{Gray}) \end{aligned} \quad (5.3.1)$$

Although no attempt was made in the modulator design to improve this symbol error to bit error ratio, a relatively simple coding scheme could be implemented to correct for this.

								LOGIC STATE					
								X1	X2	X3			
x	x	x	x		x	x	x	x	1	1	1	↕	1 BIT ERROR
x	x	x	x		x	x	x	x	1	1	0	↕	2 BIT ERRORS
x	x	x	x		x	x	x	x	1	0	1	↕	1 BIT ERROR
x	x	x	x		x	x	x	x	1	0	0	↕	3 BIT ERRORS
x	x	x	x		x	x	x	x	0	1	1	↕	1 BIT ERROR
x	x	x	x		x	x	x	x	0	1	0	↕	2 BIT ERRORS
x	x	x	x		x	x	x	x	0	0	1	↕	1 BIT ERROR
x	x	x	x		x	x	x	x	0	0	0	↕	

FIGURE 5.3.2 AN ILLUSTRATION OF THE 64-STATE QAM STATE SPACE TO BIT ERROR RELATIONSHIP

9

CHAPTER 6

CHAPTER 6.

6.1 Thesis Summary

The first chapter in this thesis was introductory in nature and presented the reasons for the selection of NLA 64-state QAM for further research. In comparing the performance of various 64-ary modulation techniques, rectangular 64-state APK was selected over the other candidates because of its comparable performance and its realizability. Section 1.5 compared the implementation of two rectangular 64-state APK modulation techniques namely: 8-L QAM and NLA 64-state QAM. It was found that the nonlinear application of NLA 64-state QAM could lead to a significant gain in transmit power efficiency and that the parallel modulation application could result in design simplification and flexibility over 8-L QAM. The results of this comparison warranted our selection of NLA 64-state QAM as a potentially attractive highly spectral efficient modulation technique.

Chapter 2 presented a description of the prototype modem that was implemented for this research. Our prototype modem had the following design parameters: a 64-state QAM/NLA 64-state QAM switchable modulation technique, a bit rate of 384 kb/s, and a carrier frequency of 1 MHz.

The modulator design consisted of a serial-to-parallel converter, predistortion equalizers and low-pass filters which could be switched in or out, quadrature modulators, hardlimiters

which could be switched in or out, and a combiner. The serial-to-parallel converter was used to convert the input serial 384 kb/s data stream into six parallel 64 kb/s data streams. The predistortion equalizers were manually adjustable 4 tap predistortion equalizers set to minimize the ISI at the receiver's threshold detector input. The low-pass filters were modified fifth order Butterworth filters used to limit the transmitted spectrum. The predistortion equalizers and low-pass filters could be switched in or out of the signal path depending on whether 64-state QAM or NLA 64-state QAM was the desired modulation technique. Quadrature modulators implemented with double balanced mixers were used to quadrature modulate the prototype's 1 MHz carrier signal. Hardlimiters were used to simulate the nonlinear device in a NLA 64-state QAM modulator. A linear three-to-one combiner was used to sum the three quadrature modulated signals to form the 64-state QAM or NLA 64-state QAM signal.

The demodulator design consisted of a quadrature demodulator, eight-to-two level converters, and parallel-to-serial converters. No carrier or clock recovery subsystems were included in the laboratory prototype modem. The quadrature demodulator was used to demodulate the incoming 64-state QAM or NLA 64-state QAM signals into two eight level filtered data streams. The same low-pass filters used in the 64-state QAM modulator were used in this quadrature demodulator to remove the

higher harmonic components after carrier multiplication and to remove unwanted signals. Eight-to-two level converters implemented with analog-to-digital converters were used to convert each multilevel filtered signal into three binary data streams. A parallel-to-serial converter was used to convert the six 64 kb/s binary data streams into one serial 384 kb/s data stream representing the recovered data.

Chapter 3 presented a description of the computer simulation models developed for this research to analyze the performance of 64-state QAM systems. The transmission and hardware impairments modelled include adjacent and cochannel interference, signal level anomaly, amplitude distortions, group delay distortions, and selective fading.

Our computer simulation model was based on the equivalent baseband concept. The 64-state QAM system models were broken down into blocks where, for a given system, certain blocks are included and others excluded. These blocks included: QPSK signal generator, 64 QAM signal generator, nonlinear amplifier, transmit filter, group delay distortion model, amplitude distortion model, selective fade model, weighted summer, adjacent and cochannel interference summer, receive filter, and sampler and threshold detector with P_e determination.

The P_e calculations consider the combined effects of ISI and noise. The optimum sampling instant was selected for the simulation run by selecting the sampling point which

minimized the P_e of the run for a given value of E_b/N_0 . The detector "demodulated" the received data into its two quadrature component parts. For each component part the detector evaluated the probability that the sampled symbol would not remain within the correct decision region for a specified value of N_0 . The detector averaged these probabilities over the entire symbol sequence for each value of E_b/N_0 to determine the P_e versus E_b/N_0 data. The corresponding equations were given in section 3.3.

Chapter 4 presented the performance of 64-state QAM systems with commonly encountered transmission and hardware impairments. The results were obtained using the computer simulation models described in Chapter 3 and Appendix B.

In section 4.2 we evaluated the cochannel and adjacent channel performance of a 64-state QAM system. The adjacent channel data indicated that threshold degradations of less than 0.3 dB result from interference levels that are 18 dB above the desired receiver level. This high level of adjacent channel rejection is important from a propagation and operation standpoint. The cochannel data indicates that the modulation technique is highly sensitive to in-band interference. The impact of these results is, that a high level of receiver selectivity must be maintained for satisfactory adjacent channel performance.

Section 4.3 evaluated the performance of a 64-state QAM system with anomalous amplifier power levels and phase. The

results of this study indicated that if level variations were present, a monitoring of the received eye diagram and a readjusting of the decision threshold would be needed to maintain reasonable performance. The study also indicated that the transmit amplifiers phase must be maintained within 2 or 3 degrees.

In sections 4.4 and 4.5 we evaluated the performance of 64-state QAM systems with hardware or environment related channel amplitude and group delay distortions. Amplitude and group delay distortions of the linear, parabolic, and sinusoidal form were considered. The amplitude distortion results indicated that for a given amount of distortion within the channel bandwidth, 64-state QAM was least affected by linear amplitude distortion followed by parabolic and sinusoidal. In a similar comparison with group delay distortions, the results indicated that 64-state QAM was least affected by parabolic distortion followed by sinusoidal and linear.

The selective fading performance of a 64-state QAM system was evaluated in section 4.6. The results indicated that a .05 dB minimum or nonminimum fade centered in the transmit spectrum would degrade the P_e performance by at least 2.4 dB unless techniques were used to combat it. The techniques which might be used to control fades were briefly discussed. However, for this thesis, no attempt was made to determine which techniques to use or how to implement them.

6.2 Suggested Research Topics

The study of modulation techniques with bandwidth efficiencies of over 4 b/s/Hz is just now in its infancy but, because of industry trends this will not last for long. The novelty of 64-state QAM leaves the field of suggested research topics wide open. However, directly related to NLA 64-state QAM, in Chapter 4 a study of the effects of anomalous signal levels was undertaken. This provided a good analysis of the effects of power amplifier power level variations. The effects of power amplifier phase variations, however, were not thoroughly analyzed. Phase variations which can occur due to temperature, aging, and field replacement of an amplifier could have serious consequences. Thus, a further analysis to that presented in Chapter 4 would be very useful.

The simulation programs described in Chapter 2, provide a flexible and powerful tool for analysis. However, because of the immensity of the simulation arrays and the program's complexity an extremely long CPU time is typically required to generate any given set of results (i.e. in the order of 30 minutes on a VAX-11). It would be advantageous to be able to relate any given set of impairments to a specific quantity of degradation. This would represent the next obvious step to be taken with the results given in Chapter 4.

APPENDIX A

APPENDIX A

Technical Information - 64-state QAM Modem

A.1 SERIAL-TO-PARALLEL CONVERTER

A.1.1 Function

The Serial-to-Parallel Converter Unit is used in the 64-state QAM modulator to convert the incoming 384 kb/s data stream into six 64 kb/s parallel data streams. The unit also produces a 64 kHz symbol clock from the 384 kHz master clock.

A.1.2 Circuit Description

A.1.2.1 General

The serial-to-converter circuits can be split into two basic sections. One section performs the dividing of the data and the other performs the dividing of the clock. A technical summary of the serial-to-parallel is given in Table A.1.1. Refer to Fig. A.1.1 for the circuit diagram of the unit. Fig. A.1.2 shows the unit's circuit board.

A.1.2.2 Clock Divide

The 384 kHz master clock enters the unit and is applied to the divide-by-six counter, U1. The output of U1 is used to clock the latch and leaves the unit as the 64 kHz symbol clock.

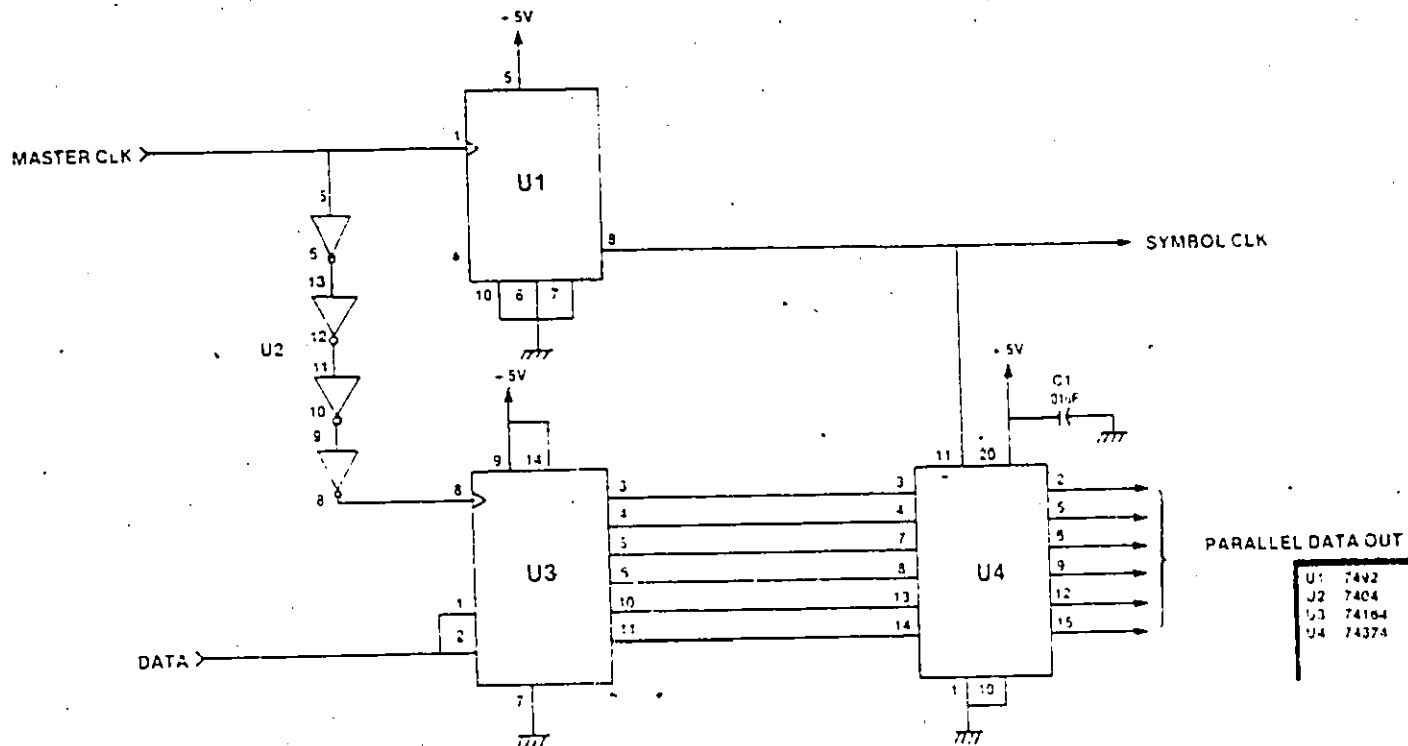
A.1.2.3

The incoming 384 kb/s data in NRZ format is applied to parallel-out serial shift register, U3. The six parallel output data streams of U3 are then clocked through the latch, U4, with

Table A.1.1

Technical summary

Master Clock Input	TTL level, 384 kHz (NRZ)
Data Input	TTL level, pseudo-random, 384 kb/s (NRZ)
Symbol Clock Output	TTL level, 64 kHz (NRZ)
Data Outputs	TTL level, 64 kb/s (NRZ)
Voltage Requirements	+ 5 Vdc



PARALLEL DATA OUT

U1	7442
U2	7404
U3	74164
U4	74374

FIGURE A.1.1 SERIAL-TO-PARALLEL CIRCUIT DIAGRAM

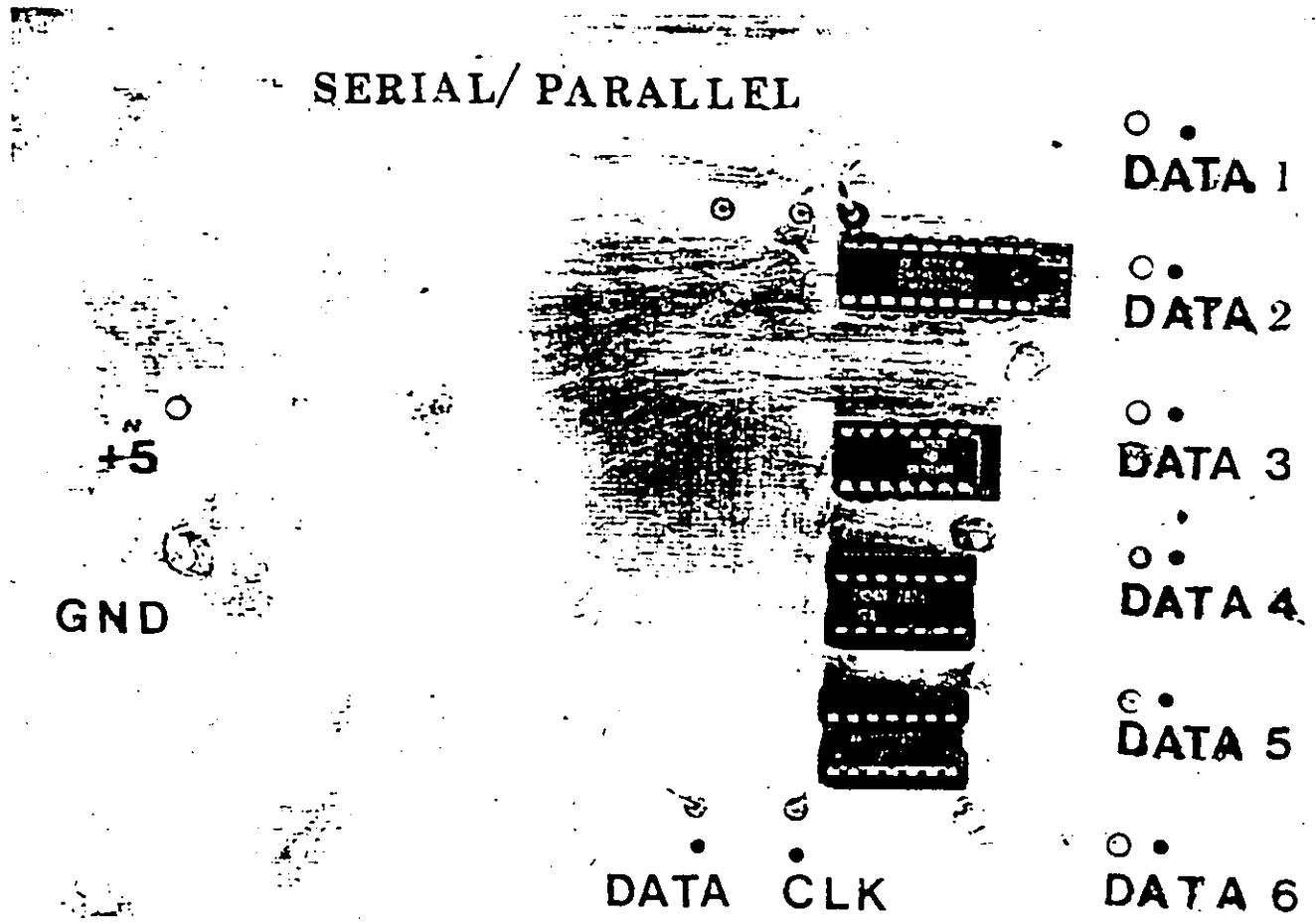


FIGURE A.1.2 SERIAL-TO-PARALLEL CIRCUIT BOARD

the 64 kHz clock. The six 64kb/s data streams leave the unit as the DATA1 through DATA6 signals.

A.2 PREDISTORTION EQUALIZER/LOW PASS FILTER

A.2.1 Function

The Predistortion Equalizer/Low Pass Filter unit is used in the 64-state QAM modulator to predistort and filter the data prior to modulation. Within the unit, the data signal is predistorted to minimize the ISI at the receiver's threshold detector input. The equalized data is then filtered and passed to the quadrature modulator unit. The insertion of the predistortion equalizer/low-pass filter unit in the data paths is controlled by an external switch. This is done on a redundant basis with this unit in all six data paths.

A.2.2 Circuit Description

A.2.2.1 General

The predistortion equalizer/low-pass filter unit contains a predistortion equalizer circuit and a low-pass filter circuit. Refer to Table A.2.1 for a technical summary of the unit. The circuit diagram of the unit is given in Fig. A.2.1 and the circuit board is shown in Fig. A.2.2.

A.2.2.2 Predistortion Equalizer

The incoming data in NRZ format enters the unit and is applied to a delay circuit, U1, to align the data with the other parallel data signals. The delayed data is applied to the

4-tap predistortion equalizer circuit consisting of flip-flops U2-A, U2-B, U3-B. The tap settings may be adjusted using the potentiometers R4, R8, R12, and R16.

A.2.2.3 Low Pass Filter

The output of the predistortion equalizer is amplified and passed to the low-pass filter circuitry. The filter has a fourth order Butterworth frequency response with one additional pole and a 3 dB cutoff frequency of 34 kHz. The level of the output signal is adjusted using potentiometer R21.

Table A.2.1

Technical Summary

Clock Input	TTL level, 64 kHz (NRZ)
Data Input	TTL level, 64 kb/s (NRZ)
Data Output	± 0.8 Vp nominal, 64 kb/s filtered and equalized
Voltage Requirements	+5 Vdc +15 Vdc -15 Vdc

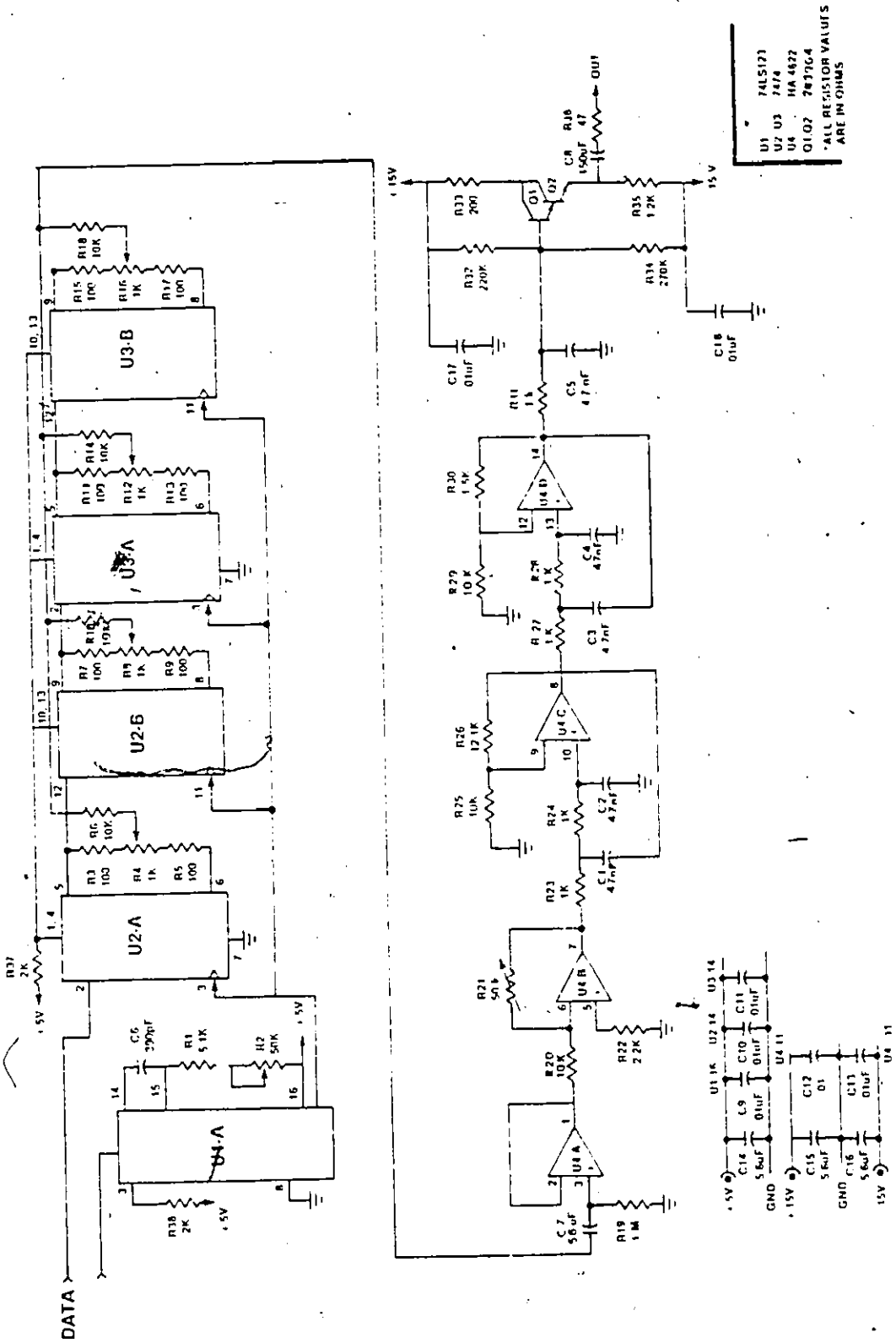
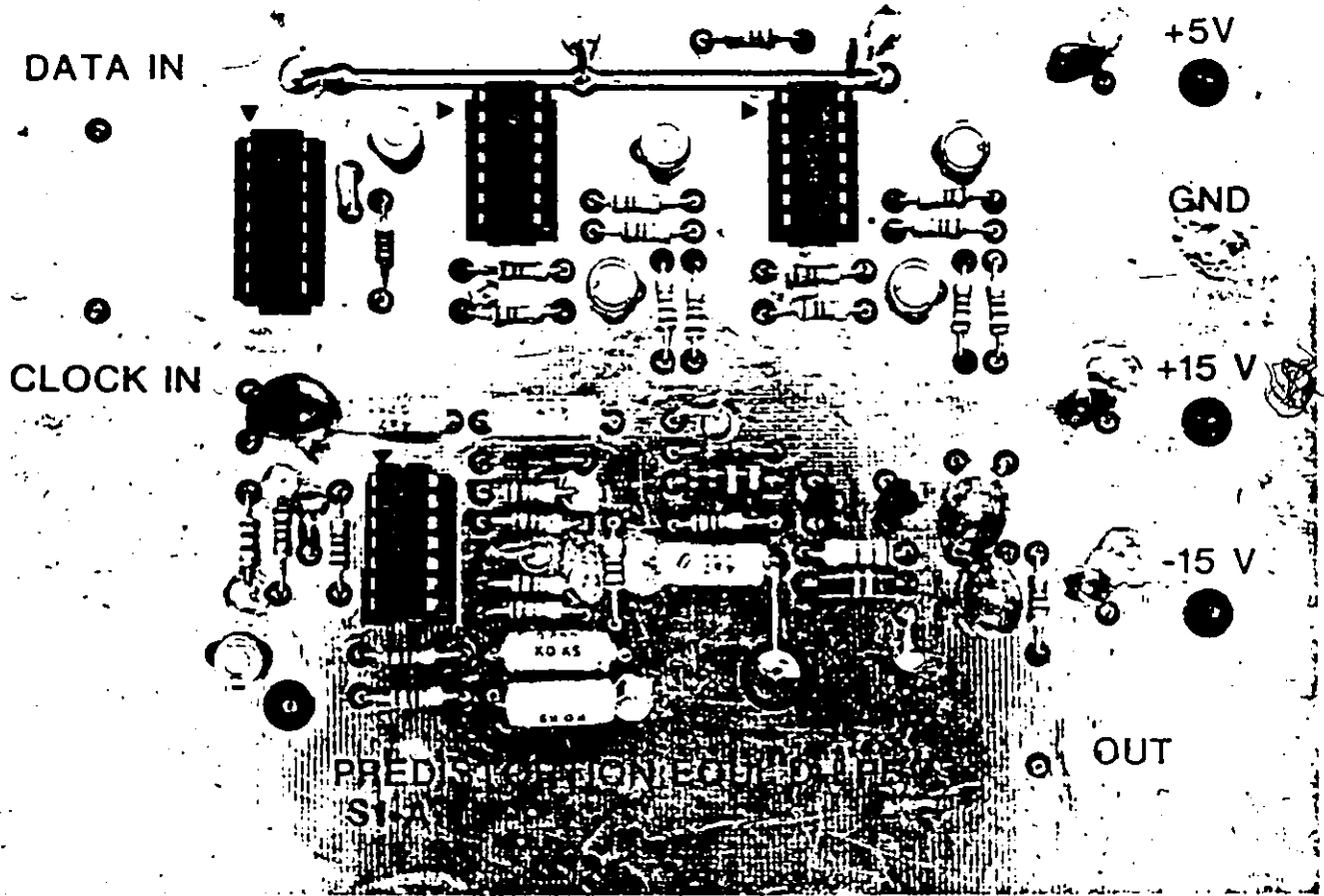


FIGURE A.2.1 PREDISTORTION EQUALIZER AND LOW-PASS FILTER CIRCUIT DIAGRAM



- FIGURE A.2.2 PREDISTORTION EQUALIZER LOW-PASS FILTER
CIRCUIT BOARD

A.3 QUADRATURE MODULATOR

A.3.1 Function

The Quadrature Modulator unit is used in the 64-state QAM modem to amplitude modulate two 1 MHz quadrature carriers with two data streams 'I' and 'Q'. The modulated signals are combined and passed to subsequent units. This is done on a redundant basis with three Quadrature Modulator units in the 64-state QAM modulator.

A.3.2 Circuit Description

A.3.2.1 General

Refer to Table A.3.1 for a technical summary. Because of the quadrature relationship between the carriers, and the modulation of each carrier, the output signal is designated as a QPSK signal. Fig. A.3.1 is the unit circuit diagram and Fig. A.3.2 shows the circuit board.

A.3.2.2 Carrier Phase Shift

The input 1 MHz carrier signal is split and applied to the phase shift circuitry consisting of IC's U2-A and U2-B. The level and phase of the two carrier signals is set with the potentiometers R1, R2, R21, and R22, respectively. The outputs of the circuitry are two quadrature carrier signals of equal amplitudes.

A.3.2.3 QPSK Modulator

The unit accepts two filtered or unfiltered data streams,

'I' and 'Q', and buffers and applies them to mixers U3 and U4, respectively. Buffering provides appropriate data levels and impedance matching for the mixers. Potentiometers R6 and R26 are used to set the levels of the input 'I' and 'Q' data streams respectively. The modulated output signal of each mixed is passed to the output combiner circuit, U1. The output from U1 is a QPSK modulated signal with the third and higher harmonics suppressed by at least 30 dB.

Table A.3.1

Technical Summary

Carrier Input	1.5 Vp-p sine wave at 1 MHz
Data Inputs	NRZ with no dc component at 64 kb/s filtered or unfiltered
Output Signal	80 mVp-p nominal centered at 1 MHz
Voltage Requirements	+15 Vdc -15 Vdc

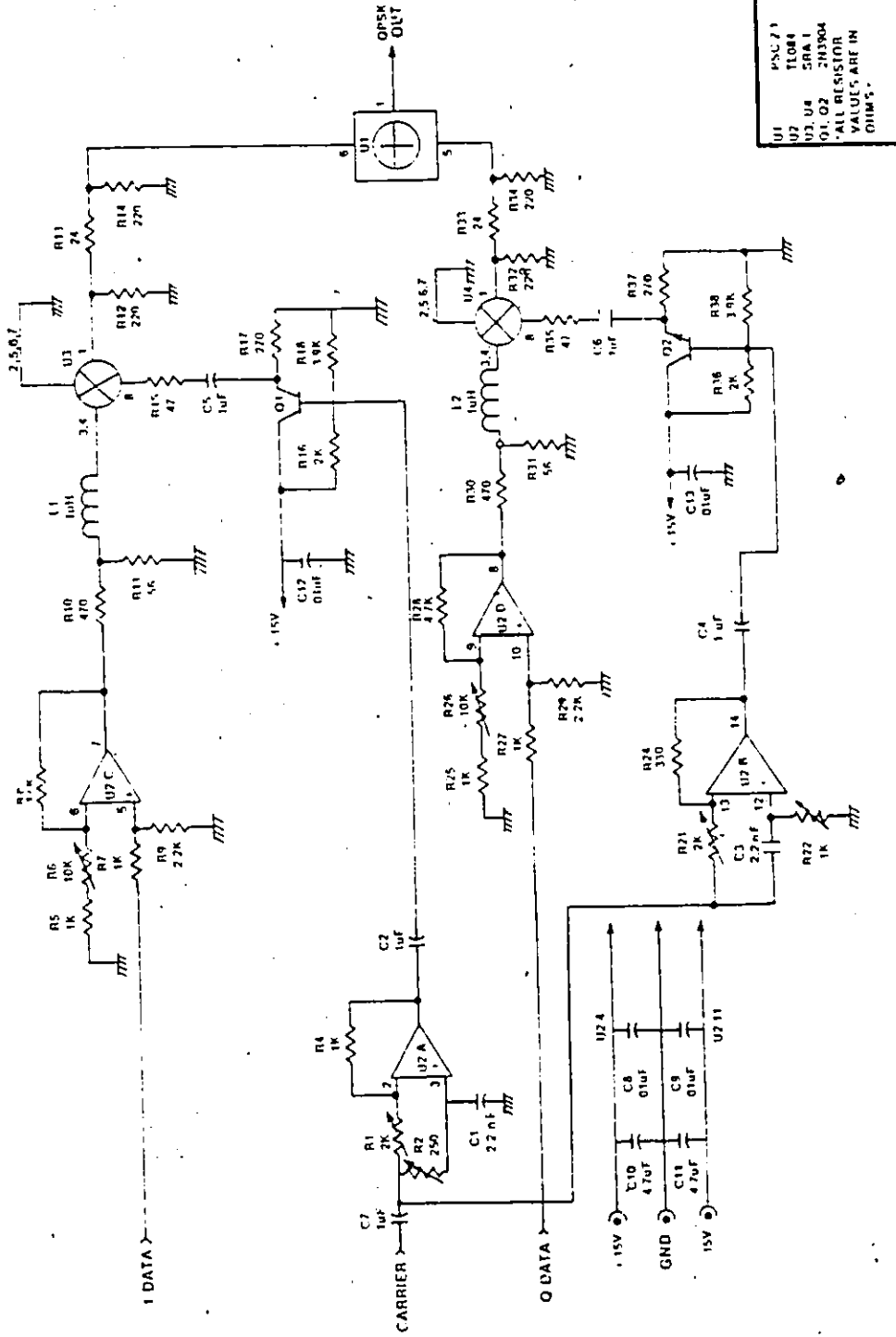


FIGURE A.3.1 QUADRATURE MODULATOR CIRCUIT DIAGRAM

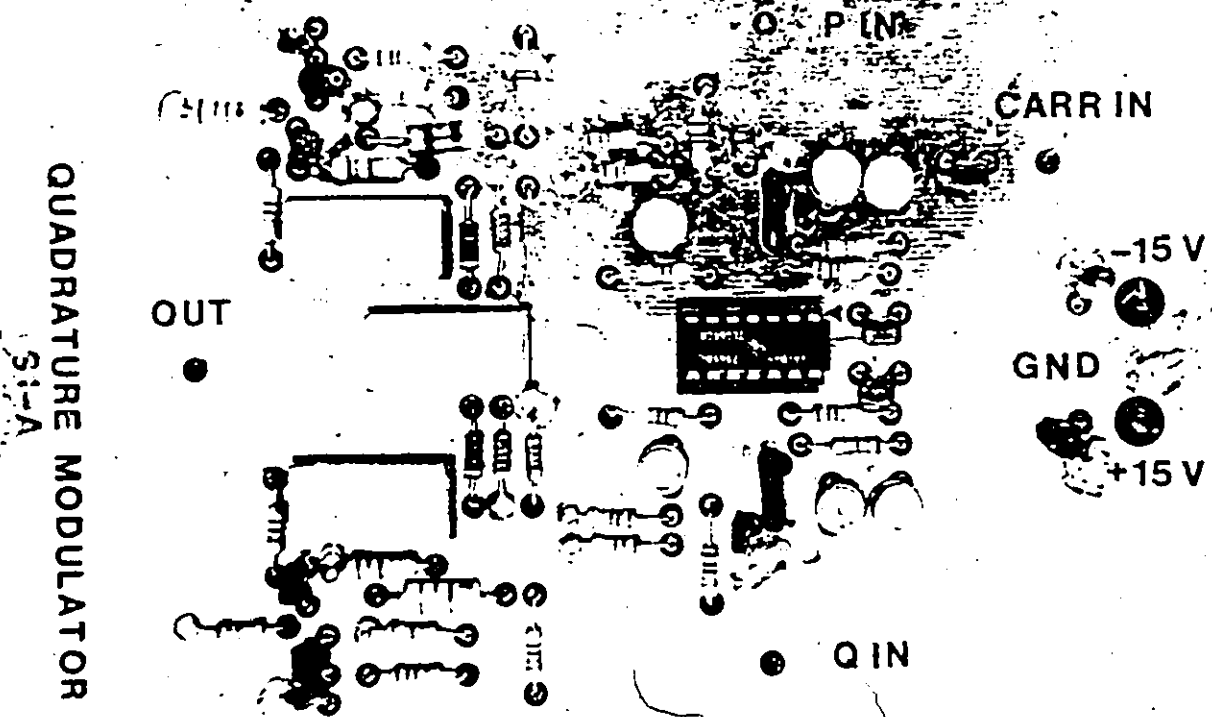


FIGURE A.3:2 QUADRATURE MODULATOR CIRCUIT BOARD

A.4 HARD LIMITER

A.4.1 Function

The Hard Limiter unit is used in the NLA 64-state QAM modulator to limit the QPSK modulated signals. The unit received QPSK modulated signals from the three quadrature modulator units and produces three hard limited QPSK signals. The insertion of the hard limiter unit in the signal path is controlled from an external switch.

A.4.2 Circuit Description

A.4.2.1 General

The hard limited unit consists of three hard limiter circuits, one for each QPSK signal. Refer to Fig. A.4.1 for the hard limiter circuit diagram. The unit's technical summary is provided in Table A.4.1.

A.4.2.2 Hard Limiter Circuit

Each QPSK modulated signal enters the unit and is buffered and passed to a hard limiter circuit. The limiter circuit compares the incoming signal to a 0 Vdc reference voltage. The hard limited signal is passed through a 4 dB, 50 ohm pad to the output of the unit. The three output signals are applied to the combiner unit.

Table A.4.1

Input Signal	80 mVp-p nominal, QPSK signal centered at 1 MHz
Output signal	100 mVp-p nominal, hard limited QPSK signal centered at 1 MHz
Voltage Requirements	+ 5 Vdc -15 Vdc

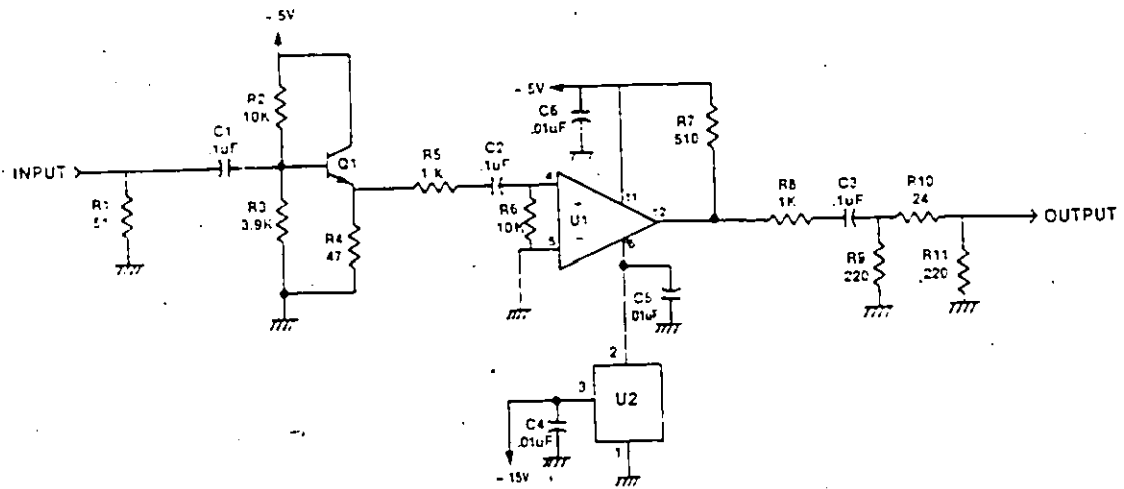


FIGURE A.4.1 HARD LIMITER CIRCUIT DIAGRAM

A.5 COMBINER

A.5.1 Function

The combiner unit is used in the transmitter side of the 64-state QAM modem. The unit receives three QPSK signals from a hard limiter unit or QPSK modulator units and produces a 64-state QAM signal. The output signal of the unit is passed to subsequent receiver units.

A.5.2 Circuit Description

A.5.2.1 General

The combiner unit weights and sums three QPSK modulated signals. A technical summary of the combiner is given in Table A.5.1. Refer to Fig. A.5.1 for the circuit diagram of the unit and Fig. A.5.2 for the circuit board.

A.5.2.2 Weighting

QPSK signals entering the combiner unit are amplified to specified power levels by U1, U2 or U3. The output power level of the signal from U1 is 12 dB higher than that from U3 and 6 dB higher than that from U2. The amplified signals are passed to the summing circuitry.

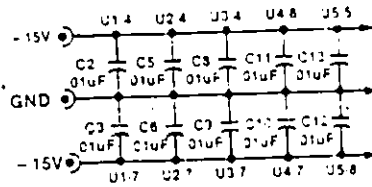
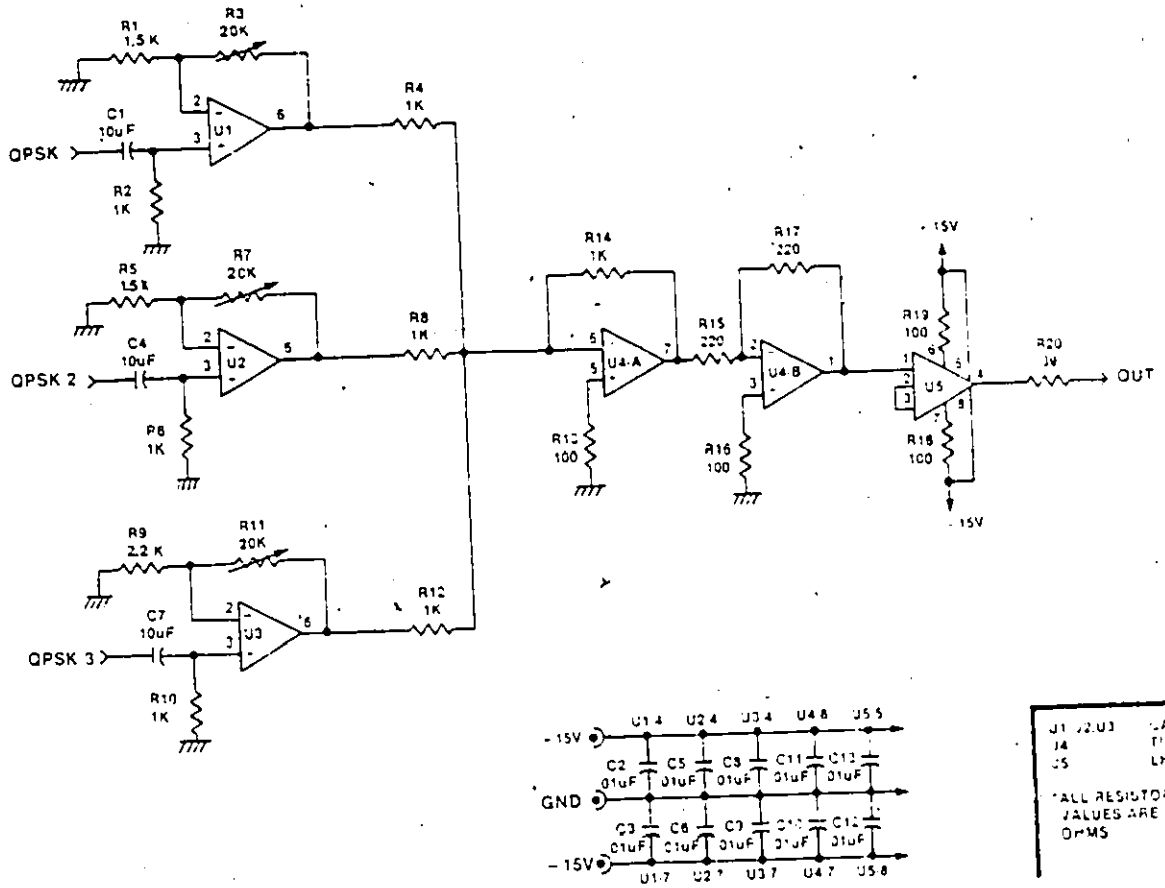
A.5.2.3 Summing

The inputs to the summing circuitry are combined and passed to two inverting operational amplifiers U4-A and U4-B. The summed output of these IC's is applied to a buffer circuit, U5 and passed to the output of the unit as the 64-state QAM signal.

Table A.5.1

Technical summary

Signal Inputs	QPSK at 1 MHz, 80 mVp-p nominal or hardlimited QPSK at 1 MHz, 100 mVp-p nominal
Signal Output	64-state QAM, 300 mVp-p nominal or NLA 64-state QAM, 300 Vp-p nominal
Voltage Requirements	+ 15 Vdc - 15 Vdc



U1, U2, U3	LA3100
U4	TJ82
U5	LH0033

ALL RESISTOR VALUES ARE IN OHMS

FIGURE A.5.1 COMBINER CIRCUIT DIAGRAM

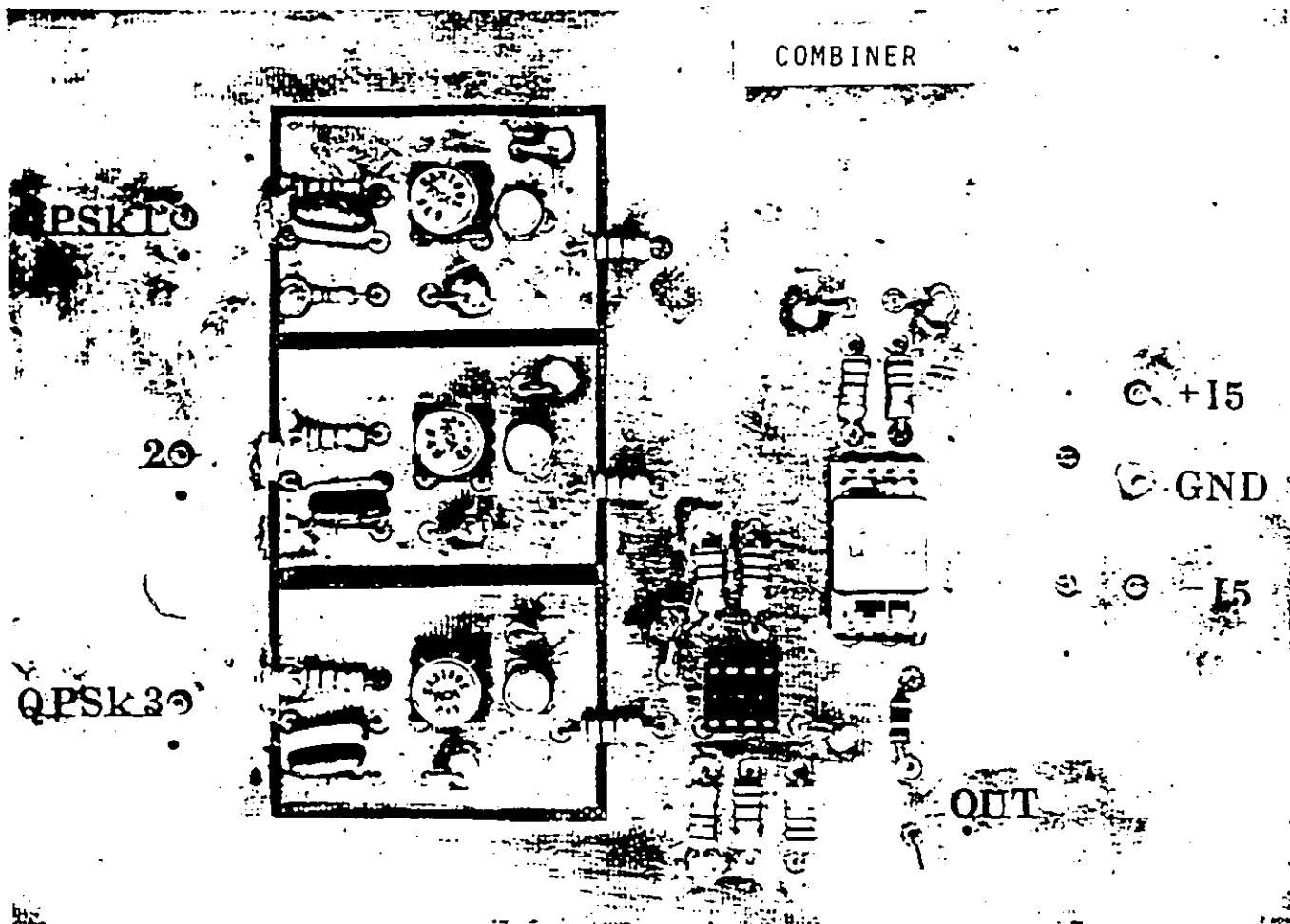


FIGURE A.5.2 COMBINER CIRCUIT BOARD

A.6 QUADRATURE DEMODULATOR

A.6.1 Function

The Quadrature Demodulator unit together with the post detection low-pass filter unit demodulates the 1 MHz modulated signal and recovers the symbol streams. Because the carrier and symbol timing signals are hardwired, no carrier or symbol timing recovery circuitry is needed.

A.6.2 Circuit Description

A.6.2.1 General

Refer to Table A.6.1 for a technical summary. The Demodulator unit accepts a 1 MHz 64-state QAM signal and extracts the 'I' and 'Q' symbol streams. Fig. A.6.1 is the circuit diagram of the demodulator. The circuit board is shown in Fig. A.6.2.

A.6.2.2 Carrier Phase shift

The 1 MHz carrier signal is split and applied to the phase shift circuitry consisting of IC's U1-A and U1-B. This circuitry provides impedance matching for the mixers and the appropriate carrier levels and phases for the mixer. The outputs of this circuitry are two quadrature carrier signals in-phase with the modulated input signal.

A.6.2.3 Quadrature Demodulator

The 64-state QAM signal is split in U2 and U3 to provide one signal for the future implementation of a carrier recovery circuit and identical signals to two mixers, U4, and U5. The quadrature carriers are applied to the mixers. One mixer extracts

the 'I' symbol stream, and the other mixer extracts the 'Q' symbol stream. The 'I' and 'Q' streams are forwarded to separate post-detection low-pass filters.

Table A.6.1

Technical Summary

Input Carrier Signal	1 Vp-p sine wave at 1 MHz
Input Modulated Signal	100 mVp-p nominal centered at 1 MHz
Signal Outputs	70 mVp-p nominal at 64 kBaud
Voltage Requirements	+15 Vdc -15 Vdc

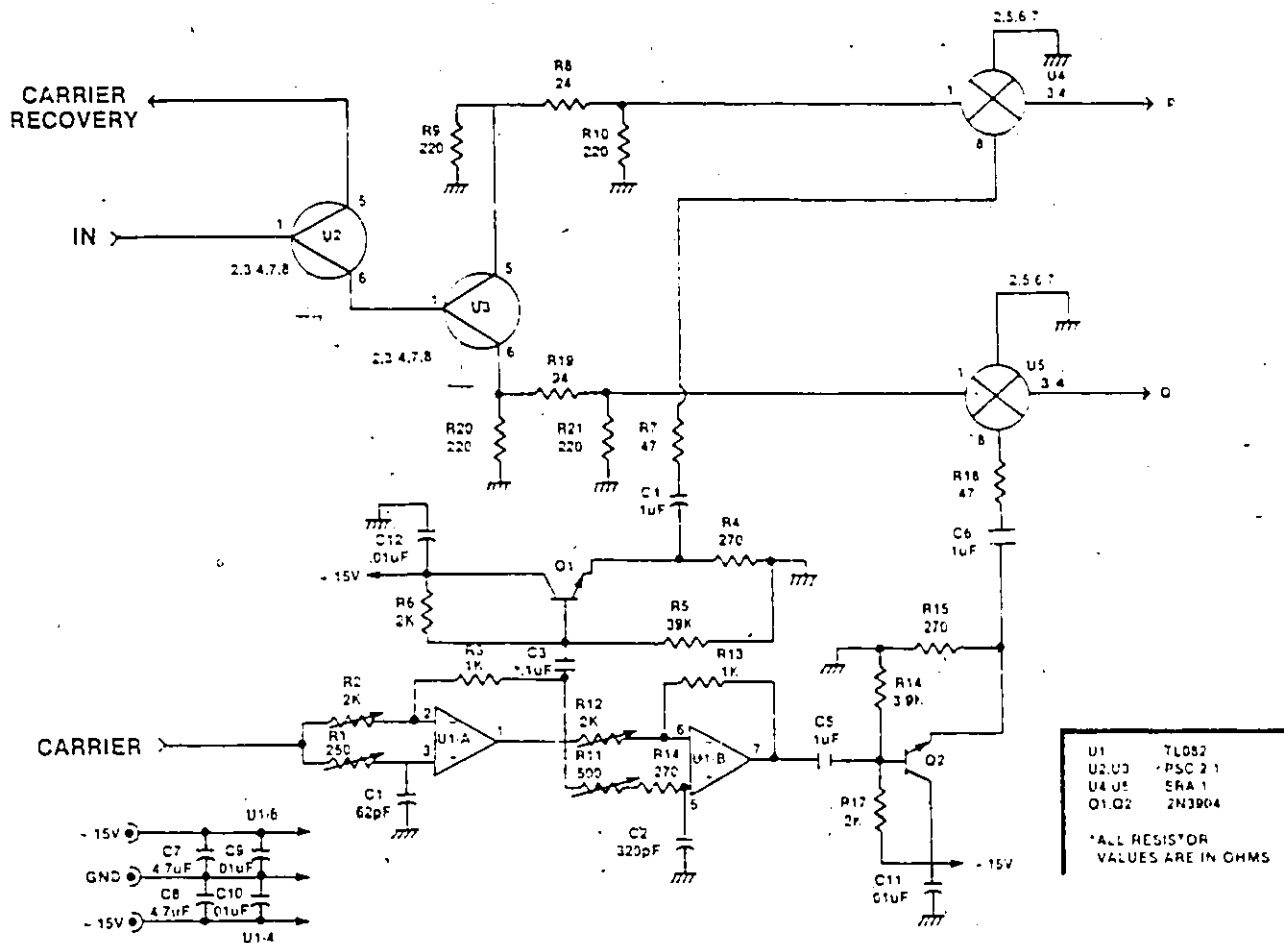


FIGURE A.6.1 QUADRATURE DEMODULATOR CIRCUIT DIAGRAM

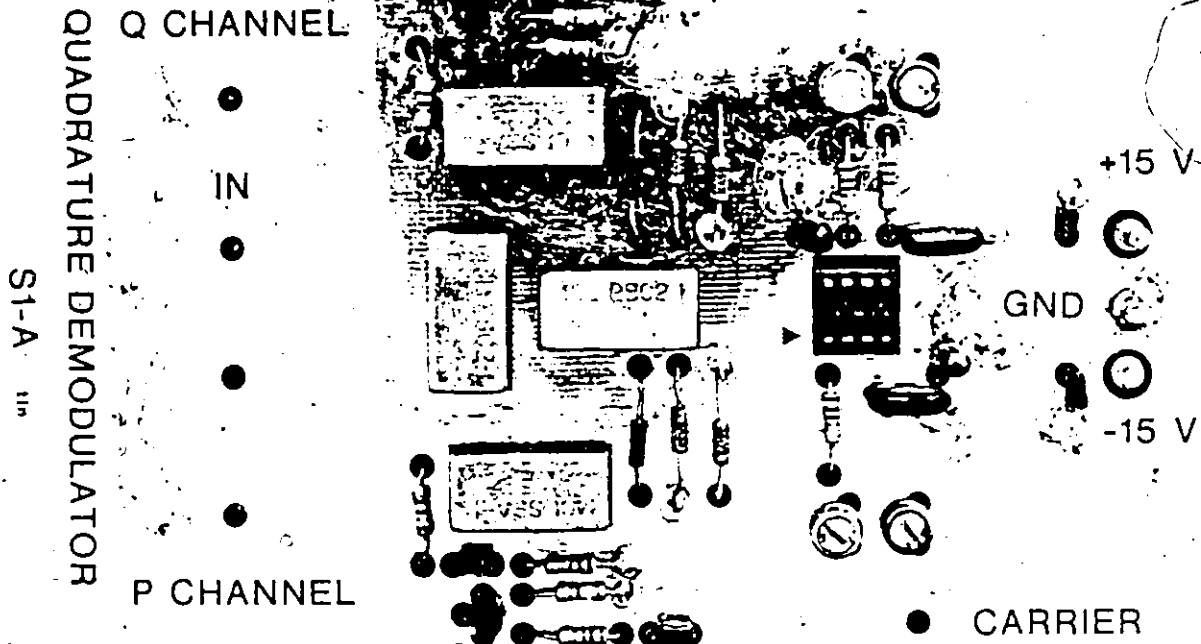


FIGURE A.6.2 QUADRATURE DEMODULATOR CIRCUIT BOARD

A.7 POST DETECTION LOW PASS FILTER

A.7.1 Function

The Post Detection Low Pass Filter unit is used in the 64-state QAM demodulator to remove noise, interference, and second order harmonics. This unit also amplifies and level-shifts the filtered signal. The ± 2.5 Vp filtered output signal is passed to subsequent units.

A.7.2 Circuit Description

A.7.2.1 General

A technical summary of the low-pass filter unit is given in Table A.7.1. Refer to Fig. A.7.1 for the circuit diagram.

A.7.2.2 Low-Pass Filter

The in-phase or quadrature signals from the quadrature demodulator enter the unit and are applied to the low-pass filter circuitry. The filter comprised of IC's U4-B and U4-C has a 3 dB cutoff frequency of 36 kHz, and a fourth order Butterworth frequency response with one additional pole.

A.7.2.3 Amplifier and Level Shifter

The filtered signal is passed to the amplifier and level shifting circuitry. The output amplitude of the 8-level filtered signal is set using potentiometers R21 and R41. A 0 Vdc center voltage of the output signal is adjusted using potentiometer R38.

Table A.7.1

Technical summary

Input Signal	70 mVp-p nominal
Output Signal	± 2.5 Vp 8-level filtered data at 64 kBaud
Voltage Requirements	+ 15 Vdc - 15 Vdc

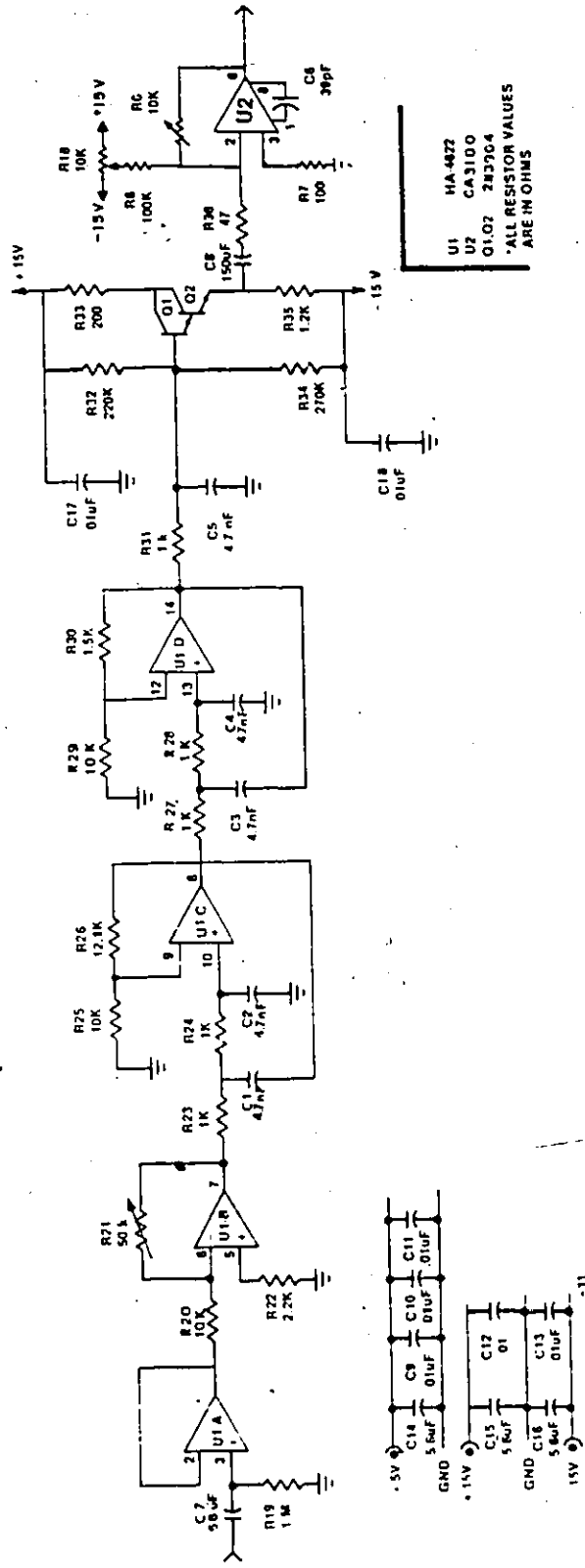


FIGURE A.7.1 LOW-PASS FILTER CIRCUIT DIAGRAM

A.8 EIGHT-TO-TWO LEVEL CONVERTER/PARALLEL-TO-SERIAL CONVERTER

A.8.1 Function

The Eight-to-Two Level/Parallel-to-Serial Converter Unit is used in the 64-state QAM demodulator to convert the demodulated signals into a single 384 kb/s data stream. The unit receives the 'I' and 'Q' demodulated signals from the post detection low-pass filter units and the symbol clock, which is hardwired, and center samples the demodulated signals. The sampled signals are converted into digital data streams and then multiplexed into a single data stream representing the recovered data.

A.8.2 Circuit Description

A.8.2.1 General

As the name of the unit implies, the circuits can be split into two basic sections. One section performs the sampling threshold detection, and the other section performs the parallel-to-serial conversion. A technical summary of the unit is given in Table A.8.1 for the circuit diagram and Fig. A.8.2 for the circuit board.

A.8.2.2 Eight-to-Two Level Converter

The 64 kHz symbol clock enters the unit and is applied to variable delay circuits, U2 and U4. The delay of the clock through these units is adjusted, using R27, R28, and R7, R8 respectively. This enables the demodulated data at the samplers,

U5, and U9 to be center sampled at the maximum eye opening. The sampled symbols are each analog-to-digital converted, U6 and U8, into three parallel bit streams. The delay of the symbol clock into U6 and U8 is set using R31, R32 and R11, R12.

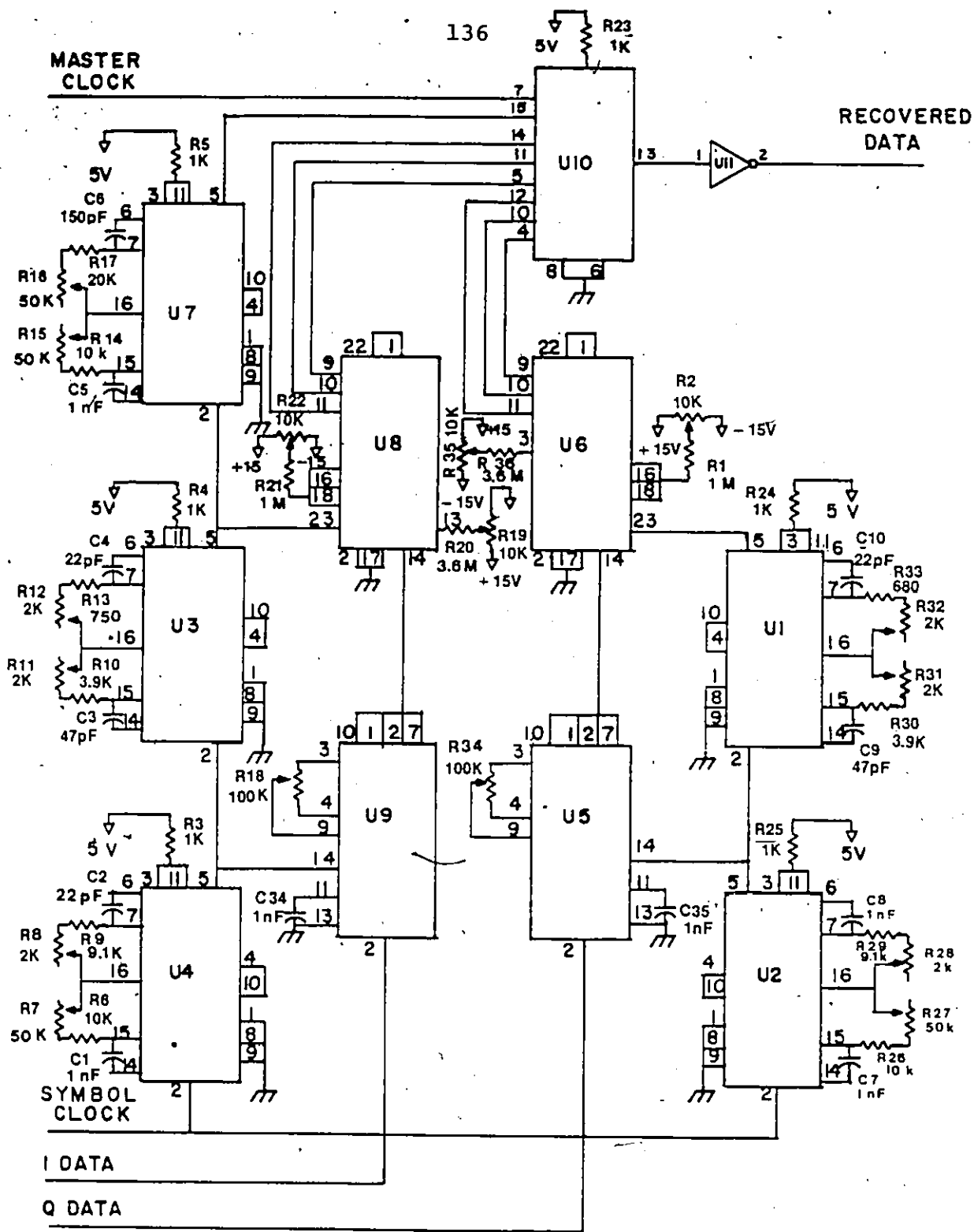
A.8.2.3 Parallel-to-Serial Converter

The six parallel 64 kb/s data streams are multiplexed into a single 384 kb/s data stream in U10. The 64 kb/s data streams are read into U10 with a delayed symbol clock, the delay is adjusted using R15 and R16, and read out with the 384 kb/s master clock.

Table A.8.1

Technical Summary

Symbol Clock Input	TTL level, 64 kHz (NRZ)
Demodulated Input Signals	+/- 2.5 Vp 8-level filtered data at 64 kBaud
Master Clock Input	TTL level, 384 kHz (NRZ)
Data Output	TTL level, pseudo-random, 384 kb/s (NRZ)
Voltage Requirement	+ 5 Vdc +15 Vdc -15 Vdc



UNLESS OTHERWISE SPECIFIED:

- RESISTOR VALUES ARE IN OHMS \pm 5%, 1/4 W.

- U1,U2,U3,U4,U7 74LS123
- U5,U9 AD583
- U6,U8 ADC82
- U11 74166
- U10 7404

FIGURE A.8.1 EIGHT-TO-TWO LEVEL CONVERTER/PARALLEL-TO-SERIAL CONVERTER CIRCUIT DIAGRAM

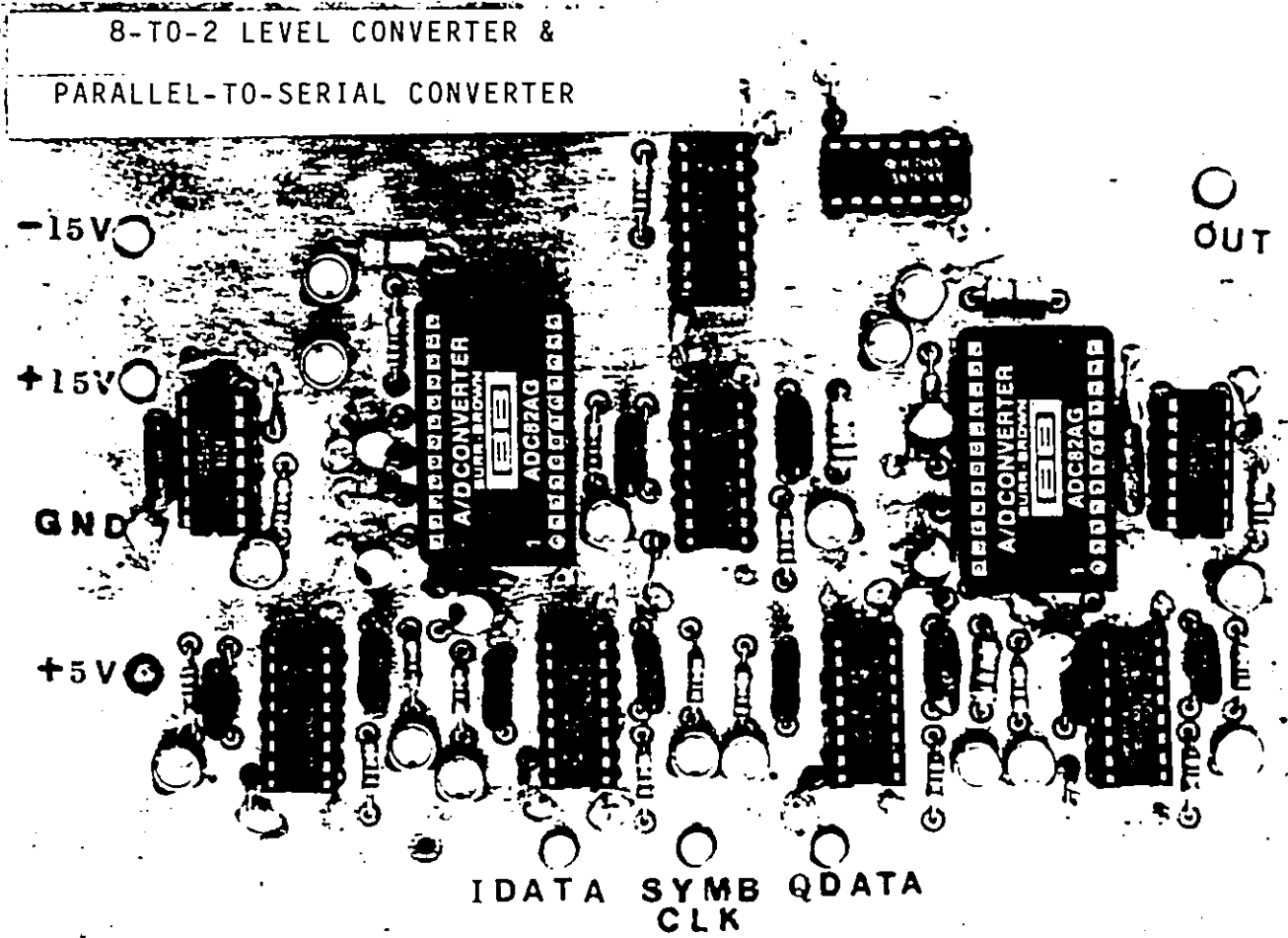


FIGURE A.8.2 EIGHT-TO-TWO LEVEL CONVERTER/PARALLEL-TO-SERIAL CONVERTER CIRCUIT BOARD

APPENDIX, B

APPENDIX B

B.1 Introduction

This appendix contains listings of the computer programs which were used to evaluate the performance of 64-state QAM systems. It has been included in this thesis for completeness at the request of Dr. Feher. The programs are based on those given in DCL report 214. They are written in FORTRAN IV and ran on AMDHAL V7A and VAX-11 computers using FORTRAN IV G LEVEL and FORTRAN IV PLUS compilers respectively.

Three programs for the analysis of 64-state QAM are given in the succeeding sections. The first simulates linearly amplified 64-state QAM in a channel with practically encountered amplitude and group delay characteristics. A block diagram of this simulation model is depicted in Fig. B.1.1. The second program simulates NLA 64-state QAM where the nonlinear devices modelled include an HPA/TWT and a hardlimiter. Figure B.1.2 shows a block diagram of this second simulation model. The third program, whose block diagram is shown in Fig. B.1.3, is used in the study of the effects of cochannel and adjacent channel interference.

In all three programs the simulation is based on the equivalent baseband concept and many of the same subroutines are used in the programs. The subroutines which are common to all of

the programs will be listed with the first program. Only those subroutines peculiar to the other programs will be listed with them.

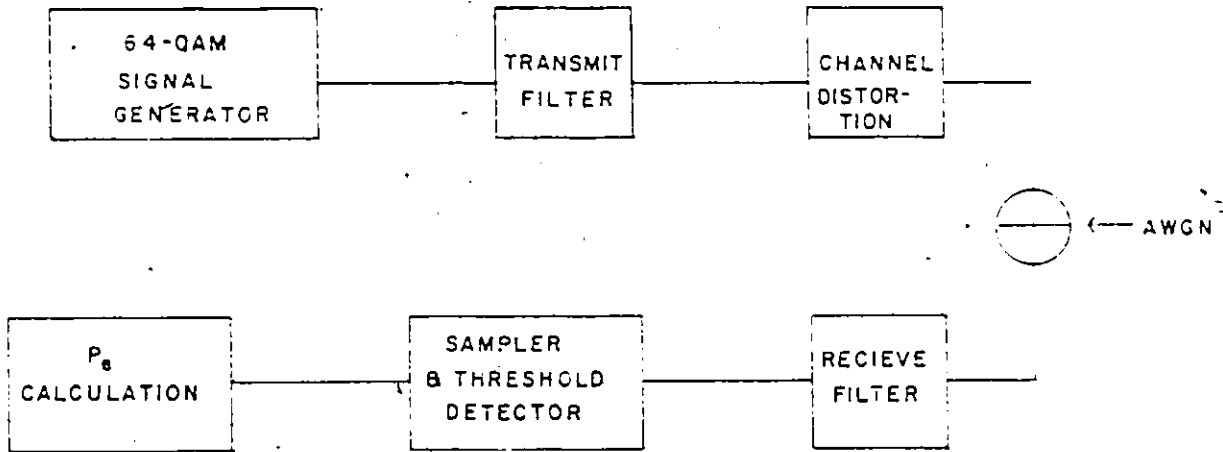


FIGURE B.1.1 64-STATE QAM SIMULATION MODEL

```

C*****
C PROGRAM FOR SIMULATION OF 64-QAM WITH CHANNEL DISTORTIONS
C THE PROGRAM IS BASED ON DCL REPORT #112 BY DR. V. ARUNACHALAM.
C COPYRIGHT UNIVERSITY OF OTTAWA.
C
C BY TRICIA HILL
C*****
COMPLEX DATA(65536),TF(65536)
DIMENSION PEI(25),EBNO(25),NI(2048),NQ(2048)
DIMENSION XARRAY(27),YARRAY(27)
C
C INITIALIZE PROGRAM.
C SET PARAMETERS FOR RUN
C
COMMON /NUMB1/ FBW,ALPHA,LDIM,IOFF,LSAMPL
COMMON /NUMB2/ NSNR,NSYMB,BAUD
FBW=7.5
ALPHA=0.4
LDIM=65536
IOFF=0
LSAMPL=32
NSNR=25
NSYMB=2047
BAUD=15.0
NFILTR=2
NRUNS=5
ISIN=1
C END OF INITIALIZATION.
C
C START OF COMPUTATIONS.
C
DO 100 NR=1,NRUNS
CALL LOAD64(DATA,NI,NQ)
CALL RCOSTX(TF)
C
C SELECT CHANNEL DISTORTION
C
CALL LINAMP(Z,TF)
CALL PARAMP(P,TF)
CALL SINAMP(ISIN,D,K,TF)
CALL LINGD(B,TF)
CALL PARGD(S,TF)
K=4
C=6.0*(NR-1)
CALL SINGD(ISIN,C,K,TF)
C CALL RUMAMP(B,FO,TF)
C CALL RUMPHA(B,FO,IMIN,TF)
CALL FILTER(DATA,TF)
CALL ENERGY(DATA,EB){ CALL RCOSRX(TF)
CALL HHGG(TF,PNOISE)
CALL FILTER(DATA,TF)
CALL SYNCRO(DATA,PNOISE,NI,NQ,MI,MQ,EB)
CALL DECODE(DATA,PNOISE,MI,MQ,NI,NQ,

```

```
#EBNO,PEI,EB)
```

```
C  
C CALL THE DRAWING ROUTINE.  
C  
C DO 99 I=1,NSNR  
C XARRAY(I)=EBNO(I)  
C 99 YARRAY(I)=PEI(I)  
C CALL DRAW(XARRAY,YARRAY,NR,NRUNS)  
C  
C 100 CONTINUE  
C STOP  
C *****  
C END OF MAIN PROGRAM.  
C *****  
C END
```

```

*****
C   LOAD64
C
C   THIS SUBROUTINE GENERATES A BASEBAND 64-QAM SIGNAL.
C   INPUT PARAMETERS: LDIM,IOFF,LSAMPL
C   OUTPUT PARAMETERS: DATA,NI,NQ
C
C   LDIM      -THE DIMENSION OF THE COMPLEX DATA ARRAY.
C   IOFF     -THE NUMBER OF SAMPLES THE Q CHANNEL DATA IS
C             OFFSET FROM THE I CHANNEL DATA.
C   LSAMPL   -THE NUMBER OF SAMPLES PER SYMBOL.
C   DATA    -THE COMPLEX DATA ARRAY IN THE TIME DOMAIN.
C   NI       -THE I CHANNEL SYMBOL ARRAY.
C   NQ       -THE Q CHANNEL SYMBOL ARRAY.
C
C   THIS SUBROUTINE GENERATES TWO 8-LEVEL SYMBOL ARRAYS,
C   NI AND NQ, AND THE BASEBAND 64-QAM DATA ARRAY. A GENERATOR
C   POLYNOMIAL OF DEGREE 11 IS USED TO GENERATE A PRBS OF NRZ
C   DATA FROM THE PRIMER DATA NY.  $G(X)=1+X^{2}+X^{11}$ 
C   A SEQUENCE OF  $2^{11}$  DATA SYMBOLS IS GENERATED WITH THE FIRST
C   SYMBOL REPEATED AS THE LAST SYMBOL. THIS SEQUENCE IS SHIFTED
C   FIVE TIMES TO PROVIDE FIVE ADDITIONAL SEQUENCES. THE TWO
C   SETS OF THREE SEQUENCES ARE THEN 8-TO-2 LEVEL CONVERTED
C   TO FORM THE I CHANNEL SYMBOLS AND THE Q CHANNEL SYMBOLS.
C   THESE SYMBOLS ARE THEN LOADED IN THE COMPLEX DATA ARRAY
C   WITH A SET NUMBER OF SAMPLES REPRESENTING EACH SYMBOL(LSAMPL).
C   THE REAL PART OF THE DATA ARRAY CORRESPONDS TO THE I COMPONENT
C   AND THE IMAGINARY PART CORRESPONDS TO THE Q COMPONENT.
*****

```

```

C
SUBROUTINE LOAD64(DATA,NI,NQ)
COMPLEX DATA(1)
DIMENSION NY(11),NI(1),NQ(1),NX(2048)
COMMON /NUMB1/ FBW,ALPHA,LDIM,IOFF,LSAMPL
C DATA NX(1),NX(2),NX(3),NX(4),NX(5),NX(6),NX(7),NX(8),NX(9),
C #NX(10),NX(11),NX(12)/-1,-1,-1,-1,-1,-1,-1,-1,-1,-1,-1/
DATA NY(1),NY(2),NY(3),NY(4),NY(5),NY(6),NY(7),NY(8),NY(9),
#NY(10),NY(11)/-1,-1,1,1,1,1,-1,-1,-1,-1,-1/
DATA JLAST,JTAP/11,1/
KKK=2**JLAST
KK=KKK-(1+JLAST)
DO 6 I=1,JLAST
NX(I)=NY(I)
6 CONTINUE

C
C GENERATE 2**JLAST -1 LENGTH SEQUENCE USING GIVEN DATA AND
C GENERATOR POLYNOMIAL.
C
DO 1 J=1,KK
I=J+JLAST
NX(I)=NX(J)*NX(J+2)
NX(I)=0-NX(I)
1 CONTINUE

C
C GENERATE 6 CYCLICALLY SHIFTED VERSIONS OF ORIGINAL
C SEQUENCE OF LENGTH 2**JLAST.
C
K1=1
K2=2
K3=3
K4=4
K5=5
K6=6
DO 2 I=1,KKK
IF (K1.EQ.KKK) K1=1
IF (K2.EQ.KKK) K2=1
IF (K3.EQ.KKK) K3=1
IF (K4.EQ.KKK) K4=1
IF (K5.EQ.KKK) K5=1
IF (K6.EQ.KKK) K6=1
NI(I)=(NX(K1)*4) + (NX(K3)*2) + NX(K5)
NQ(I)=(NX(K2)*4) + (NX(K4)*2) + NX(K6)

C
C LOAD INTO SAMPLE ARRAY, 16 SAMPLES PER SYMBOL
J1=(I-1)*LSAMPL+1
J2=I*LSAMPL
DO 3 J3=J1,J2
3 DATA(J3)=CMPLX(FLOAT(NI(I)),FLOAT(NQ(I)))
K1=K1+1
K2=K2+1
K3=K3+1

```

```
K4=K4+1
K5=K5+1
K6=K6+1
2 CONTINUE
IF(IOFF.EQ.0) RETURN
LL=LDIM-1
DO 4 I=1, IOFF
XX=AIMAG(DATA(I))
DO 5 K=1, LL
5 DATA(K)=CMPLX(REAL(DATA(K)), AIMAG(DATA(K+1)))
4 DATA(LDIM)=CMPLX(REAL(DATA(LDIM)), XX)
RETURN
END
C
```

```

*****
C
C   RCOSTX:
C
C   THIS SUBROUTINE DEVELOPS THE TRANSFER FUNCTION OF A SQUARE
C   ROOT OF RAISED-COSINE FILTER WITH 1/SINX EQUALIZATION; WITH
C   ROLL-OFF 'ALPHA' AND A 3dB BANDWIDTH OF 'FBW'.
C
C   INPUT PARAMETERS: ALPHA, LSAMPL, BAUD, LDIM, FBW
C   OUTPUT PARAMETER: TF
C
C   ALPHA      -THE AMOUNT OF BANDWIDTH USED IN EXCESS OF THE
C               MINIMUM NYQUIST BANDWIDTH DIVIDED BY THE NYQUIST
C               BANDWIDTH.
C   LSAMPL     -THE NUMBER OF SAMPLES PER SYMBOL.
C   BAUD       -THE SYMBOL RATE IN MBaud.
C   LDIM       -THE DIMENSION OF THE COMPLEX TF ARRAY.
C   FBW        -THE LOW-PASS FILTER 3dB BANDWIDTH IN MHz.
C   TF         - RESULTANT COMPLEX TRANSFER FUNCTION OF THE FILTER.
C
C   THE TRANSFER FUNCTION IS MODELLED AS FOLLOWS:
C
C   TF(f)=PI*f*T/(SIN(PI*f*T)   FOR 0<f<FN(1-ALPHA)
C   TF(f)=PI*f*T/(SIN(PI*f*T))*SQRT(.5*(1-SIN(PI*(f-FN)))/
C   2*ALPHA*FN                 FOR FN(1-ALPHA)<f<FN(1+ALPHA)
C   TF(f)=0                    FOR f>FN(1+ALPHA)
C
C   WHERE   PI=3.1415927
C           FN=NYQUIST FREQUENCY
C           T=SYMBOL DURATION.
C
*****

```


C

```

SUBROUTINE RCOSTX(TF)
  COMPLEX TF(65536)
  COMMON /NUMB1/ FBW,ALPHA,LDIM,IOFF,LSAMPL
  COMMON /NUMB2/ NSNR,NSYMB,BAUD
  SBANDW=BAUD*LSAMPL
  NO=LDIM/2
  NO1=NO+1
  IF (ALPHA.EQ.0) ALPHA=0.0001
  FN=LDIM*(FBW/SBANDW)
  F1=(1.-ALPHA)*FN
  F2=(1.+ALPHA)*FN
  IFN=IFIX(FN)
  IF1=IFIX(F1)+1
  IF2=IFIX(F2)+1

```

C

C

C

```

THE AMPLITUDE CHARACTERISTICS

```

```

  A1=3.141516/(2.*FLOAT(IFN))
  DO 8 I=2,IF1
  TF(I)=CMPLX(1.0,0.0)
  J=I-1

```

C

C

C

```

X/SIN(X) EQUALIZATION

```

```

  A2=(FLOAT(J)*A1)/(SIN(FLOAT(J)*A1))
  TF(I)=CMPLX(A2,0.0)
8 CONTINUE
  JK=IF1+1
  DO 9 J=JK,IF2
  I=J-1

```

C

C

C

```

ROOT OF RAISED COSINE

```

```

  A3=(FLOAT(I)*A1)/(SIN(FLOAT(I)*A1))
  A=(3.141516/(2.0*ALPHA))*((FLOAT(I)/FLOAT(IFN))-1.)
  TF(J)=CMPLX(SQRT(0.5*(1.0-SIN(A))),0.0)
  TF(J)=TF(J)*CMPLX(A3,0.0)
8 CONTINUE
  JH=IF2+1
  DO 10 I=JH,NO1
  TF(I)=CMPLX(0.0,0.0)
10 CONTINUE
  NO2=NO1+1
  DO 5 I=NO2,LDIM
  TF(I)=CONJG(TF(LDIM+2-I))
5 CONTINUE
  RETURN
  END

```

C

```

*****
C.  LINAMP:
C
C  THIS SUBROUTINE DEVELOPS THE TRANSFER FUNCTION OF A CHANNEL
C  WITH LINEAR AMPLITUDE CHARACTERISTICS AND MULTIPLIES IT WITH
C  THE INPUT TRANSFER FUNCTION.
C
C  INPUT PARAMETERS: TF,Z,ALPHA,LSAMPL,BAUD,LDIM
C  OUTPUT PARAMETER: TF
C
C  TF      -THE COMPLEX TRANSFER FUNCTION OF THE CHANNEL IN
C           THE FREQUENCY DOMAIN.
C  Z       -THE AMPLITUDE SLOPE IN dB/MHz.
C  ALPHA   -THE AMOUNT OF BANDWIDTH USED IN EXCESS OF THE
C           MINIMUM NYQUIST BANDWIDTH DIVIDED BY THE NYQUIST
C           BANDWIDTH.
C  LSAMPL  -THE NUMBER OF SAMPLES PER SYMBOL.
C  BAUD    -THE SYMBOL RATE IN MBaud.
C  LDIM    -THE DIMENSION OF THE COMPLEX TF ARRAY..
C
C  THE AMPLITUDE DISTORTION ,A(f), MODIFIES THE INPUT
C  TRANSFER FUNCTION TF(f) AS FOLLOWS:
C
C  IF   $A(f)=10^{(Z*f/20)}$ 
C
C  THEN THE OUTPUT TRANSFER FUNCTION IS
C
C        $=TF(f)*A(f)$ 
C
C  WHERE f IS IN MHz.
C
C  NOTE THAT AT f=0 THE AMPLITUDE FUNCTION IS NORMALIZED TO 1.
C
*****

```

C

```
SUBROUTINE LINAMP(Z,TF)
COMMON /NUMB1/ FBW,ALPHA,LDIM,IOFF,LSAMPL
COMMON /NUMB2/ NSNR,NSYMB,BAUD
COMPLEX TF(1)
SBANDW=FLOAT(LSAMPL)*BAUD
NO1=LDIM/2 + 1
NO2=NO1 + 1
AI=Z*SBANDW/FLOAT(LDIM)
DO 10 I=1,NO1
AJ=(I-1)*AI/20.
TF(I)=TF(I)*(10.**AJ)
10 CONTINUE
DO 20 I=NO2,LDIM
AZ=(LDIM+2-I)*AI/20.
TF(I)=TF(I)/(10.**AZ)
20 CONTINUE
RETURN
END
```

C

```

C*****
C  PARAMP:
C
C  THIS SUBROUTINE DEVELOPS THE TRANSFER-FUNCTION OF A CHANNEL
C  WITH PARABOLIC AMPLITUDE CHARACTERISTICS AND MULTIPLIES IT WITH
C  THE INPUT TRANSFER FUNCTION.
C
C  INPUT PARAMETERS: TF,P,ALPHA,LSAMPL,BAUD,LDIM
C  OUTPUT PARAMETER: TF
C
C  TF      -THE COMPLEX TRANSFER FUNCTION OF THE CHANNEL IN
C          THE FREQUENCY DOMAIN.
C  Z1      -THE PARABOLIC AMPLITUDE PARAMETER IN dB/MHz**2.
C  ALPHA   -THE AMOUNT OF BANDWIDTH USED IN EXCESS OF THE
C          MINIMUM NYQUIST BANDWIDTH DIVIDED BY THE NYQUIST
C          BANDWIDTH.
C  LSAMPL  -THE NUMBER OF SAMPLES PER SYMBOL.
C  BAUD    -THE SYMBOL RATE IN MBaud.
C  LDIM    -THE DIMENSION OF THE COMPLEX TF ARRAY.
C
C  THE PARABOLIC AMPLITUDE DISTORTION ,A(f), MODIFIES THE
C  INPUT TRANSFER FUNCTION TF(f) AS FOLLOWS:
C
C  IF  $A(f) = 10^{(Z1 * f * f / 20)}$ 
C
C  THEN THE OUTPUT TRANSFER FUNCTION IS
C
C      =TF(f)*A(f)
C
C  WHERE f IS IN MHz.
C
C  NOTE THAT AT f=0 THE PARABOLIC AMPLITUDE FUNCTION IS
C  NORMALIZED TO 1.
C*****

```

C

```
SUBROUTINE PARAMP(Z1,TF)
COMMON /NUMB1/ FBW,ALPHA,LDIM,IOFF,LSAMPL
COMMON /NUMB2/ NSNR,NSYMB,BAUD
COMPLEX TF(1)
SBANDW=FLOAT(LSAMPL)*BAUD
NO1=LDIM/2 + 1
NO2=NO1 + 1
AI=Z1*((SBANDW/FLOAT(LDIM))**2.)
DO 10 I=1,NO1
AJ=((I-1)**2.)*AI/20.
TF(I)=TF(I)*(10.**AJ)
10 CONTINUE
DO 11 I=NO2,LDIM
TF(I)=TF(LDIM+2-I)
11 CONTINUE
RETURN
END
```

C

```

*****
C   SINAMP:
C
C   THIS SUBROUTINE DEVELOPS THE TRANSFER FUNCTION OF A CHANNEL
C   WITH SINUSOIDAL AMPLITUDE CHARACTERISTICS AND MULTIPLIES IT
C   WITH THE INPUT TRANSFER FUNCTION.
C
C   INPUT PARAMETERS: TF,D,ISIN,K,ALPHA,LSAMPL,BAUD,LDIM
C   OUTPUT PARAMETER: TF
C
C   TF       -THE COMPLEX TRANSFER FUNCTION OF THE CHANNEL IN
C             THE FREQUENCY DOMAIN.
C   D        -THE AMPLITUDE OF SINUSOID IN dB.
C   K        -PARAMETER INDICATING WHETHER DISTORTION IS SINE OR
C             COSINE (EITHER 1 OR 0).
C   C        -THE NUMBER OF PERIODS OF THE SINUSOID WITHIN THE
C             NYQUIST BANDWIDTH.
C   ALPHA    -THE AMOUNT OF BANDWIDTH USED IN EXCESS OF THE
C             MINIMUM NYQUIST BANDWIDTH DIVIDED BY THE NYQUIST
C             BANDWIDTH.
C   LSAMPL   -THE NUMBER OF SAMPLES PER SYMBOL.
C   BAUD     -THE SYMBOL RATE IN MBaud.
C   LDIM     -THE DIMENSION OF THE COMPLEX TF ARRAY.
C
C   THE SINUSOIDAL AMPLITUDE DISTORTION ,A(f), MODIFIES THE
C   INPUT TRANSFER FUNCTION TF(f) AS FOLLOWS:
C
C   IF  A(f)= 10**(D*SIN(2*PI*C*f/FN)/20)   FOR K=1
C   OR  A(f)= 10**(D*COS(2*PI*C*f/FN)/20)   FOR K=0
C
C   THEN THE OUTPUT TRANSFER FUNCTION IS
C
C           =TF(f)*A(f)
C
C   WHERE FN IS IN THE NYQUIST BANDWIDTH
C   AND PI=3.141592.
C
C   NOTE THAT AT f=0 THE SINE AMPLITUDE FUNCTION IS
C   NORMALIZED TO 1 AND AT f=FN/4*C THE COSINE AMPLITUDE
C   FUNCTION IS NORMALIZED TO 1.
*****

```

C

```
SUBROUTINE SINAMP(K,D,C,TF)
COMMON /NUMB1/ FBW,ALPHA,LDIM,IOFF,LSAMPL
COMMON /NUMB2/ NSNR,NSYMB,BAUD
COMPLEX TF(1)
SBANDW=FLOAT(LSAMPL)*BAUD
NO1=LDIM/2 + 1
NO2=NO1 + 1
AJ=SBANDW/FLOAT(LDIM)
C1=BAUD/C
IF(K.EQ.1) GO TO 50
DO 10 I=1,NO1
AZ=D*COS(2.*3.141592*AJ*(FLOAT(I)-1.)/C1)/20.
TF(I)=TF(I)*(10.**AZ)
10 CONTINUE
DO 20 I=NO2,LDIM
TF(I)=TF(LDIM+2-I)
20 CONTINUE
RETURN
50 DO 30 I=1,NO1
AZ=D*SIN(2.*3.141592*AJ*(FLOAT(I)-1.)/C1)/20.
TF(I)=TF(I)*(10.**AZ)
30 CONTINUE
DO 40 I=NO2,LDIM
AZ=D*SIN(2.*3.141592*AJ*(FLOAT(LDIM+2-I)-1.)/C1)/20.
TF(I)=TF(I)/(10.**AZ)
40 CONTINUE
RETURN
END
```

C

```

C*****
C  LINGD:
C
C  THIS SUBROUTINE DEVELOPS THE PHASE RESPONSE OF A CHANNEL
C  WITH LINEAR GROUP DELAY CHARACTERISTICS AND ADDS IT TO THE
C  PHASE OF THE INPUT TRANSFER FUNCTION.
C
C  INPUT PARAMETERS: TF,B,ALPHA,LSAMPL,BAUD,LDIM
C  OUTPUT PARAMETER: TF
C
C  TF      -THE COMPLEX TRANSFER FUNCTION OF THE CHANNEL IN
C           THE FREQUENCY DOMAIN.
C  B      -THE DELAY SLOPE IN ns/MHz.
C  ALPHA  -THE AMOUNT OF BANDWIDTH USED IN EXCESS OF THE
C           MINIMUM NYQUIST BANDWIDTH DIVIDED BY THE NYQUIST
C           BANDWIDTH.
C  LSAMPL -THE NUMBER OF SAMPLES PER SYMBOL.
C  BAUD   -THE SYMBOL RATE IN MBaud.
C  LDIM   -THE DIMENSION OF THE COMPLEX TF ARRAY.
C
C  THE GROUP DELAY IS MODELLED AS FOLLOWS:
C
C       $T(f) = B * f * 10.^{-9}$       sec
C
C  WHERE f IS IN MHz.
C
C  IN TERMS OF PHASE, THIS CAN BE REWRITTEN AS
C
C       $\text{PHI}(f) = \text{PI} * B * f * f * 10.^{-3}$       radians
C
C  WHERE PI=3.14159.
C
C  THIS PHASE IS ADDED TO THAT OF THE INPUT CHANNEL.
C  THE RESULTANT CHANNEL TRANSFER FUNCTION IS PASSED
C  OUT OF THE SUBROUTINE IN ARRAY TF.
C*****

```


C
SUBROUTINE LINGD(B,TF)
COMMON /NUMB1/ FBW,ALPHA,LDIM,IOFF,LSAMPL
COMMON /NUMB2/ NSNR,NSYMB,BAUD
COMPLEX TF(1)
SBANDW=FLOAT(LSAMPL)*BAUD
NO1=LDIM/2 + 1
NO2=NO1-1
DO 10 I=1,NO1
AI=FLOAT(I-1)*SBANDW/FLOAT(LDIM)
PHI=3.141592*(B/(10.**3.))*(AI**2.)
TF(I)=TF(I)*CMPLX(COS(PHI),-SIN(PHI))
10 CONTINUE
DO 20 I=NO2,LDIM
TF(I)=TF(LDIM+2-I)
20 CONTINUE
RETURN
END
C

```

C*****
C
C PARGD:
C
C THIS SUBROUTINE DEVELOPS THE PHASE RESPONSE OF A CHANNEL
C WITH PARABOLIC GROUP DELAY CHARACTERISTICS AND ADDS IT TO THE
C PHASE OF THE INPUT TRANSFER FUNCTION.
C
C INPUT PARAMETERS: TF,S,ALPHA,LSAMPL,BAUD,LDIM
C OUTPUT PARAMETER: TF
C
C TF -THE COMPLEX TRANSFER FUNCTION OF THE CHANNEL IN
C THE FREQUENCY DOMAIN.
C S -THE PARAMETER FOR PARABOLIC GROUP DELAY IN ns/MHz**2.
C ALPHA -THE AMOUNT OF BANDWIDTH USED IN EXCESS OF THE
C MINIMUM NYQUIST BANDWIDTH DIVIDED BY THE NYQUIST
C BANDWIDTH.
C LSAMPL -THE NUMBER OF SAMPLES PER SYMBOL.
C BAUD -THE SYMBOL RATE IN MBaud.
C LDIM -THE DIMENSION OF THE COMPLEX TF ARRAY.
C
C THE GROUP DELAY IS MODELLED AS FOLLOWS:
C
C  $T(f) = S * f * f * 10. ** -9$  sec
C
C
C IN TERMS OF PHASE, THIS CAN BE REWRITTEN AS
C
C  $PHI(f) = 2 * PI * S * f * f * f * 10. ** -3/3$  radians
C
C WHERE PI=3.14159
C AND f IS IN MHz.
C
C THIS PHASE IS ADDED TO THAT OF THE INPUT CHANNEL.
C THE RESULTANT CHANNEL TRANSFER FUNCTION IS PASSED
C OUT OF THE SUBROUTINE IN ARRAY TF.
C*****

```

C

```
SUBROUTINE PARGD(P1,TF)
COMMON /NUMB1/ FBW,ALPHA,LDIM,IOFF,LSAMPL
COMMON /NUMB2/ NSNR,NSYMB,BAUD
COMPLEX TF(1)
SBANDW=FLOAT(LSAMPL)*BAUD
NO1=LDIM/2 + 1
NO2=NO1 + 1
DO 20 I=1,NO1
AI=FLOAT(I-1)*SBANDW/FLOAT(LDIM)
PHI=2.*3.141592/3.*((P1*(AI**3.))/(10.**3.))
TF(I)=TF(I)*CMLPX(COS(PHI),-SIN(PHI))
20 CONTINUE
DO 21 I=NO2,LDIM
TF(I)=CONJG(TF(LDIM+2-I))
21 CONTINUE
RETURN
END
```

20

21

C

C

10

11

50

12

13

60

C

```

SUBROUTINE SINGCD(ISIN,C,K,TF)
COMMON /NUMB1/ FBW,ALPHA,LDIM,IOFF,LSAMPL
COMMON /NUMB2/ NSNR,NSYMB,BAUD
COMPLEX TF(1)
SBANDW=FLOAT(LSAMPL)*BAUD
NO1=LDIM/2 + 1
NO2=NO1 + 1
C1=BAUD/K
IF (ISIN.EQ.1) GO TO 50
DO 10 I=1,NO1
AI=FLOAT(I-1)*SBANDW/FLOAT(LDIM)
PHI=(C*C1/(10.**3.))*SIN(2.*3.141592*AI/C1)
TF(I)=TF(I)*CMPLX(COS(PHI),-SIN(PHI))
CONTINUE
DO 11 I=NO2,LDIM
TF(I)=CONJG(TF(LDIM+2-I))
CONTINUE
GO TO 60
DO 12 I=1,NO1
AI=FLOAT(I-1)*SBANDW/FLOAT(LDIM)
PHI=(C*C1/(10.**3.))*COS(2.*3.141592*AI/C1)
TF(I)=TF(I)*CMPLX(COS(PHI),SIN(PHI))
CONTINUE
DO 13 I=NO2,LDIM
TF(I)=TF(LDIM+2-I)
CONTINUE
RETURN
END

```

```

C*****
C
C   RUMAMP:
C
C   THIS SUBROUTINE MODELS THE AMPLITUDE TRANSFER CHARACTERISTICS
C   OF A SELECTIVELY FADING CHANNEL USING RUMMLER'S THREE RAY
C   MODEL.
C
C   INPUT PARAMETERS:TF,B,FO,LSAMPL,BAUD,LDIM
C   OUTPUT PARAMETER:TF
C
C   TF           -THE COMPLEX TRANSFER FUNCTION OF THE CHANNEL IN
C                 THE FREQUENCY DOMAIN.
C   B            -THE NOTCH DEPTH BETWEEN 0 AND .999P.
C   FO           -THE CENTER FREQUENCY OF THE NOTCH IN MHz.
C   LSAMPL       -THE NUMBER OF SAMPLES PER SYMBOL.
C   BAUD         -THE SYMBOL RATE IN MBaud.
C   LDIM         -THE DIMENSION OF THE COMPLEX TF ARRAY.
C
C
C   THE AMPLITUDE TRANSFER CHARACTERISTIC AJ(f) IS MODELLED
C   AS FOLLOWS:
C
C   AJ(f)=SQRT(1 + B**2 - 2*B*COS(2*PHI*T*(f-FO)))
C
C   WHERE T IS 6.31 nsec (RUMMLERS FINDINGS)
C
C   THE OUTPUT CHANNEL TRANSFER FUNCTION BECOMES
C
C           =TF(f)*AJ(f)
C
C   WHERE AJ(f) IS IN dB.
C*****

```

C

```

SUBROUTINE RUMAMP(B,FO,TF)
COMMON /NUMB1/ FBW,ALPHA,LDIM,IOFF,LSAMPL
COMMON /NUMB2/ NSNR,NSYMB,BAUD
COMPLEX TF(1)
DELTAF=FLOAT(LSAMPL)*BAUD/FLOAT(LDIM)
NO1=LDIM/2 + 1
NO2=NO1 + 1
AK=2.*3.14159265*6.31*10**~3
X=0.0
DO 10 I=1,NO1
AI=AK*((I-1)*DELTAF - FO)
AJ=SQRT(1.0 + (B**2) - 2*B*COS(AI))
A=20.*ALOG10(AJ)
TF(I)=TF(I)*AJ
IF (A .LT. X) X=A
10 CONTINUE
DO 11 I=NO2,LDIM
TF(I)=TF(LDIM+2-I)
11 CONTINUE
X=-X
WRITE(6,23) X
23 FORMAT(5X,'NOTCH DEPTH ',F8.2,' IN dB')
RETURN
END

```

```

C*****
C  RUMPHA:
C
C  THIS SUBROUTINE DEVELOPS THE PHASE RESPONSE OF A SELECTIVELY
C  FADING CHANNEL USING RUMMLER'S THREE RAY MODEL AND ADDS IT
C  TO THE PHASE OF THE INPUT TRANSFER FUNCTION.
C
C  INPUT PARAMETERS:TF,B,FO,IMIN,LSAMPL,BAUD,LDIM
C  OUTPUT PARAMETER:TF
C
C  TF      -THE COMPLEX TRANSFER FUNCTION OF THE CHANNEL IN
C           THE FREQUENCY DOMAIN.
C  B       -THE NOTCH DEPTH BETWEEN 0 AND .999.
C  FO      -THE CENTER FREQUENCY OF THE NOTCH IN MHz.
C  IMIN    -PARAMETER INDICATING WHETHER FADE IS MINIMUM OR
C           NONMINIMUM PHASE FADE.
C  LSAMPL  -THE NUMBER OF SAMPLES PER SYMBOL.
C  BAUD    -THE SYMBOL RATE IN MBaud.
C  LDIM    -THE DIMENSION OF THE COMPLEX TF ARRAY.
C
C  THE PHASE PHI (f) OF RUMMLERS NOTCH CAN BE MODELLED
C  AS FOLLOWS:
C
C  PHI(f)=Arc TAN(+B*SIN((f-FO)*T)/(1-B*COS((f-F)*T)))
C           IMIN=0 {NON-MINIMUM PHASE}
C           =Arc TAN(-B*SIN((f-FO)*T)/(1-B*COS((f-F)*T)))
C           IMIN=1 {MINIMUM PHASE}
C
C  WHERE T IS 6.31 nsec (RUMMLERS FINDINGS)
C
C  THIS PHASE IS ADDED TO THAT OF THE INPUT CHANNEL.
C*****

```


c

```
SUBROUTINE RUMPHA(B,FO,IMIN,TF)
COMMON /NUMB1/ FBW,ALPHA,LDIM,IOFF,LSAMPL
COMMON /NUMB2/ NSNR,NSYMB,BAUD
```

```
COMPLEX TF(1)
SBANDW=FLOAT(LSAMPL)*BAUD
NO1=LDIM/2 + 1
NO2=NO1 + 1
DO 20 I=1,NO1
F=FLOAT(I-1)*SBANDW/FLOAT(LDIM)
WT=(F-FO)*6.31*10**3
ARG=B*SIN(WT)/(1.0-B*COS(WT))
IF(IMIN.EQ.1) ARG=-ARG
PHI=ATAN(ARG)
TF(I)=TF(I)*CMPLX(COS(PHI),-SIN(PHI))
20 CONTINUE
DO 21 I=NO2,LDIM
TF(I)=CONJG(TF(LDIM+2-I))
21 CONTINUE
RETURN
END
```

```
C*****  
C FILTER:  
C  
C THE FOLLOWING SUBROUTINE PERFORMS THE FILTERING  
C PROCESS ON THE DATA SEQUENCE.  
C INPUT PARAMETERS: DATA,TF,LDIM  
C OUTPUT PARAMETERS: DATA  
C  
C DATA -THE COMPLEX DATA ARRAY IN THE TIME DOMAIN. ON  
C THE INPUT TO THE SUBROUTINE THE DATA HAS NOT BEEN  
C -FILTERED BY THE GIVEN FILTER. ON THE OUTPUT  
C IT IS THE FILTERED DATA.  
C TF -THE COMPLEX TRANSFER FUNCTION ARRAY IN THE  
C FREQUENCY DOMAIN.  
C LDIM -THE DIMENSION OF THE COMPLEX DATA AND TF ARRAYS.  
C  
C THE INPUT DATA IN THE TIME DOMAIN IS FAST FOURIER TRANSFORMED  
C (FFT) TO THE FREQUENCY DOMAIN AND MULTIPLIED WITH THE TRANSFER  
C FUNCTION OF THE FILTER. THIS PRODUCT IS THEN INVERSE  
C TRANSFORMED BACK TO THE TIME DOMAIN TO COMPLETE THE FILTERING  
C PROCESS. THE FFT2C ALGORITHM FROM THE INTERNATIONAL  
C MATHEMATICAL AND STATISTICAL LIBRARIES IS USED TO PERFORM  
C THE FOURIER TRANSFORM AND ITS INVERSE.  
C*****
```

C
SUBROUTINE FILTER(DATA,TF)
COMPLEX DATA(1),TF(1)
DIMENSION IWK(17)
COMMON /NUMB1/ FBW,ALPHA,LDIM,IOFF,LSAMPL
CALL FFT2C(DATA,16,IWK)
DO 1 I=1,LDIM
1 DATA(I)=CONJG(DATA(I)*TF(I))
CALL FFT2C(DATA,16,IWK)
DO 2 I=1,LDIM
2 DATA(I)=CONJG(DATA(I))/FLOAT(LDIM)
RETURN
END
C


```

SUBROUTINE RCOSRX(TF)
  COMPLEX TF(65536)
  COMMON /NUMB1/ FBW, ALPHA, LDIM, IOFF, LSAMPL
  COMMON /NUMB2/ NSNR, NSYMB, BAUD
  SBANDW=BAUD*LSAMPL
  NO=LDIM/2
  NO1=NO+1
  IF (ALPHA.EQ.0) ALPHA=0.0001
  FN=LDIM*(FBW/SBANDW)
  F1=(1.-ALPHA)*FN
  F2=(1.+ALPHA)*FN
  IFN=IFIX(FN)
  IF1=IFIX(F1)+1
  IF2=IFIX(F2)+1

```

C
C
C

AMPLITUDE CHARACTERISTIC

```

  A1=3.141592/(2.*FLOAT(IFN))
  DO 8 I=2, IF1
  TF(I)=CMPLX(1.0,0.0)
  J=I-1
  TF(I)=CMPLX(1.,0.0)
8 CONTINUE
  JK=IF1+1
  DO 9 J=JK, IF2
  I=J-1

```

C
C
C

ROOT OF RAISED COSINE

```

  A=(3.141592/(2.0*ALPHA))*((FLOAT(I)/FLOAT(SFN))-1.)
  TF(J)=CMPLX(SQRT(0.5*(1.0-SIN(A))),0.0)
9 CONTINUE
  JH=IF2+1
  DO 10 I=JH, NO1
  TF(I)=CMPLX(0.0,0.0)
10 CONTINUE
  NO2=NO1+1
  DO 5 I=NO2, LDIM
  TF(I)=CONJG(TF(LDIM+2-I))
5 CONTINUE
  RETURN
  END

```

```
C*****
C ENERGY.
C THIS SUBROUTINE CALCULATES THE ENERGY PER BIT.
C INPUT PARAMETERS: DATA,BAUD,LDIM
C OUTPUT PARAMETERS: EB
C
C DATA -THE COMPLEX DATA ARRAY IN THE TIME DOMAIN.
C BAUD -THE SYMBOL RATE IN MBAUD.
C LDIM -THE DIMENSION OF THE COMPLEX DATA ARRAY.
C EB -THE ENERGY PER BIT.
C
C THE ENERGY PER SYMBOL ES FOR AN INPUT SYMBOL I+JQ IS GIVEN
C BY  $ES=(I**2 + Q**2)/TS$  WHERE TS IS THE SYMBOL DURATION.
C AND WITH 6 BITS PER SYMBOL THE ENERGY PER BIT IS GIVEN BY
C EB=ES/6.
C*****
```

C

```
SUBROUTINE ENERGY(DATA,EB)
  COMPLEX DATA(1)
  COMMON /NUMB2/ NSNR,NSYMB,BAUD
  COMMON /NUMB1/ FBW,ALPHA,LDIM,IOFF,LSAMPL
  WATTS=0.
  DO 1 I=1,LDIM
  WATTS=WATTS+((CABS(DATA(I)))**2.)
1  CONTINUE
  WATTS=WATTS/(FLOAT(LDIM))
  EB=WATTS/(6.*BAUD)
  WRITE (6,40) WATTS,EB
40  FORMAT(10X,F15.6,5X,E15.8)
  RETURN
  END
```

JL

```
C*****
C
C   HHGG:
C
C   THIS SUBROUTINE COMPUTES THE NORMALIZED NOISE POWER.
C   INPUT PARAMETERS: TF,LDIM,LSAMPL,BAUD
C   OUTPUT PARAMETERS: PNOISE
C
C   .TF       -THE COMPLEX TRANSFER FUNCTION ARRAY IN THE
C             FREQUENCY DOMAIN.
C   LDIM      -THE DIMENSION OF THE COMPLEX TF ARRAY.
C   LSAMPL    -THE NUMBER OF SAMPLES PER SYMBOL.
C   BAUD      -THE SYMBOL RATE IN MBaud.
C   PNOISE    -THE NORMALIZED NOISE POWER.
C
C   THE NOISE IN THE SYSTEM IS ASSUMED TO BE ADDITIVE WHITE
C   GAUSSIAN NOISE WITH A NORMALIZED DOUBLE-SIDED POWER
C   SPECTRAL DENSITY OF ONE-HALF (NO=1).
C   PNOISE=1/2*INTEGRAL(TF(F)**2)
C*****
```


C
SUBROUTINE HRGG(TF,PNOISE)
COMPLEX TF(1)
COMMON /NUMB1/ FBW,ALPHA,LDIM,IOFF,LSAMPL
COMMON /NUMB2/ NSNR,NSYMB,BAUD
SUM=0.0
SBANDW=BAUD*LSAMPL
DO 1 L=1,LDIM
HH=(CABS(TF(L)))**2
1 SUM=SUM+HH
PNOISE=SUM*SBANDW/FLOAT(LDIM)/2.
WRITE (6,2) PNOISE
2 FORMAT(5X,'PNOISE=',F7.3,/)
RETURN
END
C

C
 C *****
 C SYNCRO:
 C THE FOLLOWING SUBROUTINE SYNCHRONIZES THE RECEIVED DATA.
 C INPUT PARAMETERS: DATA,PNOISE,NI,NQ,EB,LDIM,IOFF,LSAMPL,NSYMB
 C OUTPUT PARAMETERS: DATA,MI,MQ

C DATA -THE COMPLEX DATA ARRAY IN THE TIME DOMAIN.
 C PNOISE -THE NORMALIZED NOISE POWER.
 C NI -THE I CHANNEL SYMBOL ARRAY.
 C NQ -THE Q CHANNEL SYMBOL ARRAY.
 C EB -THE AVERAGE ENERGY PER BIT.
 C MI -THE I CHANNEL OPTIMUM SAMPLING POINT.
 C MQ -THE Q CHANNEL OPTIMUM SAMPLING POINT.
 C LDIM -THE DIMENSION OF THE COMPLEX DATA ARRAY.
 C IOFF -THE NUMBER OF SAMPLES THE Q CHANNEL DATA IS
 C OFFSET FROM THE I CHANNEL DATA.
 C LSAMPL -THE NUMBER OF SAMPLES PER SYMBOL.
 C NSYMB -THE DIMENSION OF THE NI AND NQ ARRAYS.

C THIS SUBROUTINE SYNCHRONIZES THE RECEIVED DATA WITH RESPECT
 C TO THE ORIGINAL TRANSMITTED DATA (IF POSSIBLE) AND DETERMINES
 C THE OPTIMUM SAMPLING INSTANT. THE RECEIVED DATA IS SHIFTED
 C TO THE RIGHT UNTIL AT LEAST ONE SAMPLE OF EACH SYMBOL IS
 C OF THE SAME SIGN +/- AS THE ORIGINAL TRANSMITTED DATA.
 C THE OPTIMUM SAMPLING INSTANT FOR EACH CHANNEL IS DETERMINED
 C BY SHIFTING THE SAMPLING INSTANT OF EACH SYMBOL TO THE
 C RIGHT UNTIL, FOR A GIVEN VALUE OF EB/NO (IN THIS CASE 19 dB),
 C THE MINIMUM P_e IS FOUND. THE I AND Q CHANNEL'S OPTIMUM SAMPLING
 C INSTANT, WHICH CAN VARY FROM 1 TO LSAMPL, IS STORED FOR USE
 C IN THE DECODE ROUTINE IN MI AND MQ RESPECTIVELY.

C *****

C

```

SUBROUTINE SYNCRO(DATA,PNOISE,NI,NQ,MI,MQ,EB)
INTEGER Q7FLAG
COMPLEX DATA(1),AMP
DIMENSION NI(1),NQ(1)
COMMON /NUMB1/ FBW,ALPHA,LDIM,IOFF,LSAMPL
COMMON /NUMB2/ NSNR,NSYMB,BAUD
NERROR=0
IF (IOFF.EQ.0) GO TO 111
DO 6 K=1,IOFF
XX=AIMAG(DATA(LDIM))
DO 7 KK=2,LDIM
7. DATA(KK)=CMPLX(REAL(DATA(KK)),AIMAG(DATA(KK-1)))
6. DATA(1)=CMPLX(REAL(DATA(1)),XX)

```

C

C

C

111

```

SYNCHRONIZE THE RECEIVED DATA

```

```

NOLD=0

```

```

NOF=0

```

```

K=1

```

300 CONTINUE

```

NEW=0

```

```

DO 200 J=1,NSYMB

```

```

J1=K+(J-1)*LSAMPL

```

```

IF(J1.GT.LDIM) J1=J1-LDIM

```

```

AXBAR=REAL(DATA(J1))

```

```

AYBAR=AIMAG(DATA(J1))

```

```

SS=AXBAR*NI(J)

```

```

IF (SS .GT. 0.) NEW=NEW+1

```

```

SS=AYBAR*NQ(J)

```

```

IF (SS .GT. 0.) NEW=NEW+1

```

200 CONTINUE

```

IF(NOLD.GE.NEW) GO TO 399

```

```

NOLD=NEW

```

```

NOF=K

```

399 K=K+1

```

LFU=2*NSYMB

```

C

C

C

```

SHIFT RECEIVED DATA RIGHT UNTIL ALL SYMBOLS ARE LINED UP

```

```

IF (NOLD.LT.LFU AND.K.LE.LDIM) GO TO 300

```

```

NOF=NOF-1

```

```

IF (NOF.EQ.0) GO TO 230

```

```

LO=LDIM-1

```

```

DO 250 I=1,NOF

```

```

AMP=DATA(1)

```

```

DO 240 J=1,LO

```

```

DATA(J)=DATA(J+1)

```

240 CONTINUE

```

DATA(LDIM)=AMP

```

250 CONTINUE

C

C OPTIMIZE THE SAMPLING INSTANT

C 230 MI=1

MQ=1

EOI=FLOAT(NSYMB) + 1.

EQQ=FLOAT(NSYMB). + 1.

VARIAN=PNOISE*EB/19.

SIGMA=SQRT(VARIAN)

DO 80 J=1,LSAMPL

EI=0.

EQ=0.

DO 70 K=1,NSYMB

C VERIFY THAT NO SAMPLED SYMBOL IS IN ERROR

J1=(K-1)*LSAMPL+J

AXBAR=(REAL(DATA(J1))+REAL(DATA(J1+1)))/2.

AYBAR=(AIMAG(DATA(J1))+AIMAG(DATA(J1+1)))/2.

INDEXI=0

SS=FLOAT(NI(K))*AXBAR

IF (SS .LT. 0.) INDEXI=1

AMPX=ABS(AXBAR)

AMPI=ABS(FLOAT(NI(K)))

THR1I=AMPI - 1.0

THR2I=AMPI + 1.0

I7FLAG=0

IF (AMPI.EQ. 7.0) GO TO 30

IF ((AMPX.GE.THR2I).OR.(AMPX.LE.THR1I)) INDEXI=1

GO TO 40

30 IF(AMPX.LE.THR1I) INDEXI=1

I7FLAG=1

40 CONTINUE

INDEXQ=0

SS=FLOAT(NQ(K))*AYBAR

IF(SS .LT. 0.) INDEXQ=1

AMPY=ABS(AYBAR)

AMPQ=ABS(FLOAT(NQ(K)))

THR1Q=AMPQ - 1.0

THR2Q=AMPQ + 1.0

Q7FLAG=0

IF (AMPQ.EQ. 7.0) GO TO 50

IF ((AMPY.GE.THR2Q).OR.(AMPY.LE.THR1Q)) INDEXQ=1

GO TO 60

50 IF(AMPY.LE.THR1Q) INDEXQ=1

Q7FLAG=1

60 CONTINUE

IF(INDEXI.EQ.1) EI=EI + 1.

IF(INDEXQ.EQ.1) EQ=EQ + 1.

C COMPUTE THE PROBABILITY OF ERROR FOR THIS SYMBOL AT EB/NO=19dB

C D1=ABS(AMPX-THR1I)

C ARG=D1/(SIGMA*SQRT(2.))

C CHECK IF ARG IS LARGE INWHICH CASE PE IS INSIGNIFICANT

C

```

IF (ARG.GT.12.) ARG=12.
EI=EI + ERFC(ARG)/2.
IF (I7FLAG .EQ. 1) GO TO 65
D2=ABS(THR2I-AMPX)
ARG=D2/(SIGMA*SQRT(2.))
IF (ARG.GT.12.) ARG=12.
EI=EI + ERFC(ARG)/2.
65 D1=ABS(AMPY-THR1Q)
ARG=D1/(SIGMA*SQRT(2.))
IF (ARG.GT.12.) ARG=12.
EQ=EQ + ERFC(ARG)/2.
IF (Q7FLAG .EQ. 1) GO TO 70
D2=ABS(THR2Q-AMPY)
ARG=D2/(SIGMA*SQRT(2.))
IF (ARG.GT.12.) ARG=12.
EQ=EQ + ERFC(ARG)/2.
70 CONTINUE
IF (EOI.LE.EI) GO TO 75
EOI=EI
MI=J
75 CONTINUE
IF (EOQ.LE.EQ) GO TO 80
EQ=EQ
MQ=J
80 MOFF=IABS(MI-MQ)
IF (MOFF.NE.0) WRITE(6,90) MOFF
OFF=(FLOAT(MI) + FLOAT(NOF))/FLOAT(LSAMPL)
90 FORMAT(5X,'SAMPLING POINTS FOR I AND Q CHANNELS DIFFER BY',
#I2,' SIXTEENTHS OF THE SYMBOL INTERVAL',/)
WRITE(6,95) OFF
95 FORMAT(5X,'RECEIVED DATA IS DELAYED BY ',F7.3,' SYMBOLS',/)
RETURN
END

```

```

C
C*****
C  DECODE:
C  THE FOLLOWING SUBROUTINE DECODES THE RECEIVED DATA.
C  INPUT PARAMETERS: DATA,PNOISE,MI,MQ,NI,NQ,EB,LSAMPL,NSNR,NSYMB
C  OUTPUT PARAMETERS: EBNO,PE
C
C  DATA      -THE COMPLEX DATA ARRAY IN THE TIME DOMAIN.
C  PNOISE     -THE NORMALIZED NOISE POWER.
C  MI         -THE I CHANNEL OPTIMUM SAMPLING POINT.
C  MQ         -THE Q CHANNEL OPTIMUM SAMPLING POINT.
C  NI         -THE I CHANNEL SYMBOL ARRAY.
C  NQ         -THE Q CHANNEL SYMBOL ARRAY.
C  EB         -THE AVERAGE ENERGY PER BIT.
C  EBNO       -THE ARRAY CONTAINING THE EB/NO VALUES CONSIDERED.
C  PE         -THE Pe ARRAY FOR THE GIVEN EB/NO VALUES.
C  LSAMPL     -THE NUMBER OF SAMPLES PER SYMBOL.
C  NSNR       -THE NUMBER OF PE VERSUS EBNO VALUES CALCULATED.
C  NSYMB      -THE DIMENSION OF THE NI AND NQ ARRAYS.
C
C  THIS SUBROUTINE CHECKS FOR AN ERROR AT THE SAMPLING INSTANT
C  AND TERMINATES THE RUN IF ONE IS FOUND. THIS ERROR SIGNIFIES
C  AN UNACCEPTABLY HIGH Pe AND AS SUCH FURTHER CALCULATION IS
C  POINTLESS. FLAGS ARE SET (I7FLAG OR Q7FLAG) WHICH INDICATE THE
C  ORIGINAL TRANSMITTED I OR Q SYMBOL WAS AN ENDPOINT. THE
C  APPROPRIATE Pe EQUATION IS THEN USED TO CALCULATED THE Pe
C  FOR THAT SYMBOL.
C
C  FOR THE END POINTS THE  $PE=1/2*ERFC(D1/(SIGMA*SQSRT(2)))$ 
C
C  AND FOR THE INNER POINTS THE  $PE=1/2*ERFC(D1/(SIGMA*SQRT(2))) +$ 
C   $1/2*ERFC(D2/(SIGMA*SQRT(2)))$ .
C
C  WHERE  SIGMA=SQRT(VARIAN)
C         D1  =[[SAMPLE] - THR1]
C         D2  =[[THR2-[SAMPLE]]
C         THR1 =[[NI] {OR [NQ]} -1
C         THR2 =[[NI] {OR [NQ]} +1
C
C  THIS CALCULATION IS REPEATED FOR ALL THE SYMBOLS IN THE
C  SEQUENCE.
C*****

```

```

C
SUBROUTINE DECODE(DATA, PNOISE, MI, MQ, NI, NQ, EBNO, PE, EB)
INTEGER Q7FLAG
COMPLEX DATA(1), AMP
DIMENSION EBNO(1), PE(1), NI(1), NQ(1)
COMMON /NUMB1/ FBW, ALPHA, LDIM, IOFF, LSAMPL
COMMON /NUMB2/ NSNR, NSYMB, BAUD
NERROR=0
DO 1 I=1, NSNR
1 PE(I)=0.
C CHECK FOR AN ERROR AT THE SAMPLING INSTANT, ONLY THOSE
C ERRORS IN ADJACENT LEVELS ARE CONSIDERED
3 DO 2 K=1, NSYMB
J1=(K-1)*LSAMPL+MI
J2=(K-1)*LSAMPL + MQ
AXBAR=(REAL(DATA(J1))+REAL(DATA(J1+1)))/2.
AYBAR=(AIMAG(DATA(J2))+AIMAG(DATA(J2+1)))/2.
INDEXI=0
SS=FLOAT(NI(K))*AXBAR
IF(SS .LT. 0.) INDEXI=1
AMPX=ABS(AXBAR)
AMPI=ABS(FLOAT(NI(K)))
THR1I=AMPI - 1.0
THR2I=AMPI + 1.0
I7FLAG=0
IF(.AMPI.EQ. 7.0) GO TO 30
IF((AMPX.GE.THR2I).OR.(AMPX.LE.THR1I)) INDEXI=1
GO TO 40
30 IF(AMPX.LE.THR1I) INDEXI=1
I7FLAG=1
40 CONTINUE
INDEXQ=0
SS=FLOAT(NQ(K))*AYBAR
IF(SS .LT. 0.) INDEXQ=1
AMPY=ABS(AYBAR)
AMPQ=ABS(FLOAT(NQ(K)))
THR1Q=AMPQ - 1.0
THR2Q=AMPQ + 1.0
Q7FLAG=0
IF(AMPQ.EQ. 7.0) GO TO 50
IF((AMPY.GE.THR2Q).OR.(AMPY.LE.THR1Q)) INDEXQ=1
GO TO 60
50 IF(AMPY.LE.THR1Q) INDEXQ=1
Q7FLAG=1
60 CONTINUE
IF((INDEXI.EQ.1).OR.(INDEXQ.EQ.1)) NERROR=NERROR+1

C
C COMPUTE THE PROBABILITY OF ERROR FOR THIS SYMBOL.
C THE VARIABLES ARE AS FOLLOWS: M IS EB/NO IN dB; PNOISE IS
C 1/2*INTERGAL ([ H(F)**2] DF); AND VARIAN = NO*PNOISE.
C FOR THE END POINTS (7FLAG=1) THE PE=1/2*ERFC(D1/(SIGMA*SQSRT(2)))
C AND FOR THE INNER POINTS THE PE=1/2*ERFC(D1/(SIGMA*SQRT(2))) +

```

```

C      1/2*ERFC(D2/(SIGMA*SQRT(2))).
C
DO 4 M=1,NSNR
VARIAN=PNOISE*EB*(10.**(-0.1*FLOAT(M)))
SIGMA=SQRT(VARIAN)
D1=ABS(AMPX-THR1I)
ARG=D1/(SIGMA*SQRT(2.))
C      CHECK IF ARG IS LARGE INWHICH CASE PE IS INSIGNIFICANT
C      CHECK IF SYMBOL IS IN ERROR. IF IT IS TERMINATE RUN
C
IF (INDEXI.EQ.1) GO TO 153
IF (ARG.GT.12.) ARG=12.
PEI=ERFC(ARG)/2.
IF (I7FLAG .EQ. 1) GO TO 100
D2=ABS(THR2I-AMPX)
ARG=D2/(SIGMA*SQRT(2.))
IF (ARG.GT.12.) ARG=12.
PEI=PEI + ERFC(ARG)/2.
100 D1=ABS(AMPY-THR1Q)
ARG=D1/(SIGMA*SQRT(2.))
IF (INDEXQ.EQ.1) GO TO 153
IF (ARG.GT.12.) ARG=12.
PEQ=ERFC(ARG)/2.
IF (Q7FLAG .EQ. 1) GO TO 110
D2=ABS(THR2Q-AMPY)
ARG=D2/(SIGMA*SQRT(2.))
IF (ARG.GT.12.) ARG=12.
PEQ=PEQ + ERFC(ARG)/2.
110 IF(PEI.LT.1.E-15) PEI=0.
IF(PEQ.LT.1.E-15) PEQ=0.
4 PE(M)=PE(M)+PEI+PEQ
2 CONTINUE
DO 5 I=1,NSNR
PE(I)=PE(I)/FLOAT(NSYMB)
5 EBNO(I)=FLOAT(I)
PRINT 150
150 FORMAT(5X,'EB/NO',10X,'PROB. OF ERROR',/)
WRITE (6,151) (EBNO(I),PE(I),I=1,NSNR)
151 FORMAT(5X,F5.1,10X,E13.6)
WRITE (6,152) NERROR
152 FORMAT(/5X,'ERRORS=',I5,/)
GO TO 155
153 PRINT 154
154 FORMAT (10X,'SYMBOL WAS IN ERROR, RUN WAS TERMINATED',/)
155 CONTINUE
RETURN
END

```

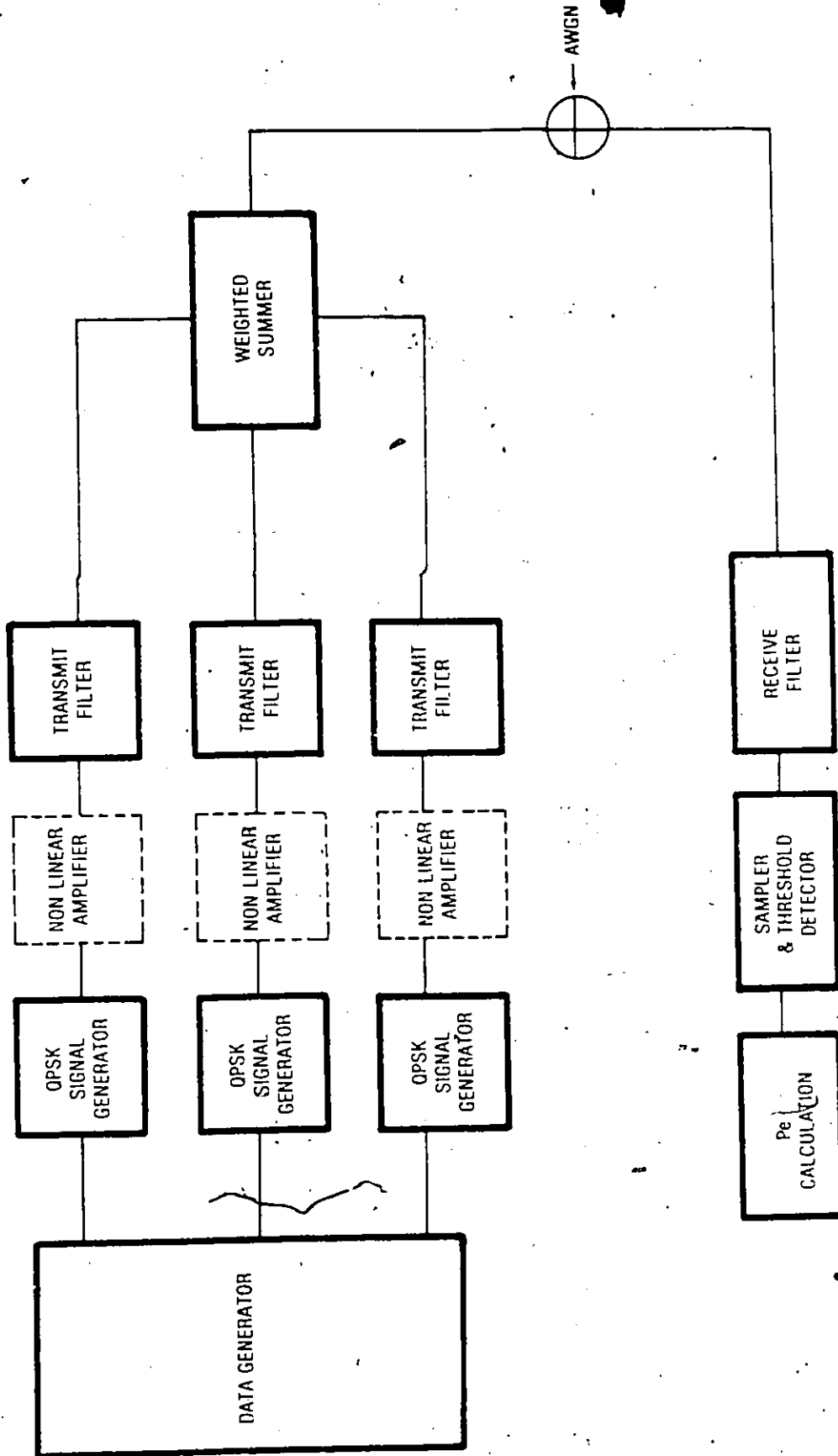



FIGURE B.1.1.2 NLA 64-STATE QAM SIMULATION MODEL

```

C*****
C PROGRAM FOR SIMULATION OF 64-QAM IN A NONLINEAR CHANNEL
C MODIFIED BY TRICIA HILL FROM DCL REPORT #112 BY DR.V.ARUNACHALAM
C*****
COMPLEX DATA(16384),DATA2(16384),TF(16384)
REAL MPO
  DIMENSION PEI(25),EBNO(25),NI(2048),NQ(2048)
  DIMENSION XARRAY(27),YARRAY(27)

C
C INITIALIZE PROGRAM.
C SET THE PARAMETERS FOR THE RUN
C
COMMON /NUMB1/ FBW,ALPHA,LDIM,IOFF,LSAMPL
COMMON /NUMB2/ NSNR,NSYMB,BAUD
COMMON /INPUT/ NI,NQ
FBW=60.0
BACKOF=0.0
ALPHA=0.4
LDIM=16384
IOFF=0
LSAMPL=8
NSNR=25
NSYMB=2047
BAUD=60.0
NRUNS=1
KM=1
NFILTR=2
IORDER=4
C END OF INITIALIZATION.
C
xC START OF COMPUTATIONS.
C
CALL RCOSTX(TF)
C
C THIS PROGRAM GENERATES THREE QPSK SIGNALS AND SUMS THEM.
C EACH QPSK SIGNAL IS GENERATED IN LOAD4, FILTERED
C AND THEN SUMMED TO GENERATE 64-QAM.
C
NUM=1
CALL LOAD4 (DATA,NUM)
CALL HLIM(DATA)
C CALL POWER(DATA,MPO)
C CALL HPA(DATA,BACKOF,PSHIFO,MPO)
C CALL PHASE(DATA,PSHIFO)
CALL FILTER(DATA,TF)
NUM=3
CALL LOAD4(DATA2,NUM)
CALL HLYM(DATA2)
C CALL POWER(DATA2,MPO)
C CALL HPA(DATA2,BACKOF,PSHIFO,MPO)
C CALL PHASE(DATA2,PSHIFO)
CALL FILTER(DATA2,TF)

```

```
CALL SUM(DATA, DATA2, NUM)
NUM=5
CALL LOAD4(DATA2, NUM)
CALL HLIM(DATA2)
C   CALL POWER(DATA2, MPO)
C   CALL HPA(DATA2, BACKOF, PSHIFO, MPO)
C   CALL PHASE(DATA2, PSHIFO)
CALL FILTER(DATA2, TF)
CALL SUM(DATA, DATA2, NUM)
CALL RCOSRX (TF)
CALL HHGG(TF, PNOISE)
CALL ENERGY(DATA, EB)
CALL FILTER(DATA, TF)
CALL SYNCRO(DATA, PNOISE, MI, MQ, EB)
CALL DECODE(DATA, PNOISE, MI, MQ,
#EBNO, PEI, EB)
C
C   CALL THE DRAWING ROUTINE.
C
DO 99 I=1, NSNR
XARRAY(I)=EBNO(I)
99  YARRAY(I)=PEI(I)
C   CALL DRAW(XARRAY, YARRAY, KM, NRUNS)
100 CONTINUE
STOP
END
```

```

7cC*****
C   LOAD4:
C
C   THIS SUBROUTINE GENERATES AN BASEBAND QPSK SIGNAL.
C   INPUT PARAMETERS: LDIM,IOFF,LSAMPL
C   OUTPUT PARAMETERS: DATA,NI,NQ
C
C   LDIM      -THE DIMENSION OF THE COMPLEX DATA ARRAY.
C   IOFF      -THE NUMBER OF SAMPLES THE Q CHANNEL DATA IS
C              OFFSET FROM THE I CHANNEL DATA.
C   LSAMPL    -THE NUMBER OF SAMPLES PER SYMBOL.
C   NUM       -THE PARAMTER INDICATING WHICH QPSK DATA ARRAY.
C   DATA     -THE COMPLEX DATA ARRAY IN THE TIME DOMAIN.
C   NI        -THE I CHANNEL SYMBOL ARRAY.
C   NQ        -THE Q CHANNEL SYMBOL ARRAY.
C
C   THIS SUBROUTINE GENERATES TWO 2-LEVEL SYMBOL ARRAYS,
C   NI AND NQ, AND THE BASEBAND QPSK DATA ARRAY.  A GENERATOR
C   POLYNOMIAL OF DEGREE 11 IS USED TO GENERATE A PRBS OF NRZ
C   DATA FROM THE PRIMER DATA NY.   $G(X)=1+X^{**2}+X^{**11}$ 
C   A SEQUENCE OF  $2^{**11}$  DATA SYMBOLS IS GENERATED WITH THE FIRST
C   SYMBOL REPEATED AS THE LAST SYMBOL.  THIS SEQUENCE IS SHIFTED
C   TO PROVIDE THE ADDITIONAL SEQUENCE TO FORM THE I CHANNEL
C   SYMBOLS AND THE Q CHANNEL SYMBOLS.
C   THESE SYMBOLS ARE THEN LOADED IN THE COMPLEX DATA ARRAY
C   WITH A SET NUMBER OF SAMPLES REPRESENTING EACH SYMBOL(LSAMPL).
C   THE REAL PART OF THE DATA ARRAY CORRESPONDS TO THE I COMPONENT
C   AND THE IMAGINARY PART CORRESPONDS TO THE Q COMPONENT.
C*****

```

{
C

```

SUBROUTINE LOAD4(DATA,NUM)
COMPLEX DATA(1)
DIMENSION K(6),NY(11),NI(2048),NQ(2048),NX(2048)
COMMON /NUMB1/ FBW,ALPHA,LDIM,IOFF,LSAMPL
COMMON /INPUT/ NI,NQ
DATA NY(1),NY(2),NY(3),NY(4),NY(5),NY(6),NY(7),NY(8),NY(9),
#NY(10),NY(11)/-1,-1,1,1,1,-1,-1,-1,-1,-1/
DATA JLAST,JTAP/11,1/
KKK=2**JLAST
KK=KKK-(1+JLAST)
DO 6 I=1,JLAST
NX(I)=NY(I)
6 CONTINUE

```

C
C
C
C

```

GENERATE 2**JLAST -1 LENGTH SEQUENCE USING GIVEN DATA AND
GENERATOR POLYNOMIAL..

```

1

```

DO 1 J=1,KK
I=J+JLAST
NX(I)=NX(J)*NX(J+2)
NX(I)=0-NX(I)
1 CONTINUE

```

C
C
C
C

```

GENERATE 6 CYCLICALLY SHIFTED VERSIONS OF ORIGINAL
SEQUENCE OF LENGTH 2**JLAST FOR THE SAMPLE ARRAY.

```

```

K(1)=1
K(2)=2
K(3)=3
K(4)=4
K(5)=5
K(6)=6
DO 2 I=1,KKK
DO 5 J=1,6
5 IF (K(J) .EQ. KKK) K(J)=17c
IF (NUM .NE. 1) GO TO 4
NI(I)=(NX(K(1))*4) + (NX(K(3))*2) + NX(K(5))
NQ(I)=(NX(K(2))*4) + (NX(K(4))*2) + NX(K(6))

```

C
C
C

```

LOAD QPSK DATA INTO SAMPLE ARRAY, 8 SAMPLES PER SYMBOL

```

```

4 NUMI=NUM
II=K(NUMI)
NUMQ=NUM+1
IQ=K(NUMQ)
J1=(I-1)*LSAMPL+1
J2=I*LSAMPL
DO 3 J3=J1,J2
3 DATA(J3)=CMPLX(FLOAT(NX(II)),FLOAT(NX(IQ)))
DO 7 J=1,6
7 K(J)=K(J) + 1

```

2 CONTINUE
END

```
C
C*****
C HLIM:
C THIS SUBROUTINE SIMULATES A HARD LIMITER
C INPUT PARAMETERS: DATA,LDIM
C OUTPUT PARAMETERS: DATA
C
C DATA -THE COMPLEX DATA ARRAY IN THE TIME DOMAIN.
C LDIM -THE DIMENSION OF THE COMPLEX DATA ARRAY.
C
C THE OUTPUT SIGNAL OF THE HARDLIMITER RELATIVE TO AN INPUT
C SIGNAL OF  $I(t) + jQ(t)$  IS GIVEN BY
C
C  $I(t) = I(t) / \sqrt{I(t)^2 + Q(t)^2}$ 
C  $Q(t) = Q(t) / \sqrt{I(t)^2 + Q(t)^2}$ 
C*****
```

C

```
SUBROUTINE HLIM(DATA)
COMPLEX DATA(1)
COMMON /NUMB1/ FBW, ALPHA, LDIM, IOFF, LSAMPL
DO 10 I=1, LDIM
10 DATA(I)=DATA(I)/CABS(DATA(I))
RETURN
END
```

C

C
C*****

C HPA:

C THIS SUBROUTINE SIMULATES THE EQUIVALENT BASEBAND
C NONLINEARITY OF THE HUGHES 261-H TWT. COURTEOUSY OF
C DR. V. ARUNACHALAM
C INPUT PARAMETERS: DATA, LDIM, BAKOFF, MPO
C OUTPUT PARAMETERS: DATA, PSHIFT

- C DATA -THE COMPLEX DATA ARRAY IN THE TIME DOMAIN.
- C LDIM -THE DIMENSION OF THE COMPLEX DATA ARRAY.
- C BAKOFF -THE BACKOFF OF THE DEVICE IN dB.
- C MPO -THE MEAN POWER OF THE INPUT DATA SIGNAL.
- C PSHIFT -THE PHASE SHIFT OF THE DATA RESULTING FROM THIS
C SUBROUTINE.

C THE NONLINEAR DEVICE IS SIMULATED USING TWO POLYNOMIALS P(R)
C AND Q(R). THE OUTPUT DATA IMAGINARY AND REAL COMPONENTS
C CAN BE WRITTEN AS:

C REAL DATA= P(R)*X- Q(R)*Y
C IMAGINARY DATA= P(R)*Y + Q(R)*X

C WHERE X IS THE NORMALIZED DATA'S REAL COMPONENT
C Y IS THE NORMALIZED INPUT DATA'S IMAGINARY COMPONENT
C AND R IS THE NORMALIZED ENVELOPE OF THE INPUT SIGNAL.

C FOR DEVICES OPERATING WITH "BAKOFF" db BACKOFF THE
C NORMALIZED INPUT SIGNAL IS MULTIPLIED BY
C $10^{-(BAKOFF)/10}/\sqrt{MPO}$ TO FORM THE NORMALIZED INPUT
C DATA.

C*****

C

```

SUBROUTINE HPA(DATA,BAKOFF,PSHIFT,MPO)
COMMON /NUMB1/ FBW,ALPHA,LDIM,IOF,LSMP
COMPLEX DATA(1)
REAL MPO
DATA ZPMAX,ZQMAX,VMAX,VO/1.068,0.928,1.414,1./
DATA A1,A3,A5,A7,A9,A11,A13,A15,A17/1.916288,-9.358132E-1,
#1.942392E-1,-2.832262E-2,1.840305E-2,-4.282407E-3,0.0,0.0,0.0/
DATA B1,B3,B5,B7,B9,B11,B13,B15,B17/-5.9659E-2,1.907669,
#-1.846724,8.615552E-1,-1.990954E-1,1.815157E-2,0.0,0.0,0.0/
P(X)=(((((((A17*X**2+A15)*X**2+A13)*X**2+A11)*X**2+A9)*
#X**2+A7)*X**2+A5)*X**2+A3)*X**2+A1
ZP(X)=P(X)*X
Q(X)=(((((((B17*X**2+B15)*X**2+B13)*X**2+B11)*X**2+B9)*
#X**2+B7)*X**2+B5)*X**2+B3)*X**2+B1
ZQ(X)=Q(X)*X
Z(X)=SQRT(ZP(X)**2+ZQ(X)**2)
TWTIN=VO*10.**(-BAKOFF/20.)
PSHIFT=ATAN(ZQ(TWTIN*1.414)/ZP(TWTIN*1.414))
WRITE (6,2) BAKOFF,PSHIFT
2  FORMAT(5X,'HPA INPUT BACKOFF:',F4.1,' DB',
# '   OUTPUT PHASE SHIFT:',F7.3,/)
CALL POWER(DATA,MPO)

FNORMI=TWTIN/SQRT(MPO)
DO 11 I=1,LDIM
DATA(I)=DATA(I)*FNORMI
11 CONTINUE
DO 10 I=1,LDIM
X=REAL(DATA(I))
Y=AIMAG(DATA(I))
R=SQRT(X**2+Y**2)
IF(R.GT.VMAX) GOTO 12
DATA(I)=CMPLX(P(R)*X-Q(R)*Y,P(R)*Y+Q(R)*X)
GO TO 10
12 DATA(I)=CMPLX(ZPMAX*X-ZQMAX*Y,ZQMAX*X+ZPMAX*Y)/R
10 CONTINUE
RETURN
END

```

```
C
C*****
C  SUM:
C
C  THE FOLLOWING SUBROUTINE SUMS THE TWO QPSK DATA ARRAYS INTO
C  DATA1.
C  INPUT PARAMETERS:  DATA1,DATA2,NUM,LDIM
C  OUTPUT PARAMETERS:  DATA1
C
C  DATA1,DATA2 -THE COMPLEX DATA ARRAYS IN THE TIME DOMAIN.
C  NUM          -THE PARAMTER INDICATING WHICH QPSK DATA ARRAY.
C  LDIM         -THE DIMENSION OF THE COMPLEX DATA ARRAY.
C
C  DATA1 IS ADDED TO DATA2 /NUM-1 TO FORM THE OUTPUT DATA1
C  ARRAY. AS A FINAL STEP, DATA1 IS MULTIPLIED BY 4 TO
C  OBTAIN THE CORRECT DATA LEVELS.
C*****
```

C
SUBROUTINE SUM (DATA1,DATA2,NUM)
COMPLEX DATA1(1),DATA2(1)
COMMON /NUMB1/ FBW,ALPHA,LDIM,IOFF,LSAMPL
DO 1 I=1,LDIM
DATA1(I)=DATA1(I) + (DATA2(I)/(NUM -1))
IF (NUM .EQ. 5) DATA1(I)=DATA1(I)*4.
1 CONTINUE
RETURN
END

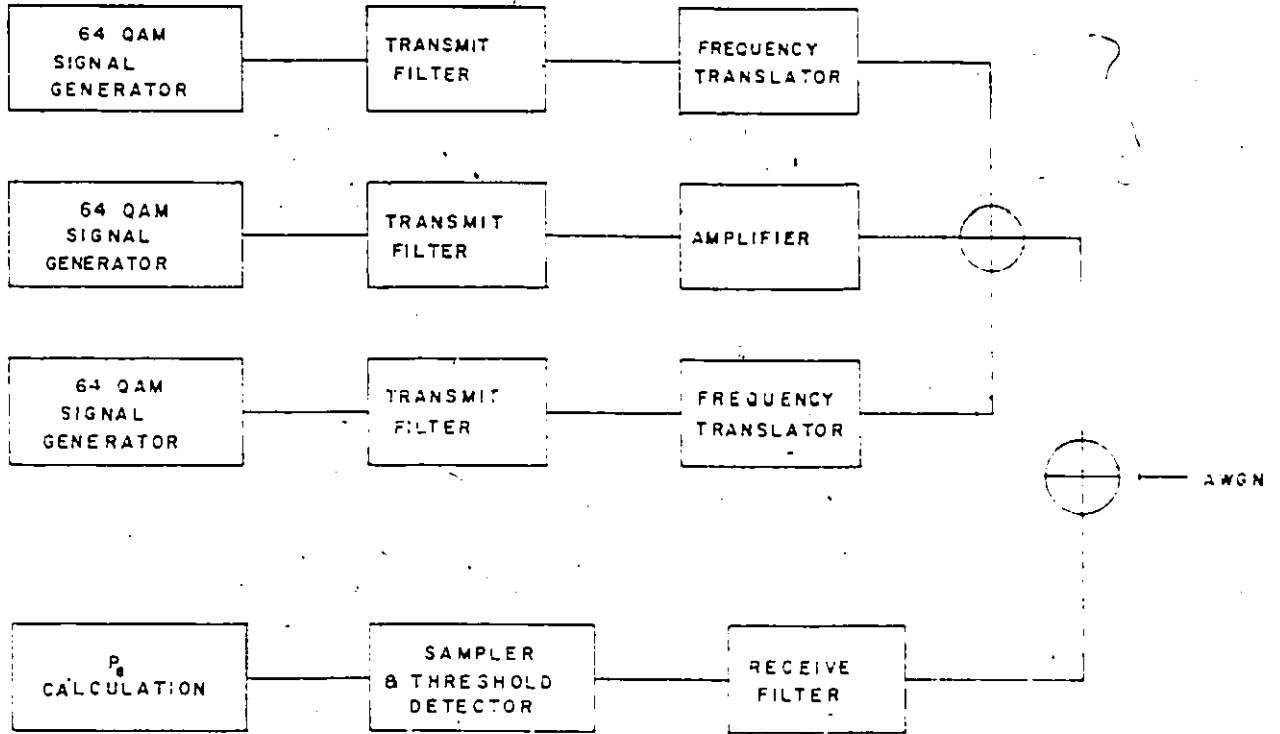


FIGURE B.1.3 64-STATE QAM COCHANNEL AND ADJACENT CHANNEL SIMULATION MODEL

```

C*****
C PROGRAM FOR THE SIMULATION OF 64-QAM WITH ADJACENT CHANNEL
C AND COCHANNEL INTERFERENCE.
C COPYRIGHT UNIVERSITY OF OTTAWA
C
C BY TRICIA HILL
C*****
COMMON /NUMB1/ FBW,ALPHA,LDIM,IOFF,LSAMPL
COMMON/NUMB2/ NSNR,NSYMB,BAUD
COMPLEX DATA1(32768),TF(32768),TFTX(32768),DATA2(32768)
#,TFRX(32768),DATA3(32768)
DIMENSION PEI(25),EBNO(25),NI(2048),NQ(2048),PO(25)
DIMENSION XARRAY(27),YARRAY(27)
REAL MP1,MP2,MP3

C
C INITIALIZE PROGRAM.
C SET PARAMETERS FOR RUN
C
NSYMB=2048
LSAMPL=16
BAUD=15.
NSNR=25
NRUNS=4
FBW=7.5
ALPHA=0.4
LDIM=32768
IOFF=0
DATA FOF1,FOF2,FOF3/-20.,0.,20./
DATA PSHIF3,PSHIF1/3.64,1.70/
DATA ITSH1,ITSH3/0,0/
DATA AT1,AT3/100.0,-27.0/
DO 19 I=1,NSNR
PO(I)=0.0
19 CONTINUE
PO1=0.0
DO 500 KM=1,NRUNS
ACIR1=-1*AT1
ACIR3=-1*AT3
SSS1=FLOAT(ITSH1)/(16.*.06)
SSS3=FLOAT(ITSH3)/(16.*.06)
ITSHI1=ITSH1+672
ITSHI3=ITSH3+72

C
C END OF INITIALIZATION.
C
C START OF COMPUTATIONS.
C
CALL RCOSTX(TFTX)
CALL RCOSRX(TFRX)

C
C CHANNEL 1
C

```

```

CALL LOAD64(DATA1,NI,NQ)
CALL FILTER(DATA1,TFTX)
CALL SACI(DATA1,FOF1)
CALL PHASE(DATA1,PSHIF1)
CALL TIMSHF(DATA1,ITSHI1)
CALL ATT(DATA1,AT1)
CALL FILTER(DATA1,TFRX)
CALL POWER(DATA1,MP1,PF1)

```

C
C
C

CHANNEL 2

```

33 CALL LOAD64(DATA2,NI,NQ)
CALL FILTER(DATA2,TFTX)
CALL ENERGY(DATA2,EB)
CALL FILTER (DATA2,TFRX)
CALL POWER(DATA2,MP2,PF2)

```

C
C
C

CHANNEL 3

```

CALL LOAD64(DATA3,NI,NQ)
CALL FILTER(DATA3,TFTX)
CALL SACI(DATA3,FOF3)
CALL PHASE(DATA3,PSHIF3)
CALL TIMSHF(DATA3,ITSHI3)
CALL ATT(DATA3,AT3)
CALL FILTER(DATA3,TFRX)
CALL POWER(DATA3,MP3,PF3)

```

C
C

ADD CHANNEL 1 AND CHANNEL 3 INTERFERENCE TO CHANNEL 2.

```

DO 20 I=1,LDIM
20 DATA2(I)=DATA1(I)+DATA2(I)+DATA3(I)

```

C
C
C

AT THE RECEIVER.

```

35 CALL HHGG(TFRX,PNOISE)
CALL SYNCRO(DATA2,PNOISE,NI,NQ,MI,MQ,EB)
CALL DECODE(DATA2,PNOISE,MI,MQ,NI,NQ,EBNO,PEI,EB)
DO 23 I=1,NSNR
PO(I)=PEI(I)+PO(I)
IF((PEI(I).LT..1E-03.AND.PEI(I).GT..1E-04).AND.(KM.EQ.1)) KL=I
23 CONTINUE
PO1=(PEI(KL)**2.)+PO1
ITSH1=ITSH1-1
PSHIF1=PSHIF1+.66
PSHIF3=PSHIF3-.23
ITSH3=ITSH3+1
500 CONTINUE
DO 64 I=1,NSNR
PO(I)=PO(I)/FLOAT(NRUNS)
64 CONTINUE

```

C
C

CALCULATE THE STANDARD DEVIATION.

```
C
  PO1=(PO1/FLOAT(NRUNS))- (PO(KL)**2.)
  PO1=ABS(PO1)
  PO1=SQRT(PO1)
  PO2=PO(KL)-PO1
  PO3=PO(KL)+PO1
  WRITE(6,150)
150  FORMAT(5X,'EB/NO',10X,'PROB. OF. ERROR', /)
  WRITE(6,172) (EBNO(I),PO(I),I=1,NSNR)
172  FORMAT(5X,F5.1,10X,E13.6)
  DO 190 I=1,NSNR
  XARRAY(I)=EBNO(I)
  YARRAY(I)=PO(I)
190  CONTINUE
  STOP
  END
```



```
C
C*****
C  S A C I :
C
C  THIS ROUTINE FREQUENCY SHIFTS THE DATA BY "FOF" MHz.
C  INPUT PARAMETERS: TF1,FOF,LDIM,LSAMPL,BAUD
C  OUTPUT PARAMETERS: TF1
C
C  TF1      -THE COMPLEX DATA SAMPLE ARRAY IN THE TIME DOMAIN.
C  FOF      -THE CHANNEL FREQUENCY OFFSET FROM THE MAIN
C           CHANNEL IN MHz.
C  LDIM     -THE DIMENSION OF THE TF1 COMPLEX ARRAY.
C  LSAMPL   -THE NUMBER OF SAMPLES/SYMBOL.
C  BAUD     -THE SYMBOL RATE IN MBaud.
C
C  THE DATA IS TRANSFORMED INTO THE FREQUENCY DOMAIN AND
C  THEN SHIFTED TO THE RIGHT (+FOF) OR LEFT (-FOF) MHz.
C  THE SHIFTED DATA IS THEN TRANSFORMED BACK TO THE TIME
C  DOMAIN.
C*****
C
```

C

```

SUBROUTINE SACI(TF1,FOF)
COMMON /NUMB1/ FBW,ALPHA,LDIM,IOFF,LSAMPL
COMMON /NUMB2/ NSNR,NSYMB,BAUD
COMPLEX TF1(32768)
COMPLEX XX
DIMENSION IWK(16)

```

C

C

C

```

TRANSFORM TO FREQUENCY DOMAIN

```

```

CALL FFT2C(TF1,15,IWK)
SBANDW=FLOAT(LSAMPL)*BAUD

```

C

C

C

```

IFOF IS THE NUMBER OF THE FREQUENCY SAMPLE REPRESENTING FOF

```

```

IFOF=IFIX(FOF*FLOAT(LDIM)/SBANDW)
IF(IFOF.EQ.0) RETURN
IF(IFOF.LT.0) GO TO 50

```

C

C

C

```

SHIFT DATA BY IFOF SAMPLES

```

```

DO 20 K=1, IFOF
XX=TF1(LDIM)
JJ=LDIM-1
DO 30 I=1, JJ
TF1(LDIM+1-I)=TF1(LDIM-I)
30 CONTINUE
TF1(1)=XX
20 CONTINUE
GO TO 100
50 IFOF=-IFOF
JJ=LDIM-1
DO 70 K=1, IFOF
XX=TF1(1)
DO 60 I=1, JJ
60 TF1(I)=TF1(I+1)
TF1(LDIM)=XX
70 CONTINUE

```

C

C

C

```

TRANSFORM BACK TO TIME DOMAIN

```

100

1

2

```

DO 1 I=1, LDIM
TF1(I)=CONJG(TF1(I))
CALL FFT2C(TF1,15,IWK)
DO 2 I=1, LDIM
TF1(I)=CONJG(TF1(I))/FLOAT(LDIM)
RETURN
END

```

```
C
C*****
C  PHASE:
C
C  THIS SUBROUTINE PHASE SHIFTS THE DATA BY "PSHIFT" RADIANS.
C  INPUT PARAMETERS: DATA, PSHIFT, LDIM
C  OUTPUT PARAMETERS: DATA
C
C  DATA      -THE COMPLEX DATA SAMPLE ARRAY IN THE TIME DOMAIN.
C  PSHIFT     -THE PHASE SHIFT IN RADIANS.
C  LDIM       -THE DIMENSION OF THE COMPLEX DATA ARRAY.
C
C  THE DATA IS MULTIPLIED BY EXP(-J*PSHIFT) TO SHIFT THE DATA.
C*****
C
```

C

```
SUBROUTINE PHASE(DATA, PSHIFT)
COMMON /NUMB1/ FBW, ALPHA, LDIM, IOFF, LSAMPL
COMPLEX EPS, DATA(32768)
EPS=CMPLX(COS(PSHIFT), -SIN(PSHIFT))
DO 10 I=1, LDIM
DATA(I)=DATA(I)*EPS
CONTINUE
RETURN
END
```

10

```
C
C*****
C  TIMSHF:
C
C  THIS SUBROUTINE SHIFTS THE DATA SAMPLES 'IT' POSITIONS.
C  INPUT PARAMETERS: DATA,IT,LDIM
C  OUTPUT PARAMETERS: DATA
C
C  DATA      -THE COMPLEX SAMPLE DATA ARRAY IN THE TIME
C             DOMAIN.  INPUT NOT SHIFTED.  OUTPUT SHIFTED.
C  IT         -THE NUMBER OF POSITIONS TO THE LEFT THE
C             DATA SAMPLES ARE SHIFTED.
C  LDIM       -DIMENSION OF THE COMPLEX DATA ARRAY.
C
C  THE SHIFTED DATA CORRESPONDS TO
C
C  DATA(J-IT)=DATA(J)
C
C  WHERE J REPRESENTS THE JTH SAMPLE OF THE DATA IN THE TIME
C  DOMAIN.
C*****7c*****
```

c

```
SUBROUTINE TIMSHF(DATA, IT)
COMMON /NUMB1/ FBW, ALPHA, LDIM, IOFF, LSAMPL
COMPLEX DATA(32768), DAT
DO 10 I=1, IT
DAT=DATA(I)
DO 20 J=2, LDIM
DATA(J-1)=DATA(J)
10 DATA(LDIM)=DAT
RETURN
END
```

```
C
C*****
C  ATT:
C
C  THIS SUBROUTINE ATTENUATES THE SIGNAL 'AT' DB.
C  INPUT PARAMETERS: DATA,AT,LDIM
C  OUTPUT PARAMETERS: DATA
C
C  DATA      -THE COMPLEX DATA SAMPLE ARRAY IN THE TIME
C              DOMAIN.  INPUT BEFORE ATTENUATION
C              OUTPUT ATTENUATED DATA.
C
C  AT         -THE ATTENUATION IN DB.
C
C  LDIM      -THE NUMBER OF SAMPLES PER CHANNEL.
C
C  THE INPUT DATA IS ATTENUATED 'AT' DB IN THIS ROUTINE.
C*****
C
```

```
C  
SUBROUTINE ATT(DATA,AT)  
COMMON /NUMB1/ FBW,ALPHA,LDIM,IOFF,LSAMPL  
COMPLEX DATA(32768)  
ATTEN=10.**(-AT/20.)  
DO 10 I=1,LDIM  
10 DATA(I)=DATA(I)*ATTEN  
RETURN  
END
```



```
C
C*****
C      POWER:
C
C      THIS SUBROUTINE CALCULATES THE MEAN POWER AND PEAK FACTOR OF
C      THE DATA.
C      INPUT PARAMTEETERS: DATA,LDIM
C      OUTPUT PARAMETERS: MP,PF
C
C      DATA      ~THE COMPLEX SAMPLE DATA ARRAY IN THE TIME
C                  DOMAIN.
C      LDIM       ~DIMENSION OF THE COMPLEX DATA ARRAY.
C      MP         ~MEAN POWER OF THE DATAA
C      PF         ~PEAK FACTOR OF THE DATA
C
C      THE MEAN POWER OF THE TIME DOMAIN DATA SIGNALS IS
C      THE SUM OF THE MEAN OPOWER OF EACH SAMPLE DIVIDED BY THE NUMBER
C      OF SAMPLES.  THE PEAK FACTOR IS THE PEAK POWER OF A SAMPLE
C      DIVIDED BY THE MEAN POWER OF THE SIGNAL.
C*****
```

C

```
SUBROUTINE POWER(DATA,MP,PF)
COMMON /NUMB1/ FBW,ALPHA,LDIM,IOFF,LSAMPL
COMPLEX DATA(32768)
REAL MP
PF=0.
MP=0.0
DO 10 I=1,LDIM
MP=MP+((CABS(DATA(I)))**2.)
IF(PF.LT.CABS(DATA(I))) PF=CABS(DATA(I))
10 CONTINUE
MP=MP/FLOAT(LDIM)/2.
PF=(PF**2.)/MP
PF=10.*ALOG10(PF)
RETURN
END
```

REFERENCES

REFERENCES

1. P. Hartman, "Digital radio technology: Present and future," IEEE Communications Magazine, July 1981.
2. K. Feher, Digital Communications Microwave Applications, Prentice-Hall Inc., Eaglewood Cliffs N.J., 1981.
3. C.M. Thomas, M.Y. Weidner and S.H. Durrani, "Digital amplitude-phase keying with m-ary alphabets", IEEE Trans. on Communications, Com-22, No. 2, Feb. 1974.
4. K. Miyauchi, S. Seki and H. Ishio, "New technique for generating and detecting multilevel signal formats", IEEE Trans. on Communication, Com-24, Feb. 1976.
5. D.H. Morais and K. Feher, "NLA-QAM: A new method for generating high power QAM signals through nonlinear amplification", IEEE Trans. on Communication, Com-30, Feb., 1982.
6. Y. Yashida, Y. Kitahara and S. Yokoyama, "6 GHz-90 Mb/s digital radio system with 16-QAM modulation", ICC, Seattle, June, 1980.
7. T. Le Gnoc, K. Feher and H. Pham Van, "Power and bandwidth efficient ISI and jitter-free transmission techniques for linear and nonlinear channels", ICC, Denver, June, 1981.
8. H. Pham Van and K. Feher, "A class of two symbol interval modems for nonlinear radio channels", NTC, New Orleans, Nov., 1981.

9. F. Jager and C. Dekker, "Tamed frequency modulation, A novel method to achieve spectrum economy in digital transmission", IEEE Trans. on Communication, Com-26, May, 1978.
10. W.R. Bennet and J.R. Davey, Data Transmission, McGraw-Hill Book Company, New York, 1965.
11. D. Predergast and K. Feher, "Switchable data modem design and evaluation (BPSK to 16-APK)", CCPC records, Montreal, Oct., 1980.
12. C.A. Holt, Electronic Circuits Digital and Analog, John Wiley and Sons, New York, 1978.
13. V. Arunachalam, "Digital Communications Group Report 112", University of Ottawa, Ottawa, 1980.
14. J.M. Wozencraft and I.M. Jacobs, Principles of Communication Engineering, John Wiley and Sons, New York, 1965.
15. G.M. Babler, "Measurements of delay distortion during selective fading", ICC, June, 1974.
16. M. Subramarian, K.C. O'Brien and P.J. Pulgris, "Phase dispersion characteristics during fade in microwave line-of-sight radio channels", B.S.T.J., Vol. 52, No. 10, Dec., 1973.
17. D.H. Morais, A. Sewerinson and K. Feher, "The effects of the amplitude and delay slope components of frequency selective fading on QPSK, offset QPSK, and 8 PSK systems", IEEE Trans. on Communication, Com-27, Dec., 1979.

18. W.D. Rummler, "A new selective fading model: Application to propagation data", B.S.T.J., Vol. 58, May-June, 1979.
19. F. Amoroso, "The bandwidth of digital data signals", IEEE Communications Magazine, Nov., 1980.
20. W.W. Mumford and E.H. Scheibe, Noise Performance Factors in Communication Systems, Horizon House-Microwave Inc., Dedham, Massachusetts, 1968
21. D.R. White, A Handbook on Electrical Filters, D. White, Germantown, 1963.
22. K. Feher, Digital Modulation Techniques in an Interference Environment, D. White, Germantown, 1977.
23. T.P. Murphy, F.M. Baker, C.L. Garner and P.J. Kruzinski, "Practical techniques for improving signal robustness", NTC, Nov., 1981.
24. P.R. Hartman and E.W. Allen, "Transmission Engineering Considerations", Technical Bulletin Rockwell International 523-0604120-102A35, Dec., 1979.